Lek. Aleksander Kiełbik

Rozprawa doktorska

Wpływ krótkich impulsów elektrycznych na komórki raka gruczołu krokowego

Promotor:

dr hab. n. med. Bartosz Małkiewicz, Klinika Urologii Małoinwazyjnej
i Robotycznej, Uniwersyteckie Centrum Urologii Uniwersytetu Medycznego im.
Piastów Śląskich we Wrocławiu

Drugi promotor:

dr hab. inż. Julita Kulbacka, Prof. UMW Katedra i Zakład Biologii Molekularnej i
Komórkowej, Wydział Farmaceutyczny, Uniwersytet Medyczny im. Piastów
Śląskich we Wrocławiu

SPIS TREŚCI:

1. Streszczenie

Według światowych danych epidemiologicznych rak prostaty (PCa, *prostate cancer*) jest diagnozowany u ponad miliona mężczyzn rocznie. Z uwagi na często powolny rozwój oraz rozpoznanie w późnym wieku, nie zawsze istnieją wskazania do leczenia radykalnego z wykorzystaniem standardowych form terapii (leczenie operacyjne, radioterapia) zwłaszcza w grupie chorych niskiego i pośredniego ryzyka z chorobą ograniczoną do narządu. Jednocześnie formy terapii zachowawczej tj. aktywny nadzór lub baczne wyczekiwanie nie zawsze są akceptowane przez pacjenta. Powyższe podkreśla potrzebę poszukiwania i rozwoju minimalnie inwazyjnych metod leczenia.

Krótkie impulsy elektryczne mogą wywołać efekt permeabilizacji czyli zwiększenia przepuszczalności błon biologicznych. Zjawisko to zostało nazwane elektroporacją. W przeciwieństwie do większości fokalnych terapii, efekt cytotoksyczny technologii opartych na elektroporacji nie wynika z uszkodzeń termicznych komórek nowotworowych, lecz z permeabilizacji ich błony komórkowej. Wstępnym etapem do wdrażania dalszych protokołów terapeutycznych opartych na elektroporacji są badania *in vitro*, które pozwalają na wyjaśnienie mechanizmów ich działania. Celem niniejszej pracy doktorskiej, opartej o cykl publikacji, jest zbadanie efektów biologicznych krótkich impulsów elektrycznych na modelach komórkowych raka gruczołu krokowego.

Do badań efektów biologicznych krótkich impulsów elektrycznych użyto cytometrii przepływowej, mikroskopii konfokalnej i fluorescencyjnej. Ponadto dokonano pomiaru przeżywalności i mobilności komórek oraz aktywności kaspaz. By zwizualizować elektoporację mikrosekundową z jonami wapnia przeprowadzono *in silico* symulację dynamiki molekularnej.

Badania potwierdzają obiecujące efekty krótkich impulsów elektrycznych na komórki raka prostaty. Elektroporacja z jonami wapnia zwiększa efekt cytotoksyczny zarówno przy zastosowaniu nano- jak i mikrosekundowych impulsów. Metoda ta może zapewnić skuteczniejszą ablację oraz zmniejszyć ryzyko wznowy miejscowej choroby. Permeabilizacja komórek przez impulsy nanosekundowe może być kontrolowana przez natężenie pola elektrycznego, jak również przez częstotliwość impulsów. Nanosekundowe impulsy o częstotliwościach MHz-owych wykazują wyraźnie zwiększoną cytotoksyczność w porównaniu do impulsów o niższych częstotliwościach. Elektroporacja impulsami nano- lub mikrosekundowymi bez jonów wapnia wywołuje apoptozę komórek nowotworu prostaty. Jeżeli komórki są eksponowane na impulsy elektryczne w buforze ze zwiększonym stężeniem jonów wapnia mechanizm ich śmierci zależy od długości impulsu. Zmniejszona mobilność komórek nowotworowych, oraz zmiany w cytoszkielecie komórek po terapii, ilustrują potencjał krótkich impulsów elektrycznych w zapobieganiu przerzutom nowotworu stercza.

2. Abstract

Every year over one million patients are diagnosed with prostate cancer (PCa). Due to slow progression and typically late age at onset, radical treatment (surgery, radiation) cannot always be indicated, especially for low and medium-risk localized PCa. Simultaneously, conservative treatment, i.e. watchful waiting and active surveillance, does not always gain acceptance from patients. The latter calls for the development of new, effective, safe, and minimally invasive therapies.

The observation that an application of pulsed electric fields (PEFs) resulted in increased permeability of the cell membrane has led to the discovery of the phenomenon called electroporation. In vitro research helps to elucidate the potential of PEFs, and constitutes the first step for further technology development. The aim of Ph.D. thesis was to evaluate the effects of pulsed electric fields on human prostate cancer models.

In the project, we used flow cytometry and confocal and fluorescence microscopy. Moreover, we performed cell viability assay, caspase activity analysis and, wound healing assay to investigate the biological effect of PEFs on PCa cells. For *in silico* investigation of calcium electroporation, we conducted the molecular dynamics simulation.

The research confirms the promising effect of PEFs on PCa cells. Electroporation with calcium has a chance to enhance the oncological outcome of the nanosecond as well as microsecond pulses. The cell membrane permeabilization by nanosecond pulses can not only be controlled by electric field intensity but also with pulse frequency. MHz compression of nanosecond PEFs bursts proved to additionally enhance the effectiveness of the therapy. The cancer cells exposed to electric pulses presented disrupted cytoskeleton and impaired mobility. Thus, PEFs have the potential to prevent or slow down the progression of metastasis. Depending on the pulse duration and the Ca^{2+} content in the electroporation buffer, the mechanism of death may differ. Standalone electroporation promotes rather an apoptotic type of cell death. Differently, for the cells electroporated in buffer containing Ca^{2+}, cell death mechanisms depend on the pulse duration. Short electric pulses showed potential for an application as focal therapy of prostate cancer.

3. Cykl publikacji stanowiących podstawę pracy doktorskiej:

1. Kiełbik, A., Szlasa, W., Saczko, J., & Kulbacka, J. (2020). Electroporation-Based Treatments in Urology. *Cancers*, *12*(8), 2208.

(IF: 6.639, Pkt. MNiSW: 140)

2. Kiełbik, A., Szlasa, W., Michel, O., Szewczyk, A., Tarek, M., Saczko, J., & Kulbacka, J. (2020). In Vitro Study of Calcium Microsecond Electroporation of Prostate Adenocarcinoma Cells. *Molecules*, *25*(22), 5406

(IF: 4.411, Pkt. MNiSW: 100)

3. Kiełbik, A., Szlasa, W., Novickij, V., Szewczyk, A., Maciejewska, M., Saczko, J., & Kulbacka, J. (2021). Effects of high-frequency nanosecond pulses on prostate cancer cells. *Scientific Reports*, 11(1), 1-10

(IF: 4.379, Pkt. MNiSW: 140)

Łączna punktacja cyklu publikacji:

Impact factor (IF): 15,429 Liczba punktów MNiSW/KBN: 380

4. Wprowadzenie do rozprawy doktorskiej

Rak gruczołu krokowego jest drugim na świecie najczęściej diagnozowanym nowotworem u mężczyzn [1]. Z badań opartych na autopsji wynika, że występuje u ok. 48-71% pacjentów powyżej 79 roku życia [2]. Według światowych danych epidemiologicznych, rak prostaty jest wykrywany u ponad miliona mężczyzn rocznie [3]. Zapadalność znacząco wzrasta z wiekiem, a 71,2% wszystkich zgonów z powodu tej choroby dotyczy pacjentów powyżej 75 roku życia [4]. Powszechne oznaczanie stężenia PSA oraz wdrożenie w ostatnich latach do codziennej praktyki nowych precyzyjnych technik obrazowania takich jak multiparametryczny rezonans magnetyczny (mpMRI - *multi-parametric magnetic resonance imaging*), spowodowało znaczący wzrost przypadków rozpoznawanych w niskim stadium zaawansowania [5]. Z uwagi na często powolny rozwój oraz rozpoznanie w późnym wieku, nie zawsze istnieją wskazania do leczenia radykalnego z wykorzystaniem standardowych form terapii (leczenie operacyjne, radioterapia) zwłaszcza w grupie chorych niskiego i pośredniego ryzyka z chorobą ograniczoną do narządu (*Low-risk and intermediate-risk localized prostate cancer*) [6]. Jednocześnie formy terapii zachowawczej tj. aktywny nadzór (*ang. active surveilance*) lub baczne wyczekiwanie (*ang. watchfull waiting*) nie zawsze są akceptowane przez pacjenta. Wysoka zapadalność oraz skutki uboczne radykalnych form terapii, podkreślają potrzebę poszukiwania i rozwoju minimalnie inwazyjnych metod leczenia. Według wytycznych Europejskiego Towarzystwa Urologicznego, w przypadku nowotworu o niskim lub pośrednim ryzyku ograniczonego do narządu możliwe jest wykorzystanie terapii fokalnych [7]. Spośród dostępnych technologii najpowszechniej wykorzystywane są ultra dźwięki o wysokim natężeniu (HIFU – *high intensity focused ultrasounds*), krioablacja oraz terapia fotodynamiczna (PDT – *photodynamic therapy*). Niemniej jednak, metody te są wciąż uznawane za eksperymentalne, ponieważ nie dysponujemy wysokiej jakości danymi uwzględniającymi długoterminowe obserwacje i efekty onkologiczne, które jednoznacznie potwierdziłyby skuteczność wymienionych metod.

Krótkie impulsy elektryczne mogą permeabilizować błony biologiczne, zwiększając ich przepuszczalność [8,9]. Zjawisko to zostało nazwane elektroporacją. Zewnętrzne pole elektryczne powoduje powstanie dodatkowego napięcia na zewnętrznej błonie komórki. Jeśli różnica potencjałów po obu jej stronach wyniesie ok. 200–250 mV dwuwarstwa lipidowa znacząco zwiększa swoją przepuszczalność [10]. Zwyczajowo, do permeabilizacji błony komórkowej, używa się serii impulsów prostokątnych. W zależności od długości ich trwania wyróżniamy elektroporację mili-, mikro-, oraz nanosekundową. Rozszczelnienie błony przez impulsy elektryczne może być nieodwracalne (IRE - *irreversible electroporation*) lub odwracalne. Nieodwracalna elektroporacja skutkuje zaburzeniem homeostazy komórki oraz indukcją procesu śmierci komórkowej [11]. Komórki odwracalnie elektroporowane po pewnym

czasie odtwarzają ciągłość błony komórkowej. Tymczasowa permeabilizacja, umożliwia dokomórkowy transport cząsteczek takich jak leki cytostatyczne, ale również białek, czy materiału genetycznego [12,13]. Impulsy elektryczne można zatem wykorzystać w celowanej chemoterapii lub jako metodę transfekcji.

Kliniczne zastosowanie elektroporacji wymaga przezskórnej lub śródoperacyjnej insercji elektrod w region, który ma zostać permeabilizowany. W tym celu najczęściej używane są elektrody igłowe, płytowe, cewnikowe lub zaciskowe. Do efektywnej elektoporacji niezbędne jest również uwzględnienie nierównomierności w przewodnictwie elektrycznym tkanek [14]. Numeryczne modelowanie tkanek oraz symulacje elektroporacji pomagają przewidzieć rozkład natężenia pola elektrycznego w celowanym regionie [15]. Do śledzenia efektów terapii aktualnie najczęściej używane są tomografia komputerowa, rezonans magnetyczny lub ultrasonografia [16,17]. Techniki te nie mogą jednak zobrazować zakresu ablacji w momencie dostarczania impulsów. Bazując na zmianach w przewodnictwie elektrycznym elektroporowanych tkanek, wciąż rozwijane i ulepszane są nowe technologie umożliwiające określenie zasięgu ablacji w czasie rzeczywistym [18].

Aktualnie, elektryczne impulsy mikrosekundowe, w ramach badań naukowych, wykorzystuje się również w fokalnej terapii nowotworu prostaty metodą nieodwracalnej elektroporacji. W przeciwieństwie do większości terapii fokalnych, efekt cytotoksyczny technologii opartych na elektroporacji nie wynika z uszkodzeń termicznych komórek rakowych, lecz z ich permeabilizacji [19]. Odmienny mechanizm oddziaływania i precyzyjna lokalizacja miejsc dostarczania impulsów elektrycznych potencjalnie pozwalają na minimalizację efektów ubocznych oraz poprawę wyników funkcjonalno-czynnościowych m.in szybszą regeneracje kompleksu zwieracza cewki moczowej oraz zmniejszają ryzyko uszkodzenia pęczków naczyniowo-nerwowych i w konsekwencji zaburzeń erekcji [20]. Aktualnie w fazie badań klinicznych znajduje się elektroporacja nieodwracalna stosowana do celowanej lub całkowitej ablacji gruczołu krokowego oraz do leczenia wznowy lokalnej po radioterapii.

Wstępne wyniki badań klinicznych z zastosowaniem nieodwracalnej elektroporacji w raku prostaty potwierdzają skuteczność terapii oraz niskie ryzyko powikłań. Niemniej jednak u części pacjentów po zabiegu dochodzi do progresji miejscowej choroby, co sugeruje niedostateczną elektoporację komórek nowotworowych i niekompletną ablację [21]. Ryzyko wznowy lokalnej można ograniczyć, zwiększając natężenie pola elektrycznego lub liczbę impulsów. Inną metodą, która wzmacnia cytotoksyczność terapii jest dodatkowa aplikacja jonów wapnia w miejscu ablacji [22]. Metoda ta została pierwszy raz opisana przez prof. J. Gehl w 2012 [23]. Jony wapnia w komórce pełnią rolę kluczowego przekaźnika w wielu procesach fizjologicznych. Aby zachować homeostazę jonów Ca^{2+} w komórce, ich poziom musi być ściśle kontrolowany [24]. Stężenie wewnątrzkomórkowych jonów Ca^{2+} zostaje utrzymane na poziomie

20-40 nM, jednocześnie stężenie tego jonu w płynie zewnątrzkomórkowym wynosi zazwyczaj ok. 2 mM [25]. Permeabilizacja błony komórkowej, zgodnie z procesem dyfuzji, wywołuje napływ jonów wapnia do komórki. Poprzez aplikację $CaCl_2$ w miejscu elektroporacji możliwe jest zwiększenie transportu jonów wapnia oraz wzmocnienie efektu cytotoksycznego terapii. Aktualnie pierwsze próby kliniczne z zastosowaniem elektroporacji z $CaCl_2$ obejmują czerniaka, nowotwory głowy i szyi oraz raka jelita grubego [22]. Potencjalnie $CaCl_2$ z elektroporacją można wykorzystać także w terapii raka prostaty.

Kliniczne zastosowanie elektroporacji, wymaga znieczulenia ogólnego oraz całkowitego zwiotczenia mięśni [26]. Dodatkowo, by uniknąć potencjalnych arytmii, impulsy mogą być dostarczane jedynie w fazie refrakcyjnej czynności elektrycznej serca, dlatego terapia musi być zsynchronizowana z EKG [27]. Aby skutecznie ograniczyć zdolność ekscytacji komórek nerwowych oraz mięśniowych przez impulsy elektryczne możliwe jest skrócenie ich długości do przedziałów nanosekundowych. Nanosekundowe impulsy pierwszy raz zostały użyte w 2001 roku przez K. Schoenbach i S. Beebe i od tego czasu rozpoczęły się badania analizujące ich efekty biologiczne [28]. Kolejne eksperymenty ujawniły ich unikalne właściwości. Impulsy nanosekundowe wywierają efekt na wnętrze komórki, permeabilizując błony mitochondrialne oraz siateczkę endoplazmatyczną, co powoduje śmierć komórkową [29,30]. Co więcej, podobnie jak impulsy mikrosekundowe, oddziałują one także na zewnętrzną błonę komórek, doprowadzając do jej permeabilizacji. Defekty w błonie są jednak mniejsze w porównaniu do tych wywoływanych przez dłuższe impulsy [31]. Impulsy nanosekundowe mogą być potencjalnie wykorzystane w terapii ogniskowej raka prostaty. Umożliwia to uniknięcie niepożądanych skurczy mięśni szkieletowych, precyzyjniejszą kontrolę ablacji oraz przeprowadzenie zabiegu w znieczuleniu miejscowym. Możliwości wykorzystania krótkich impulsów elektrycznych do terapii raka prostaty są liczne i znacznie wykraczają poza obecnie stosowaną klinicznie elektroporację nieodwracalną. Wstępnym etapem do wdrażania dalszych protokołów terapeutycznych opartych na elektroporacji są badania *in vitro*, które pozwalają na wyjaśnienie mechanizmów ich działania.

5. Założenia i cele pracy

Założenia niniejszej pracy doktorskiej są następujące:

1. Zastosowanie standardowych form leczenia radykalnego w części przypadków raka prostaty niskiego i pośredniego ryzyka ograniczonego do narządu (low-risk and intermediate-risk localized prostate cancer) nie zawsze jest uzasadnione. Niski odsetek powikłań czynnościowo-funkcjonalnych terapii fokalnych sprawia, że stanowią one obiecującą i interesującą alternatywę terapeutyczną.
2. Elektroporacja z jonami wapnia zwiększa efekt cytotoksyczny terapii, jednak brak jest badań przedklinicznych uzasadniających celowość jej zastosowania na nowotworze prostaty.
3. Aplikując nanosekundowe impulsy elektryczne zamiast standardowo używanych mikrosekundowych, można uniknąć niepożądanego wzbudzenia komórek nerwowych i mięśniowych. Umożliwia to przeprowadzenie zabiegu w znieczuleniu miejscowym. Efekt cytotoksyczny impulsów nanosekundowych na komórki raka prostaty pozostaje jednak niezbadany.
4. Kompresja MHz-owa impulsów nanosekundowych zwiększa ich cytotoksyczność oraz zdolność permeabilizacji błon biologicznych. Pierwsze badania *in vitro* wskazują na dużą skuteczność tej technologii, jednak jej efekty cytobiologiczne wciąż pozostają nieznane.

Celem niniejszej pracy doktorskiej było zbadanie efektów biologicznych krótkich impulsów elektrycznych na modelach komórkowych raka prostaty. W pracy zostały wyróżnione dwa główne cele badawcze:

1. Szczegółowa analiza wpływu mikrosekundowych impulsów elektrycznych o wysokim napięciu na komórki DU 145 raka gruczołu krokowego (z oraz bez dodatkowej aplikacji jonów wapnia), obejmująca mechanizm śmierci komórkowej, dynamikę transportu wapnia, jak również mobilność oraz strukturę cytoszkieletu komórek prostaty po elektroporacji.
2. Analiza potencjału impulsów nanosekundowych o wysokich częstotliwościach w terapii nowotworu stercza na komórkach DU 145 i LNCaP uwzględniająca impulsy o częstotliwościach megahercowych.

Cel pracy doktorskiej zrealizowano w ramach dwóch projektów badawczych, których efektem było powstanie dwóch prac oryginalnych. Ponadto w skład cyklu publikacji włączona jest praca przeglądowa opisująca aktualny rozwój technologii opartych na elektroporacji w urologii.
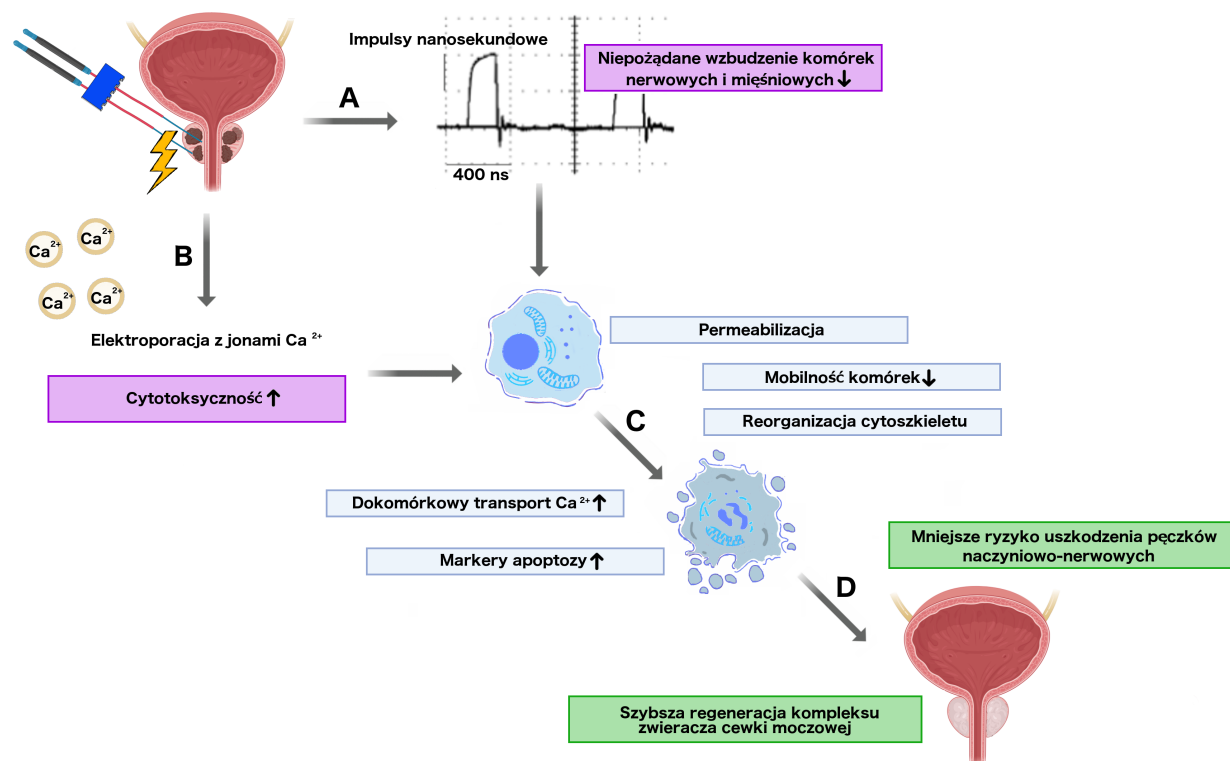
Rycina 1. Koncepcja pracy doktorskiej pt. „Wpływ krótkich impulsów elektrycznych na komórki raka gruczołu krokowego". Aplikując nanosekundowe impulsy elektryczne zamiast standardowo używanych mikrosekundowych można uniknąć niepożądanego wzbudzenia komórek nerwowych i mięśniowych (**A**). Elektroporacja z jonami wapnia zwiększa efekt cytotoksyczny terapii (**B**). Krótkie impulsy elektryczne wywołują szereg efektów biologicznych, które ostatecznie prowadzą do śmierci komórki (**C**). Odmienny mechanizm oddziaływania i precyzyjna lokalizacja miejsc dostarczania impulsów elektrycznych potencjalnie pozwala na minimalizację efektów ubocznych oraz poprawę wyników funkcjonalno-czynnościowych (**D**).

6. Materiał i metodyka badań

6.1 Omówienie materiału i metodyki badań

Eksperymenty badawcze zostały przeprowadzone w laboratorium Katedry i Zakładu Biologii Molekularnej i Komórkowej Uniwersytetu Medycznego we Wrocławiu. Ludzkie komórki raka prostaty DU 145 oraz LNCaP zostały wykorzystane jako model *in vitro* raka gruczołu krokowego. Obie linie zostały nabyte od ATCC® (American Type Culture Collection) i udostępnione do badań przez Instytut Immunologii i Terapii Doświadczalnej im. Ludwika Hirszfelda Polskiej Akademii Nauk**.** Komórki hodowano zgodnie z zaleceniami producenta.

Elektroporacja komórek i jej efektywność

Elektroporacja zawiesiny komórek została przeprowadzona przy pomocy różnych elektroporatorów. Do wytworzenia impulsów mikrosekundowych użyto elekroporatora ECM830 BTX (Syngen Biotech, Wrocław, Poland). Nanosekundowe impulsy wygenerowano przez elektroporator zaprojektowany i zbudowany w Instytucie Silnych Pól Magnetycznych (VGTU, Wilno, Litwa) przez prof. Vitalij'a Novickij'ego. Przed elektroporacją komórki zostawały zawieszone w buforze HEPES z dodatkami. Ekspozycji na krótkie impulsy elektryczne dokonano w 1 mm lub 4 mm kuwetach (VWR). Po elektroporacji materiał biologiczny poddano dalszej analizie.

Do określenia stopnia permeabilizacji komórek użyto cytometrii przepływowej. Po ekspozycji na impulsy elektryczne do zawiesiny komórek dodano fluorescencyjnego barwnika YO-PRO-1 (ThermoScientific). Ocenę intensywności wybarwienia komórek przeprowadzono przy pomocy cytometru Cube 6 (Sysmex, Polska). W badaniu tym ilość komórek wykazujących sygnał fluorescencyjny z całej populacji odzwierciedlała procent permeabilizacji.

Do oceny przeżywalności komórek wykorzystano test MTT. Po elektroporacji komórki nałożono na płytkę 96-dołkową i po 24 godzinnej inkubacji dodano odczynnik MTT. Powstałe po inkubacji kryształki rozpuszczono przy pomocy izopropanolu. Do oceny absorbancji wykorzystano czytnik wielodetekcyjny GlowMax (Promega, Walldorf, Niemcy).

Analiza śmierci komórkowej

W badaniu efektów biologicznych impulsów mikrosekundowych wykorzystano cytometrię przepływową, mikroskopię konfokalną oraz czuły test luminescencyjny.

Do badań cytometrycznych, po elektroporacji z jonami wapnia, do zawiesiny

z komórkami dodano barwniki SYTOX oraz APC połączone z Aneksyną V. Komórki apoptotyczne identyfikowano, mierząc ekspresję fosfatydyloseryny na zewnętrznej błonie cytoplazmatycznej, z którą łączy się APC sprzężone z Aneksyną V. Komórki nekrotyczne zostały wybarwione odczynnikiem SYTOX, który wnika do komórki przez uszkodzoną błonę, tworząc kompleks z kwasami nukleinowymi. Oceny komórek dokonano przy pomocy cytometru Cube 6 (Sysmex, Polska).

Do badań z zastosowaniem mikroskopii konfokalnej, po elektroporacji komórki utrwalono na szkiełkach mikroskopowych oraz wybarwiono pierwszorzędowym przeciwciałem skierowanym przeciwko kaspazie 3 oraz drugorzędowym przeciwciałem fluorescencyjnym Alexa Fluor 488. Oceny ekspresji dokonano, używając mikroskopu konfokalnego (Olympus FluoView 1000, Tokio, Japonia).

W przypadku analizy śmierci komórkowej, za pomocą czułego testu Caspase-Glo 3/7 Promega (Madison, WI, USA), komórki po elektroporacji nałożono na 96 dołkową płytkę. Następnie po 2h, 4h, 8h oraz 20h do dołów dodano reagent i dokonano odczytu luminescencji wielodetekcyjnym czytnikiem GlowMax (Promega, Walldorf, Niemcy)

Analiza mobilności komórkowej

Mobilność komórek po terapii zbadano, obserwując i analizując tempo zarastania wolnej przestrzeni pomiędzy dwiema koloniami. Aby tego dokonać, komórki hodowano w silikonowych insertach (Ibidi, Niemcy). Po wytworzeniu monowarstwy inserty zostały zdjęte, a wytworzone kolonie komórek obserwowano, aż do ich połączenia. Analizy mobilności oceny dokonano przy pomocy programu ImageJ (Version:2.1.0/1.53C; https://imagej.net/Fiji).

Ocena zmian białek cytoszkieletu

Wykorzystując mikroskopię konfokalną obserwowano zmiany w cytoszkielecie komórek po terapii. Po elektroporacji komórki nałożono i utrwalono na szkiełkach mikroskopowych. Następnie preparaty, zgodnie z instrukcją producenta, wybarwiono przeciwciałami przeciwko f-aktynie oraz zyksynie. Oceny struktury dokonano używając mikroskopu konfokalnego (Olympus FluoViewer 1000, Tokio, Japonia).

Efektywność transportu jonów wapnia

Ocenę dynamiki transportu jonów wapnia przeprowadzono przy pomocy mikroskopii fluorescencyjnej. Komórki nasadzono na nakrywkowe szkiełka mikroskopowe, a następnie inkubowano z barwnikiem Fluo-8. Odczynnik ten wnika do komórek, gdzie następnie jest rozkładany przez esterazy. Fluo-8 w połączeniu z Ca^{2+} zwiększa swoją fluorescencję,

co umożliwia obserwowanie zmian stężenia wewnątrzkomórkowego Ca^{2+}. Po inkubacji komórki elektroporowano, używając dwuigłowej elektrody kontaktowej BTX533 (BTX, Syngen Biotech, Poland). Zmiany fluorescencji obserwowano pod mikroskopem fluorescencyjnym Olympus IX53 (Olympus, Japonia), a jej oceny dokonano używając programu ImageJ (Version:2.1.0/1.53C; https://imagej.net/Fiji).

Badania metodami dynamiki molekularnej

Przy pomocy programu GROMACS 2018.3 dokonano symulacji dynamiki molekularnej w na klastrach obliczeniowych w Wydziale Teoretycznej Chemii i Fizyki Uniwersytetu w Lotaryngii (Nancy, Francja). Modelowy układ błony został utworzony przy pomocy oprogramowania CHARMM-GUI pod kontrolą wizualną VMD. Model dwuwarstwy fosfolipidowej zawierał 40% POPC (1-palmitoilo-2-oleoilo-sn-glicero-3-fosfocholina), 30% POPEE (1-palmitoilo 2-oleoilo-sn-glicero-3-fosfoetanoloamina), 16% POPCE (1-palmitoilo-2-oleoilo-sn-glicero-3- fosfoetanoloamina), 4% POPCE (1-palmitoilo-2-oleoilo-sn-glicero-3-fosfoetanoloamina), oraz 10% z cholesterolu. Do systemu wprowadzono nierównomierność rozkładu jonów po obu stronach błony. Zabieg ten wytworzył dostatecznie wysoki potencjał przezbłonowy skutkujący elektroporacją błony komórkowej. Symulacja trwała 10 nanosekund. Rezultaty zostały zwizualizowane i analizowane w programie VMD.

6.2 Analiza statystyczna

Eksperymenty laboratoryjne wykonano w co najmniej trzech powtórzeniach. Analiza statystyczna została przeprowadzona z użyciem programu GraphPad Prism 7 (La Jolla, CA, USA). Różnice pomiędzy grupami eksperymentalnymi zostały określone przez wieloczynnikową analizę wariancji lub Test t-Studenta w zależności od eksperymentu. Rezultaty zostały zaprezentowane jako średnia i odchylenie standardowe. Poziom istotności statystycznej określono jako $p < 0,05$ dla wszystkich obliczeń.

7. Podsumowanie wyników i wnioski z rozprawy doktorskiej

7.1 Omówienie wyników przeprowadzonych badań elektroporacji mikrosekundowej

Śmiertelność i permeabilizacja komórek nowotworu stercza zwiększa się wraz ze wzrastającym natężeniem pola elektrycznego. Najbardziej znaczący wzrost pemeabilizacji komórek jest widoczny pomiędzy 400 a 800 V/cm natężenia pola elektrycznego. Impulsy powyżej 1200 V/cm powodują całkowitą permeabilizację komórek i skutkują znaczącym spadkiem ich przeżywalności.

Zwiększone stężenie jonów wapnia w płynie zewnątrzkomórkowym istotnie wzmacnia efekt cytotoksyczny terapii. Synergistyczny efekt aplikacji Ca^{2+} jest najbardziej widoczny przy natężeniu pola elektrycznego o wartości 1000 V/cm. Sama inkubacja komórek z jonami wapnia, bez zastosowania impulsów, nie wpływa na przeżywalność komórek. Badania mechanizmu śmierci komórek po terapii udowodniły, że dominującym mechanizmem śmierci komórkowej po elektroporacji mikrosekundowej z jonami wapnia jest apoptoza. Elektroporowane komórki wykazują zmiany typowe dla programowanej śmierci komórkowej. Zaobserwowano zwiększoną ekspresję kaspazy-3 oraz obecność fosfatydyloseryny w zewnętrznej warstwie błony.

Elektroporacja mikrosekundowa obniża mobilność komórek nowotworu prostaty. Impulsy elektryczne powodują rozbicie włókien aktynowych oraz zaokrąglenie komórek. Obecność jonów wapnia w buforze dodatkowo wzmaga wpływ terapii na morfologię komórek. Badania dynamiki transportu Ca^{2+} potwierdziły, że dokomórkowy napływ jonów Ca^{2+} rozpoczyna się natychmiast po rozszczelnieniu błon komórkowych. Po osiągnięciu najwyższego stężenia Ca^{2+} w cytoplazmie komórki rozpoczynają wydalanie jonów wapnia. Początkowo ich stężenie maleje wykładniczo, po czym stała transportu Ca^{2+} stabilizuje się.

Dynamika molekularna wykazała, że transport jonów wapnia przez rozszczelnioną błonę komórkową jest sekwencyjny. Pomimo różnic w stężeniu wewnątrz- i zewnątrzkomórkowego Ca^{2+} nie dochodzi do natychmiastowego wyrównania ich poziomów.

7.2 Omówienie wyników przeprowadzonych badań elektroporacji nanosekundowej

Permeabilizacja komórek raka prostaty zależy od natężenia pola elektrycznego oraz częstotliwości nanosekundowych impulsów elektrycznych. Impulsy o częstotliwości MHz-owej efektywniej permeabilizują komórki. Poprzez kompresję impulsów do częstotliwości MHz-owej można obniżyć natężenie pola elektrycznego i uzyskać poziom permeabilizacji osiągany przy innych częstotliwościach i wyższym natężeniu pola.

Efekt cytotoksyczny impulsów nanosekundowych zależy od wrażliwości linii

komórkowej. Można go nasilić, podwyższając stężenie jonów wapnia w płynie zewnątrzkomórkowym. Synergiczny efekt aplikacji jonów wapnia nie zależy od częstotliwości nanosekundowych impulsów.

Również zwiększenie liczby nanosekundowych impulsów obniża przeżywalność komórek nowotworowych. Zależność ta jest dużo bardziej wyraźna w przypadku ekspozycji na impulsy o częstotliwości 1 MHz. Przy ekspozycji komórek na 500 takich impulsów uzyskano niemal 100%-ową śmiertelność komórek nowotworu prostaty.

Badanie przebiegu aktywności markerów apoptozy - kaspazy 3 i 7 po elektroporacji wskazuje na ich największą ekspresję 4 godziny po ekspozycji na impulsy elektryczne. Ekspozycja komórek na nanosekundowe impulsy w buforze bez Ca^{2+} wywołuje znaczący wzrost markerów apoptozy. Komórki elektroporowane w środowisku ze zwiększoną ilością Ca^{2+} wykazują niską aktywność kaspaz po terapii.

Analiza kształtu wykresów zmian wewnątrzkomórkowego stężenia wapnia po elektoporacji wykazuje różnice zależne od częstotliwości impulsów. Serie impulsów o częstotliwości 1 Hz i 1 kHz wywołują zdesynchronizowany napływ Ca^{2+} do komórek. Impulsy o tych częstotliwościach nie inicjują transportu jonów wapnia od razu po ekspozycji. Impulsy o częstotliwości 1 MHz powodują natychmiastowy i jednoczesny napływ Ca^{2+} do permeabilizowanych komórek.

Krótkie impulsy elektryczne o wysokich częstotliwościach powodują zmiany w cytoszkielecie komórek nowotworowych. Po ekspozycji włókna aktynowe skupiają się na obrzeżach komórki. Dochodzi także do zanikania lamellipodiów oraz włókien stresowych. Zmiany te są mniej widoczne po ekspozycji na impulsy o częstotliwości 1 Hz. Obecność Ca^{2+} w płynie zewnątrzkomórkowym w czasie elektroporacji wzmaga zmiany morfologii komórek. Ekspozycja na nanosekundowe impulsy elektryczne zmniejsza mobilność komórek nowotworu prostaty. Efekt ten jest niezależny od częstotliwości impulsów oraz od stężenia zewnątrzkomórkowego Ca^{2+}.

7.3 Wnioski

1. Krótkie impulsy elektryczne wykazały wysoką skuteczność cytotoksyczną na komórki raka gruczołu krokowego i mogą być potencjalnie wykorzystane w terapii fokalnej. Elektroporacja z jonami wapnia zwiększa cytotoksyczność terapii zarówno przy zastosowaniu nano- jak i mikrosekundowych impulsów.

2. Permeabilizacja komórek może być kontrolowana przez natężenie pola elektrycznego, jak również przez częstotliwość impulsów nanosekundowych. Nanosekundowe impulsy o częstotliwości 1 MHz wykazały wyraźnie zwiększoną cytotoksyczność w porównaniu do impulsów w niższych częstotliwościach. MHz-owa kompresja impulsów ujawniła także inną dynamikę napływu jonów wapnia po permeabilizacji. Badania potwierdzają odmienność i wyjątkową efektywność impulsów nanosekundowych o bardzo wysokich częstotliwościach.

3. Zmniejszona mobilność komórek nowotworowych po terapii ilustruje potencjał krótkich impulsów elektrycznych w zmniejszeniu ryzyka lub zapobieganiu przerzutom raka stercza. Korelacja pomiędzy zmianami w cytoszkielecie spowodowanymi przez impulsy elektryczne, a zmniejszoną mobilnością nie została jednak potwierdzona. Wnioskując, wpływ elektroporacji na mobilność komórek nie wynika jedynie z oddziaływania impulsów elektrycznych na strukturę cytoszkieletu.

4. Mechanizm śmierci komórek wywołanej impulsami elektrycznymi różni się w zależności od długości impulsu oraz obecności jonów wapnia w płynie zewnątrzkomórkowym. Elektroporacja impulsami nano- lub mikrosekundowymi bez jonów wapnia wywołuje apoptozę komórek raka prostaty. Jeżeli komórki są eksponowane na impulsy w buforze ze zwiększonym stężeniem jonów wapnia, mechanizm ich śmierci zależy od długości impulsu.

5. Badania potwierdzają obiecujące efekty krótkich impulsów elektrycznych na komórki raka gruczołu krokowego. Metoda ta może zapewnić skuteczniejszą ablację, doszczętność i tym samym zmniejszenie ryzyka nawrotów miejscowych. Dalsza przedkliniczna ewaluacja tej technologii powinna obejmować badania *in vivo*.

8. Piśmiennictwo

1. Sung H, Ferlay J, Siegel RL, Laversanne M, Soerjomataram I, Jemal A, et al. Global Cancer Statistics 2020 : GLOBOCAN Estimates of Incidence and Mortality Worldwide for 36 Cancers in 185 Countries. CA CANCER J CLIN. 2021;71(3):209–49.

2. Bell KJL, Mar C Del, Wright G, Dickinson J, Glasziou P. Prevalence of incidental prostate cancer : A systematic review of autopsy studies. Int J Cancer. 2015;137:1749–57.

3. Rawla P. Epidemiology of Prostate Cancer. World J Oncol. 2019;10(2):63–89.

4. Droz J, Balducci L, Bolla M, Emberton M, Fitzpatrick JM, Joniau S, et al. Menagement of prostate cancer in recommendations of a working group of the International Society of Geriatric Oncology. BJU Int. 2010;106:462–9.

5. Kurhanewicz J, Vigneron D, Carroll P, Coakley F. Multiparametric magnetic resonance imaging in prostate cancer : present and future. Curr Opin Urol. 2008;18:71–77.

6. Loeba S, Bjurlina M, Nicholsonb J, Tammelac TL, Pensond D, Cartere HB, et al. Overdiagnosis and Overtreatment of Prostate Cancer. Eur Urol. 2014;65(6):1046–55.

7. Donaldson IA, Alonzi R, Barratt D, Barret E, Berge V, Bott S, et al. Focal Therapy: Patients, Interventions, and Outcomes — A Report from a Consensus Meeting. Eur Urol. 2015;67:771–7.

8. Neumann E, Rosenheck K. Permeability Changes Induced by Electric Impulses in Vesicular Membranes. J Membr Biol. 1972;10:279–90.

9. Sale JH, Hamilton WA. Effects of high electric fields on micro-organisms III. Lysis of erythrocytes and protoplasts. Biochim Biophys Acta. 1968;163:37–43.

10. Teissie J, Marie-Pierre R. An Experimental Evaluation of the Critical Potential Difference. Biophys J Vol. 1993;65:409–13.

11. Brock RM, Beitel-white N, Davalos R V, Allen IC, Allen IC. Starting a Fire Without Flame : The Induction of Cell Death and Inflammation in Electroporation-Based Tumor Ablation Strategies. Front Oncol. 2020;10(July):1–9.

12. Mir LM, Orlowski S, Jr JB, Paoletti C. Electrochemotherapy Potentiation of Antitumour Effect of Bleomycin by Local Electric Pulses. Eur J Cancer. 1991;27(I):68–72.

13. Titomirov A V., Sukharev S, Kistanova E. In vivo electroporation and stable transformation of skin cells of newborn mice by plasmid DNA. BBA - Gene Struct Expr. 1991;1088(1):131–4.

14. Miklavcic D, Pavselj N. Electric Properties of Tissues. In: Wiley Encyclopedia of Biomedical Engineering. 2006. p. 1–12.

15. Selma C, Zupanic A, Kranjc S, Sakere B Al, Miklavcic D, Leroy-Willig A, et al. The influence of skeletal muscle anisotropy on electroporation : in vivo study and numerical modeling. Med Biol Eng Comput. 2010;48:637–48.

16. Vroomen LGPH, Scheffer HJ, Melenhorst MCAM. MR and CT imaging characteristics and ablation zone volumetry of locally advanced pancreatic cancer treated with irreversible electroporation. Eur Radiol. 2017;27:2521–31.

17. Neal II RE, Cheung W, Kavnoudias H, Thomson KR. Spectrum of imaging and characteristics for liver tumors treated with irreversible electroporation. J Biomed Sci Eng. 2012;5:813–8.

18. Kranjc M, Kranjc S, Bajd F, Serša G, Serša I, Miklavčič D. Predicting irreversible electroporation-induced tissue damage by means of magnetic resonance electrical impedance tomography. Sci Rep. 2017;7(10323):1–10.

19. Davalos R V, Mir LM, Rubinsky B. Tissue Ablation with Irreversible Electroporation. Ann Biomed Eng. 2005;33(2):223–31.

20. Onik G, Mikus P, Rubinsky B. Irreversible Electroporation : Implications for Prostate Ablation. Technol Cancer Res Treat. 2007;6(4):295–300.

21. Blazevski A, Scheltema MJ, Amin A, Thompson J, Lawrentschuk N, Stricker PD. Irreversible electroporation (IRE): a narrative review of the development of IRE from the laboratory to a prostate cancer tratment. BJU Int. 2019;120(3):1–28.

22. Frandsen SK, Vissing M, Gehl J. A Comprehensive Review of Calcium Electroporation — A Novel Cancer Treatment Modality. Cancers (Basel). 2020;12(290):1–20.

23. Frandsen SK, Gissel H, Hojman P, Tramm T, Eriksen J, Gehl J. Direct Therapeutic Applications of Calcium Electroporation to Effectively Induce Tumor Necrosis. Cancer Res. 2012;72(6):1336–42.

24. Clapham DE. Calcium Signaling. Cell. 2007;131:1047–58.

25. Furuya Y, Lundmo P, Short D, Gill L, Isaacs T. The Role of Calcium, pH, and Cell Proliferation in the Programmed (Apoptotic) Death of Androgen-independent Prostatic Cancer Cells Induced by Thapsigargin. Cancer Res. 1994;54:6167–75.

26. Nielsen K, Scheffer HJ, Vieveen JM, Tilborg AAJM Van, Meijer S, Kuijk C Van, et al. Anaesthetic management during open and percutaneous irreversible electroporation. Br J Anaesth. 2014;113(6):985–92.

27. Deodhar A, Dickfeld T, Single GW, Raymond H, Sofocleous CT, Maybody M, et al. Irreversible Electroporation Near the Heart: Ventricular Arrhythmias Can Be Prevented With ECG Synchronization. AJR Am J Roentgenol. 2011;196(3):1–16.

28. Schoenbach KH, Beebe SJ, Buescher ES. Intracellular Effect of Ultrashort Electrical Pulses. Bioelectromagnetics. 2001;448:440–8.

29. Tekle E, Oubrahim H, Dzekunov SM, Kolb JF, Chock PB. Selective Field Effects on Intracellular Vacuoles and Vesicle Membranes with Nanosecond Electric Pulses. Biophys J [Internet]. 2005;89(1):274–84.

30. Beebe SJ, Chen Y, Sain NM, Schoenbach KH, Xiao S. Transient Features in Nanosecond Pulsed Electric Fields Differentially Modulate Mitochondria and Viability. PLoS One. 2012;7(12):1–8.

31. Bowman AM, Nesin OM, Pakhomova ON, Pakhomov AG. Analysis of Plasma Membrane Integrity by Fluorescent Detection of Tl+ Uptake. J Membr Biol. 2010;236(1):15–26.

9. Informacja o źródłach finasowania badań

Projekty badawcze wchodzące w skład pracy doktorskiej były finansowane przez:

10. Artykuły z cyklu publikacji w formie załączników

Praca nr 1

<u>Tytuł</u>

Electroporation-Based Treatments in Urology

<u>Autorzy</u>

Kiełbik, A., Szlasa, W., Saczko, J., & Kulbacka, J.

<u>Czasopismo</u>

Cancers (2020, Vol:12; Issue: 8; pages: 2208; DOI: 10.3390/cancers12082208)

<u>Punktacja</u>

IF: 6.639, Pkt. MNiSW: 140

Electroporation-Based Treatments in Urology

Aleksander Kiełbik [1], Wojciech Szlasa [1] ![ID], Jolanta Saczko [2] ![ID] and Julita Kulbacka [2],* ![ID]

[1] Faculty of Medicine, Wroclaw Medical University, 50-367 Wroclaw, Poland;
    aleksander.kielbik@outlook.com (A.K.); wojciech.szlasa@outlook.com (W.S.)
[2] Department of Molecular and Cellular Biology, Wroclaw Medical University, 50-556 Wroclaw, Poland;
    jolanta.saczko@umed.wroc.pl
*   Correspondence: julita.kulbacka@umed.wroc.pl; Tel.: +48-71-784-0688

Abstract: The observation that an application of a pulsed electric field (PEF) resulted in an increased permeability of the cell membrane has led to the discovery of the phenomenon called electroporation (EP). Depending on the parameters of the electric current and cell features, electroporation can be either reversible or irreversible. The irreversible electroporation (IRE) found its use in urology as a non-thermal ablative method of prostate and renal cancer. As its mechanism is based on the permeabilization of cell membrane phospholipids, IRE (as well as other treatments based on EP) provides selectivity sparing extracellular proteins and matrix. Reversible EP enables the transfer of genes, drugs, and small exogenous proteins. In clinical practice, reversible EP can locally increase the uptake of cytotoxic drugs such as cisplatin and bleomycin. This approach is known as electrochemotherapy (ECT). Few in vivo and in vitro trials of ECT have been performed on urological cancers. EP provides the possibility of transmission of genes across the cell membrane. As the protocols of gene electrotransfer (GET) over the last few years have improved, EP has become a well-known technique for non-viral cell transfection. GET involves DNA transfection directly to the cancer or the host skin and muscle tissue. Among urological cancers, the GET of several plasmids encoding prostate cancer antigens has been investigated in clinical trials. This review brings into discussion the underlying mechanism of EP and an overview of the latest progress and development perspectives of EP-based treatments in urology.

Keywords: ablation techniques; electrochemotherapy; electroporation; gene therapy; prostate cancer

1. Introduction

The prevalence of kidney, prostate, and bladder cancer is increasing rapidly within the context of an ageing population [1]. Urological cancers are generally regarded as a problem predominantly concerning wealthier countries. However, risk factors such as tobacco smoking, diet, and lifestyle inevitably lead to increased prevalence among lower-income populations [1]. Easily available, safe, and economical therapies must be developed to reduce the degree of inequality in terms of incident cases and deaths due to urological cancers. The technique known as electroporation provides the possibility for efficient focal ablation, intracellular delivery of cytostatics or other molecules such as calcium, and safe gene transfection. In its simplicity, no sophisticated equipment is required, except a pulse generator and an electrode.

The present development of sensitive methods of imaging, such as multiparametric magnetic resonance imaging (mpMRI), enables precise tumor localization, biopsy guidance, and focal therapy [2]. It is estimated that one-third of patients with mpMRI-detected and biopsy-proven lesions in the prostate gland are potential candidates for focal treatment [3]. For this group of patients, methods based on electroporation, irreversible electroporation (IRE), or electrochemotherapy (ECT) constitute possible choices of treatment.

With the increasing importance of immune therapy, new gene delivery techniques are being developed at a very fast pace. Among viral and non-viral approaches, gene electrotransfer (GET) is characterized by a high safety profile, acceptable efficiency, availability, and ease of application [4]. In vivo trials of anti-tumor therapy for urological cancers have already proven their efficacy.

There are few publications dedicated to physicians describing the more detailed mechanism of electroporation and the possibilities of its applications in urology. It should not be neglected that a few vulnerabilities of electroporation (EP) still require new solutions and need to be optimized. The underlying mechanisms should be discussed more frequently to increase awareness of physicians applying this method in the clinic and to illustrate its potential for future development.

2. The Theoretical Background of EP

Physiologically all human cells possess a resting voltage on their plasma membrane ranging from −70 mV to −30 mV, which is generally provided by Na^+ and K^+ active and passive transport through the membrane [5]. The foundation of the EP was the observation that cells exposed to an external electric field change the properties of their membranes and become more permeable [6,7]. Once the cell is exposed to an external electric field, an additional component of the voltage across the membrane occurs [8]. The induced transmembrane voltage for a spherical cell with a nonconductive membrane can be calculated with Laplace's Equation (1):

$$\Delta\Phi\text{m} = \frac{3}{2}ER\cos\theta \tag{1}$$

where E is the electric field in the region of a cell, R is cell radius, and θ is the angle measured from the center of the cell to the direction of the field [8].

When the transmembrane potential reaches 200–250 mV, parts of the membrane become highly permeable [9,10]. Permeabilization is a local process, and the fraction of the permeabilized membrane strongly correlates with the electric field intensity [11,12]. The organization of the membranes permeable spots is inhomogeneous [12].

To permeabilize the cell membrane, usually, a series of electrical rectangular pulses are applied [13]. Depending on the pulse duration, there could be distinguished nanosecond, microsecond, or millisecond electroporation protocols [14]. Today, microsecond pulses find clinical application in IRE for the ablation therapy of prostate cancer [15]. The use of microsecond electric pulse in IRE for other urological tumors, such as kidney cancer (NCT01967407, NCT02828709, NCT02298608) and urinary bladder neoplasm (NCT02430623), is continually being tested in clinical trials. Further considering urological tumors, nanosecond electric pulses are studied only at the in vitro level [16].

The precise molecular mechanism of EP is not fully understood. However, some properties of pulsed electric fields (PEFs), as well as cell features affecting the electropermeabilization, remain defined. The influence of the external electric field on the transmembrane voltage varies depending on the shape of the cells. The position and orientation of cells to the electric field also determines the transmembrane voltage [17]. The density of defects in the cell membrane depend on pulse duration and number of pulses [12,13,18].

The following three modalities of electric-field-aided treatment methods can be distinguished: irreversible electroporation, electrochemotherapy and gene electrotransfer. Each of them is based on the use of a pulsed electric field which induces changes in the membranes of the target cells, making them more permeable. However, each technique differs in mechanism of action, uses different parameters of the electric field, and has varied aims of application in the clinical setting. This will be continually expanded upon and described in the following sections.

The process of electroporation is complex and should not be simplified only to the phenomenon of permeabilizing the cell membrane. The electrical field affect cell permeability and also generates a transient mechanical force that stretches the spherical membrane [19]. EP may lead to cytoskeleton destabilization and changes in membrane elasticity [20]. It was observed that electrical pulses generate

reactive oxygen species at the permeabilized loci [21]. However, Michel et al. proved that even if reactive oxygen species appear, their presence does not induce membrane permeabilization [22]. Electropermeabilization is followed by water flux and, consequently, by the osmotic swelling of cells [23]. When the cellular membrane becomes permeable, the leakage of metabolites such as ATP from the cytoplasm can be observed [24]. The intracellular ATP content is strongly related to the viability of the cells after electropermeabilization [25].

After permeabilization, the transfer of molecules such as drugs or even the insertion of exogenous proteins into the cell interior is possible [26,27]. The transfer of small molecules across the permeabilized membrane is driven by two factors—mainly by the concentration gradient across the membrane, but also by the post-pulse transmembrane potential [28]. EP enables the molecules to flow for seconds and up to a few minutes after the pulse [18]. The persistence of cells permeable state depends on the pulse duration and the number of pulses applied [29]. When applied PEFs do not overcome the irreversible electroporation threshold, the resealing of the cell membrane occurs [30–32]. The process engages multiple mechanisms. It was proven that cellular proteins and parallel the processes of endo and exocytosis contribute to cell membrane repair [33].

Generally, electroporation of tissue due to their inhomogeneity and anisotropy is difficult to foresee [34]. In electroporation, tissues should be considered as an insulator and conductor [35]. A few basic physical terms need to be reminded to clarify the dielectric properties of tissues. Permittivity is the measure of the capacitance of the material to store an electric field in the polarization of the medium. Conductivity is a measure of the ability of the material to conduct an electric current. Impedance is a measure of the opposition to the electric current in an electric circuit.

Conductivity and permittivity of tissues depend on the frequency of the applied electric pulses. Therefore, the tissue permittivity decreases in higher frequencies, and the conductivity increases. As the cell membrane becomes permeabilized, it increases its conductance [36]. The local changes in the electric field should be taken into account during individualized, patient-specific treatment planning [37]. It was observed that tumors are characterized by higher conductivity in comparison to normal tissues, probably due to regions of necrosis [38]. The phenomenon that the conductivity increases with electroporation enables it to effectively electroporate deeper structures of the tissue using lower voltages [39]. By measuring the electric conductivity changes in tissues, the cell permeabilization threshold can be estimated [40].

Controlling the real-time changes of the tissue impedance by the use of electrical impedance tomography (EIT) enables users to estimate the electroporated area [41]. Electrodes detect the changes in impedance caused by electropermeabilization. Subsequently, the obtained data is being transformed into the image of the electroporated area. Another technology—magnetic resonance electrical impedance tomography (MREIT)—combines EIT and magnetic resonance imaging (MRI). MREIT algorithms transfer the MRI image to digitally reconstruct the conductivity distribution inside the tissue. In contrast to EIT, it avoids the implementation of additional electrodes. In vivo and ex vivo research shows that MREIT can be applied in clinical electroporation-based procedures to improve the security of therapies [42,43]. In the future, we can expect the introduction of this technology in clinical settings.

As tissues are diverse and anisotropic, they possess distinct conduction properties [44]. Various tissues are characterized by a different proportion of the extracellular matrix, different water content, and irregular vascularization [35]. Inhomogeneity of conduction depends on the placement of the electrodes with respect to the major axis of tissue. If the tissue is organized in fibers, the detectable discrepancy of the longitudinal and transverse conductivity may occur [34]. In the longitudinal orientation of electrodes, the electricity is directed by cells organized in fibers, whereas in the transverse orientation, the charge has to overcome an extracellular matrix, which is less conductive than cells [35].

The pre-treatment computer simulation is helpful to plan the therapy, optimize pulse parameters, choose appropriate electrodes, and determinate their placement inside the tissue. Numerical modeling can be applied to predict the electric field distribution in inhomogeneous biological tissues.

The simulation enables clinicians to visualize the electric field density in the targeted region and to determinate the range of irreversible and reversible electroporation and to determine the temperature rise occurring due to Joule heating [45].

3. IRE

Davalos et al. showed that the application of PEFs promoting irreversible defects in the cellular lipid bilayer could be applied as a novel ablation method [46]. In contrast to other thermal tumor ablation possibilities such as microwave ablation, high-intensity focused ultrasound, or cryoablation, IRE is based on electropermeabilization and thus causes no excessive thermal effect [47] (Figure 1).
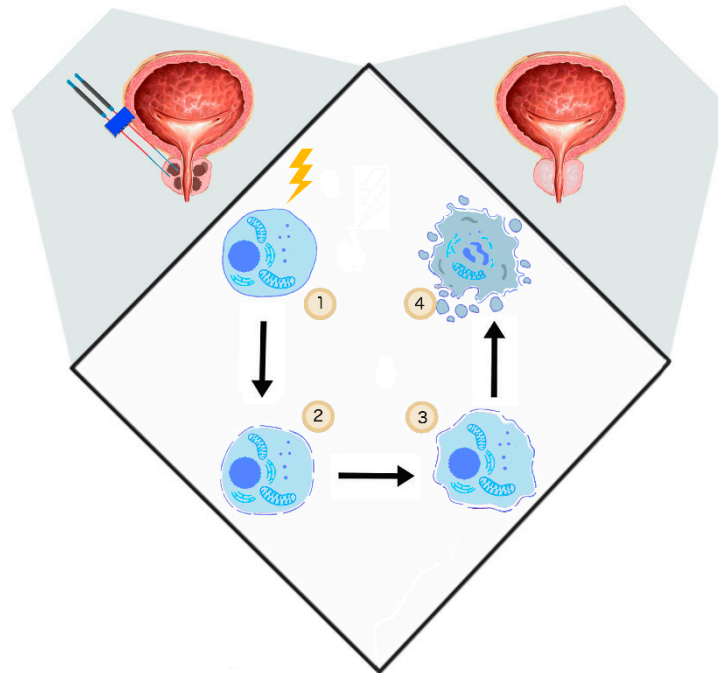

Figure 1. The general mechanism of irreversible electroporation (IRE). (1) Delivery of short electrical impulses (10–90 impulses 1000–2500 V/cm, 50–100 μs) [48], (2) cancer cell permeabilization, (3) irreversible permeabilization results in osmotic swelling [23], cytoskeleton destabilization [20], ATP depletion [24], (4) cell turns necrotic [46].

If the electric field strength is too far above the permeabilization threshold value, the permeabilized state is irreversible and results in cell destruction [46]. IRE does not require the application of chemotherapeutic agents. Several experiments investigated the specificity of IRE. It was shown that even if IRE has the potential to affect the nerves, the axonal regeneration process occurred two months after the procedure [49]. Another study on prostate gland ablation confirmed the preservation of the urethral wall, nerves, and vessels [15]. With optimal electric field parameters, IRE predominantly affects cell membrane phospholipids. Extracellular proteins, and the cell matrix are usually not affected [50].

Usually, the transmembrane potential of 1 V is sufficient to generate irreversible electroporation [46]. IRE is considered to be a non-thermal ablative method. However, the thermal effect occurs due to Joule heating and cannot be neglected. The amount of heat released is proportional to the electrode spacing and diameter and depends on repetition frequency [51]. Electrode configuration, the distance between electrodes, and the active tip length are the other factors that influence the IRE ablation zone. However, those features can be modulated during the procedure [52]. Due to the complexity of in vivo IRE procedure, pulse parameters have been established mainly experimentally. In in vivo studies, the electric field between 1000 V/cm and 2500 V/cm has been applied for IRE of the tumor. In most of the trials, the pulse durations ranged from 50 μs to 100 μs, and the pulse number varied between 10 and 90 [48].

Although IRE presents many advantages compared to other focal thermal ablation methods, there are a few issues that limit it in its clinical use. The successive ablation requires precise and parallel placement of multiple electrodes to optimize the ablation zone. IRE parameters should be personalized, since when adequately adjusted, can limit the damage caused by heat and extend the tissue ablation zone [46]. IRE is known to be minimally invasive. Nevertheless, it still requires general anesthesia and complete muscle relaxation [53]. Muscle contraction during the delivery of impulses can displace electrodes [54]. Moreover, to avoid cardiac arrhythmias, the electrical pulses need to be introduced during the refractory phase, and as a consequence, the electrode device should be synchronized with electrocardiography (ECG) [55].

In clinical practice, four different types of electrodes are used for IRE: needle, catheter, plate, and clamp. They can be applied percutaneously or intraoperatively. The endoscopic approaches for IRE ablations are currently still under development [56]. Furthermore, the endovascular IRE has been investigated for vascular smooth muscle cells. This minimally invasive method is used for creating a suitable niche for exogenous cell engraftment in regenerative surgery [57,58].

CT, MRI, and ultrasounds are often used for electroporation imaging. However, those methods cannot precisely estimate the electroporated area during the delivery of impulses [59–61]. The real-time imaging can be achieved by MREIT, which is a novel method was shortly described above.

3.1. IRE—Renal Cancer

Minimal invasive local ablation of renal cancer is an alternative treatment option for small tumors by patients who are not qualified or refuse to undergo surgery.

The effect of IRE on the porcine model was studied to investigate the histopathologic effect of renal cancer. Acute lesions, assessed 24 h after the procedure, were characterized by hemorrhagic necrosis. Three weeks after the procedure, tubules and glomeruli in the ablation zones were replaced by fibrous tissue. The extracellular matrix and transitional epithelium of the ablated pelvis generally remained intact, suggesting pelvic epithelium regeneration [62]. Urothelial regeneration was also observed in another study. MRI and intravenous urography confirmed the IRE sparring effect on renal calyxes, pelvis, and ureter [63].

The clinical study on patients with renal tumors confirmed the feasibility, safety, and efficacy of IRE as a focal ablation method [64,65]. The present clinical experience was summarized in Table 1. The procedure was performed percutaneously under general anesthesia and muscle relaxation. No significant changes in renal function were described after IRE performance. The mean procedural time was 2.1 h, including the need for general anesthesia; this might be considered as a disadvantage of IRE [64]. The post IRE imaging of the ablation zone showed similar characteristics to the marks observed after radiofrequency ablation and cryoablation [65].

Table 1. Clinical trials of IRE for small renal masses.

Type of Trial	Patients Number	Short Description	Study Outcome	Renal Function	Complications	Therapy Protocol	Ref.
Retrospective	20	IRE for focal treatment of cT1a renal cancer	initial treatment success rate of 90% (18/20). 17% (1/6) recurrence rate during a one-year follow-up	no significant differences in creatinine levels before and 6 weeks after IRE	3/20 urinary retention, 2/20 perinephric hematomas, 2/20 patients suffered from pain	3–4 electrodes, for tumors over 2.5 cm, multiple probes, 30–40 A, pulse duration 100 μs at 1 Hz, 140 pulses with electrode polarity change after 70 pulses	Trimmer et al. [65]
Prospective	42	IRE for focal treatment of cT1a renal cancer	initial treatment success rate of 93% (39/42), 83% 2-year local recurrence-free survival rate	pre and post-operative glomerular filtration rate of patients did not differ significantly	2/42 urinary retention, 4/42 perinephric hematomas, 1/42 patient suffered from pain	3–4 electrodes, for tumors over 2.5 cm, multiple probes 2000 V/cm, 100 μs at 1 Hz, 140 pulses with electrode polarity change after 70 pulses	Canvasser et al. [66]
Prospective	10	IRE for focal treatment of cT1a renal cancer	10% (1/10) recurrence rate during 6 months of follow-up	no significant differences in creatinine levels in pre-IRE tests and 1 week, 3 months, 6 months, and 12 months post-IRE tests	1/10 perinephric hematoma and pyelonephritis with fever, 1/10 blood clot in the ureter, 1/10 painful micturition, 1/10 hematuria	6 electrodes, active tip exposure 10–25 mm, 20–40 A, 100 pulses, 90 μs	Mara et al. [64]

The present European Association of Urology guidelines based on the low-quality study suggests a higher local recurrence rate for thermal ablation therapies compared to partial nephrectomy. However, simultaneously due to guidelines the focal therapy should be offered to frail and/or comorbid patients with small renal masses [67]. The new focal therapies, such as electroporation, should be developed to provide minimal-invasive treatment, suitable for comorbid patients, with the oncological outcome comparable to partial nephrectomy.

For renal cancer ablation techniques, such as radiofrequency ablation, cryoablation, and microwave ablation, are the most common techniques used [68]. However, due to the heatsink effect, their effectiveness is restricted once the targeted area is in the vicinity of blood vessels [69]. In contrary to mentioned methods, IRE is based on the permeabilization of the cell membrane, which results in cell death. It enables the treatment of tumors near critical structures with the preservation of healthy renal parenchyma and subsequent urothelial regeneration. However, to determine the oncological and functional outcome of IRE on renal cancer, more prospective studies with longer follow-up are required.

3.2. IRE—Prostate Cancer

For prostate cancer treatment, IRE has been applied for focal therapy or, in case of a spreading tumor, for the whole gland ablation. Moreover, one published clinical trial concerns IRE for recurrent cancer after radiotherapy. The present experience from chosen studies, including the oncological and functional outcome, was summarized in Table 2. Due to expert consensus, patients with intermediate-risk and unifocal or multifocal prostate cancer are the potential candidates for focal treatment [70]. In the case of prostate cancer, IRE electrodes are usually transperineally inserted under the guidance of ultrasound [71].

Ablate and resect studies investigated the histopathological outcome of the therapy four weeks after the IRE procedure. The analysis showed that the ablation resulted in a sharply demarcated, necrotic, and fibrotic area of prostate tissue. The contralateral nerve bundles, as well as nerve bundles outside the ablation area, remained untouched. Urothelium impairment of prostatic urethra occurred in 9/16 patients after IRE. Short-term follow-ups have been unable to assess the possible recovery process [72].

Table 2. Clinical trials of IRE, electrochemotherapy (ECT), and gene electrotransfer (GET) for prostate cancer.

Therapy	Type of Trial	Patients Number	Short Description	Urinary Continence	Erectile Function	Study Outcome	Therapy Protocol	Ref.
IRE	Retrospective	429	IRE for focally (123), sub-whole-gland (154), whole-gland (134) or for recurrent prostate cancer (63) after previous radical prostatectomy or radiation therapy,	IPSS-Score (urinary symptoms)- 72.8% of patients with no change or improvement; 27.2% with a decrease during the follow-up period (about 12 months)	IIEF-5 score–14/124 (11.3%) patients developed erectile dysfunction after IRE in 4/124 (3%) patients dysfunction persisted longer than one year	47/429 (10.9%) of patients with prostate cancer recurrence in 72 months follow-up (27/429 in-field and 20/429 out-of-field recurrence)	5 ± 1 electrodes; 1518.13 ± 204.05 V/cm	Guenther et al. [73]
IRE	Prospective	123	IRE for prostate gland ablation as a primary procedure; largest reported cohort of patients treated with IRE.	80/81 (98.8%) patients remained pad free and 70/75 (93.3%) remained leak-free at 12 months after treatment.	40/53 (76%) patients with normal erectile function, 9/53 (17%) with decreased, but enough for sexual activity, and 4/53 (7%) with total erectile dysfunction 12 months after treatment	23/102 (22.5%) of patients with prostate cancer recurrence 12 months after treatment (10/102 (9.8%) in-field recurrence. 13/102 (12.7%) out-of-field recurrence)	90 pulses; 1500 V/cm; 70 μs or 90 μs; 5 mm distance from vital structures; safety margin of 5 mm to 10 mm from the targeted area;	Blazevski et al. [74]
IRE (H-FIRE)	Prospective	40	H-FIRE for prostate gland ablation, as a primary procedure 8/40 patients underwent prostatectomy four weeks after treatment	40/40 (100%) patients remained pad free	14/14 (100%) patients with normal erectile function	high-frequency bipolar pulses can be safely applied for IRE of prostate cancer; oncological outcome was not evaluated	HF bipolar pulses; 250 bursts; 50 pulses in one burst; 1 burst/second; 10-s inter-burst delay; 2–6 needle electrodes; interelectrode distance <20 mm	Dong et al. [75]
IRE	Prospective	18	IRE for localized radio-recurrent prostate cancer,	8/11 (72.2%) of patients remained pad-free at six months; 10/11 (90.9%) pad-free at 12 months	2/6 (33.3%) patients with normal erectile function 6 months after treatment and 2/4 (50%) patients with normal erectile function 12 months after treatment (One patient recovered at 12 months from erectile dysfunction); a significant decrease in EPIC sexual score between baseline and six months	2/10 (20%) of patients with prostate cancer recurrence 12 months after treatment (1/10 (10%) in-field recurrence and 1/10 (10%) out-of-field recurrence)	90 pulses; 1500 V/cm; pulse; 70 μs or 90 μs; safety margin of 5 mm to 10 mm from the targeted area; active tip length 10–20 mm; interelectrode distance 7–19 mm	Scheltema et al. [76]
IRE	Prospective	63	IRE for prostate gland ablation, as a primary procedure	44/45 (98%) of patients remained pad-free at 6 months 45/45 (100%) pad-free at 12 months.	8/26 (31%) patients with erectile dysfunction at 6 months after IRE and 3/13 (23%) with erectile dysfunction 12 months after IRE.; the significant difference in EPIC sexual score between baseline and 6 months after IRE	11/48 (22.9%) of patients with prostate cancer recurrence 12 months after treatment (7/48 (14.6%) in-field recurrence and 4/48 (8.3%) out-of-field recurrence)	90 pulses; 1500 V/cm; 70 μs or 90 μs; safety margins of 5 mm or 10 mm from the targeted area; 5 mm distance from vital structures	Van Den Bos et al. [77]

Table 2. *Cont.*

Therapy	Type of Trial	Patients Number	Short Description	Urinary Continence	Erectile Function	Study Outcome	Therapy Protocol	Ref.
ECT	Case report	1	ECT for recurrence of prostate cancer by a 67-year-old patient	IPSS—no significant impairment after six months (remaining mild incontinence)	IIEF-5 score restored to the pretreatment level six months after ECT (remaining mild erectile dysfunction)	MRI six months after the treatment, showed no evidence of tumor persistence	8 min before electroporation administration of 29 mg of bleomycin i.v.; eight pulses; 100 µs; 4 Hz frequency; 1642 ± 812 V	Klein et al. [78]
GET	Prospective, two-arm	30	Patients with, biochemically recurrent prostate cancer (rising PSA but no radiological evidence of disease) received an intramuscular injection of DNA encoding PSMA+DOM C or injection followed by EP	Not evaluated	Not evaluated	Vaccination alone and with EP was well tolerated; vaccination alone showed 1.7 increase of anti-DOM IgG; vaccination with EP showed a 24.5-fold increase of anti-DOM IgG compering to baseline; responses persisted up to 18 months of follow-up	Vaccinations were administered at 0, 4, and 8 weeks, with booster doses at 24 and 48 weeks; EP was performed by two needles, which after injection served as electrodes; five pulses; 20 µs; 8.3 Hz frequency; 8 mm intra-needle distance	Low et al. [79]
GET	Prospective	15	Patients with biochemically recurrent prostate cancer without macroscopic disease received an intradermal injection of DNA encoding PSA followed by EP	Not evaluated	Not evaluated	Intradermal vaccination with skin EP is feasible; only minor discomfort occurred; vaccination with EP enhanced pre-existing or boosted PSA-specific immunity	Vaccination was administered every four weeks for five months; EP was applied immediately after each injection with two parallel rows of needles (6 needles/row); 10 pulses: 2 (1125 V/cm; 0.05 µs) and 8 (275 V/cm; 10 µs)	Eriksson et al. [80]

The clinical study of IRE reported low-grade urinary complaints. The most frequent were painful micturition and occasional incontinence, thus pads were temporarily applied to the few patients that required them. The transperineal approach resulted in a small perineal swelling, inguinal lymphadenopathy, and temporarily swollen testis. However, pain in the lower abdomen occurred without evidence of a urinary tract infection. All complications emerged during the first week after the procedure, and nearly all disappeared between the first and fourth weeks after IRE [81]. In the largest study, only a mild decrease in sexual function was observed. Among patients who were potent before treatment, 76% (40/53) did not exhibit any change in erectile function [74].

After the treatment, cancer may progress due to in-field recurrence, when the tumor is present in the ablation zone, and out-of-field recurrence from the progression of contralateral prostate gland lesions. The largest prospective studies of IRE on prostate cancer confirm that the extension of treatment margin decreases the in-field recurrence rate. Twelve months after the procedure, the in-field recurrence appeared in 9.8% (10/102) of patients. However, among the group where treatment margins were extended to 10 mm, the in-field recurrence was 2.7% (2/74). Extended ablation did not show any significant impact on out-of-field recurrence (12.1%) (9/74) [74]. The study indicates that more precise identification of patients with multifocal disease is required to reduce out-of-field recurrence. That group would benefit from whole gland ablation. $_{68}$Ga-PSMA PET fused with mpMR might provide the solution as it enables more accurate cancer detection [71].

The common danger for low-risk and arguably for intermediate-risk localized prostate cancer is overtreatment [82]. Prostatectomy and radiotherapy, although constantly developing, still involve serious risk of impotence and urine incontinence [83–85]. In careful risk stratification, better algorithms are required to determine the groups, which would benefit from focal treatment. With the development of imaging methods such as mpMRI, the use of minimal invasive focal treatments in prostate treatment will increase. Among the available approaches, high-intensity focused ultrasounds, cryotherapeutic ablation, or photodynamic therapy are the most investigated, but the data is still not sufficient to consider them as the first-line therapy. Today, electroporation for prostate cancer treatment is mainly offered within a clinical trial setting, but the therapy is rapidly developing, and treatment protocols are being enhanced. IRE, compared to other thermal ablative methods, may provide better preservation and regeneration possibilities of the urethra and neurovascular bundle. However, present studies cannot confirm this. No long-term follow-up in published studies preclude the evaluation of the exact oncological outcome. Other major deficits in the literature are the lack of the prospective randomized trial comparing IRE for prostate cancer treatment to other longer and better-investigated techniques such as high-intensity focused ultrasounds, cryotherapeutic ablation, photodynamic therapy, or radical prostatectomy. Nevertheless, for intermediate-risk prostate cancer, evaluation of the oncological outcome would require about 15 years of follow-up [71].

3.3. IRE—Urothelial Cancer

The development of a catheter electrode provides the possibility of intraluminal IRE. The feasibility study for the treatment of urothelial cancers was performed on the porcine model. The catheter-directed ablation showed the necrosis of urothelium, lamina propria, muscularis, and adventitia. However, the extracellular matrix of connective tissue remained untouched, preserving urethral integrity [86]. Short 28 day follow-up do not provide any information on the long-term situation [87]. One on-going clinical trial investigates the effect of IRE for unresectable urinary bladder cancer (NCT02430623).

3.4. High-Frequency Irreversible Electroporation

The improvement of selectivity can be provided by high frequent irreversible electroporation (H-FIRE), which uses short pulses (~1 μs). H-FIRE preferentially and proportionally to the size of the nucleus affects the cell interior. As large nuclei represent the typical feature of malignant cells, shorter pulses can more selectively target cancer cells [88]. It was also observed that H-FIRE triggers the local innate immune system and affects the tumor microenvironment promoting inflammation [89].

Moreover, H-FIRE does not cause muscle contraction. Prospectively, it might exclude intraoperative paralytics or cardiac synchronization, reducing the procedure time [90,91]. However, it was proved that H-FIRE pulses require a higher electric field to achieve the same level of cell permeabilization compared to standard monopolar pulses [91]. This phenomenon is called the cancellation effect and can be minimalized with an extension of pulse duration and interphase delay [92].

The first clinical study, which evaluated the possibility of prostate tumor ablation with H-FIRE, proved the safety for focal cancer treatment. Although several publications deny that H-FIRE causes muscle contraction, low-dose muscle relaxants were administrated before electroporation. Few patients underwent prostatectomy four weeks after the treatment. The histopathological examination revealed a well-demarcated ablation zone. The urethra, located in the ablation zone, remained intact. The examination proved its structural integrity with no evidence of necrosis in the submucosa. Sexual function and continence were preserved by all patients [75].

3.5. Immunomodulatory Effect of IRE

The immunomodulatory effect of IRE was evaluated in multiple studies. However, most of the published experimental trials concern the pancreas tumor. The major effect of IRE is a decrease of inhibitory Treg cells in the tumor microenvironment [93,94]. This effect was also observed after the application of calcium electroporation [95]. Interestingly, Beitel-White et al. presented the technology which enables the detection of a shift in Treg cell population after IRE [96]. Namely, changes in conductivity correlate with Treg cell depletion. The acquired information might influence the decision about following therapy [96]. Other studies reported the additional decrease of myeloid-derived suppressor cells in the tumor microenvironment after the performance of IRE [97]. To stimulate the immune response, lymphocytes should penetrate to the ablated sites of the tumor, and simultaneously, dendritic cells should be able to migrate and present the captured tumor antigens. The performance of IRE results in an increase of activated PD-1+ T cells in patient blood samples. IRE succeeded in boosting already existing T cell response and in its induction de novo [94]. Among lymphocytes, CD8+ and CD4+ T-cells are the main agents in anti-tumor response triggered by IRE [98,99]. Few experiments evaluated the possibility of performing IRE together with immunotherapy. The combined performance of IRE and checkpoint blockade with TLR7 stimulation resulted in a four-fold increase in IFNγ- secreting CD8+ T cells [97]. Furthermore, in another study of IRE on a murine model, an additional PD1 blockade again intensified the selective tumor infiltration by CD8+ T cells significantly prolonging the survival of mice [100]. The immunomodulatory effect of IRE can be perceived as an advantage of IRE to other ablation methods. One study compares the immunogenic effect of IRE and cryoablation. The outcome shows an enhanced infiltration of macrophages and T cells into electroporated tumor sites. A similar effect was not observed after cryoablation [101]. Among urological malignancies, the immunomodulatory effect was investigated and confirmed on murine renal tumors [102]. Considering the fast progress of immunotherapy, the application of IRE to stimulate the immune response and subsequent immunotherapy is a very promising approach. As predicted by Palucka et al., all cancers will be eventually treated with checkpoint inhibitors [103]. The application of PEFs can be utilized to boost the immune system. Nevertheless, future trials should evaluate the effectiveness of IRE and immunotherapy on urological cancers. Subsequently, the next step would be a well-designed prospective double-blind clinical study to fully confirm the efficiency of the therapy. Immunomodulatory effect of IRE raises the question of whether or not IRE could be performed before the surgery to stimulate the immune response. The study on the murine model showed the initial superiority of resection to IRE. However, after the repeated application of cancer cells, mice previously treated with IRE showed no recurrence, in contrast to mice after surgery. Furthermore, studies proved that IRE indeed triggers the vaccination effect and promotes the recognition of antigens by immune cells [97]. Beitel-White et al. suggest that surgery or other kinds of treatment in a multimodal approach should be performed at least 10 days after IRE to

enable the activation of an adaptive immune response [96]. Based on the results of these studies, it is reasonable to combine IRE, surgery, and immunotherapy in future clinical trials [97,100].

4. Electrochemotherapy

The application of the electric fields to enhance the intracellular anti-cancer drug uptake was studied and described by Mir et al. In 1991 [104]. Uptake of membrane non-permeable drugs can be locally increased when their intravenous or intratumoral administration is followed by electroporation. Clinically, in an approach commonly called electrochemotherapy, cisplatin and bleomycin are used [105]. Apart from cytostatics, intracellular uptake of calcium ions can be enhanced with electroporation as well. This novel solution showed no systemic toxicity and high efficiency in the in vitro and in vivo treatment of various cancer types [106]. In standard ECT, trains of eight 100-µs-long pulses are applied to achieve the reversible permeabilization of cells. The electroporation-mediated internalization of chemotherapeutics involves different mechanisms. During the application of PEFs, charged molecules cross the plasma membrane moved by electrophoretic forces. Subsequently, once the cell is in the permeable state, small hydrophilic molecules can enter the cell interior diffusing through the permeabilized area [107]. ECT anti-tumor effect cannot be explained only by increased uptake of cytostatics. Firstly, ECT showed high efficiency in in vivo studies as it stimulates the immune response. After the immunogenic death of electroporated cells, cancer antigens can be captured and recognized by dendritic cells and eventually increase antitumor response [108]. ECT could be considered as the adjuvant immunogen electrotransfer to peritumoral tissue [109]. The process leads to the local effects and triggers the systematic response against the metastases–abscopal effect [110]. Second, electroporation causes an increase in vessel permeability and constriction of arterioles resulting in so-called "vascular lock" [32]. The effect provides the targeted accumulation of the intravenously administrated drug [111] (Figure 2).
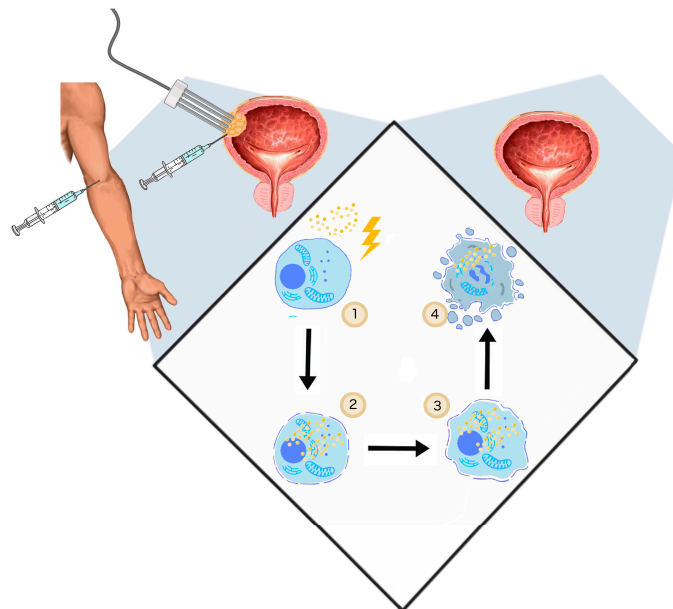

Figure 2. The general mechanism of ECT. (1) Two steps of ECT—administration of the drug (cisplatin, bleomycin) and application of PEFs (1000 V/cm, 100 µs, 9); (2) once the cell membrane gets permeabilized, the cytostatic drug penetrates to cell interior; (3) initiation of cell death by drug cytotoxicity, systemic anti-tumor reaction [108]; vasoconstriction, thus the ischemia of cancer cells [112] (4); and cell turns necrotic/apoptotic.

The data of ECT on urological cancers still remain restricted. However, with promising in vivo results, together with the technical progress of endoscopic or percutaneous approaches, the introduction of ECT in urology in the nearest future should to be expected.

4.1. ECT—Prostate Cancer

New strategies for targeted drug delivery target predominantly cancers specific antigens or use overexpressed enzymes, such as prostate-specific antigen (PSA), to enhance drug penetration [113]. The combination of drug carriers and targeting ligands, which bind to the specific antigens like prostate-specific membrane antigen (PSMA) and prostate stem cell antigen (PSCA) significantly increase the selectivity of cytostatics [114,115]. ECT is an efficient tool for selective drug delivery. However, the available data concerning prostate cancer still derives from a few experimental trials.

In vivo studies on a murine model, ECT has proved its effectiveness on prostate cancer xenografts. Bleomycin was injected into tumor sites 15 minutes before ten pulses of 500 V/cm were delivered. Bleomycin combined with ECT suppressed tumor growth, and 15 days after treatment, xenografts were not detectable [116].

One case report of ECT performed on a patient with ureter-infiltrating prostate cancer proved the feasibility of ECT in the clinic. Due to the high risk of impotence and incontinence, radiotherapy and radical prostatectomy were not feasible. Electrodes were inserted percutaneously through the perineum. The procedure was performed according to the ESOPE protocol. After six months, the MRI showed no sign of tumor persistence or lymphadenopathy. Erection and continence were preserved, indicating the effectiveness and safety of the therapy [78].

4.2. ECT—Bladder Cancer

The standard approach in non-muscle-invasive bladder cancer is transurethral resection of bladder cancer (TURB) with following the intravesical installation of cytostatics, usually mitomycin C (MMC) or epirubicin and/or intravesical Bacillus Calmette–Guérin (BCG) [67]. The therapy causes few side effects and is generally efficient for intermediate-risk patients [117]. Nevertheless, therapy failure occurs, and BCG unresponsive high-risk non-muscle-invasive tumors are associated with bad prognosis [118]. Issues such as continuous urine production and relatively short drug residence time limit the therapy effectiveness, thus leading to a higher the relapse rate [119]. There are few different approaches such as the use of hydrogels and mucoadhesive gels, which help to maintain the optimal drug concentration in the bladder [120,121]. Liposomes and nanoparticles can be applied to selectively and efficiently deliver the chemotherapeutics to the tumor site and increase the specificity of photosensitizers used in the photodynamic therapy [122]. Additionally, chemical compounds such as DMSO and hyaluronidase have been shown to upregulate the diffusion and tissue absorption of cytostatics [119]. The physical enhancement of drug delivery in the case of bladder cancer concentrates on microwave-induced hyperthermia and electromotive drug delivery. Both approaches are based on the intravesical placement of the catheter, which can either deliver microwaves to provoke the hypothermia of bladder walls or be the source of electric current, which enhance drug penetration by electrophoresis [123,124]. Although the clinical trials involving the microwave-induced hyperthermia to enhance drug delivery gave promising results, due to insufficient data, the technique is still not commonly used in clinical settings [125,126]. One clinical trial compared the effect of BCG combined with electromotive delivery of mitomycin to the BCG alone [127].

The clinical experience with ECT on bladder cancer remains restricted. One case report described the successful treatment of skin metastases of bladder cancer [128]. The other published studies investigating the in vitro and in vivo effects of ECT with bleomycin or MMC on bladder cancer cell lines and mouse bladder tumors [129–131]. Kubota et al. first presented the enhanced uptake of bleomycin in bladder tissue after application of PEFs [131]. Few studies evaluate the outcome of calcium electroporation on bladder cancer in vitro model [132,133]. The in vivo single ECT succeeded in decreasing the tumor growth rate. The further evaluation of MMC in combination with EP in the

animal studies showed an improved response to the therapy and prolonged disease-specific survival. The same research results proved the increased effectiveness of cisplatin in ECT on bladder cancer [134].

As mentioned before the combination of TURB with intravesical chemotherapy and/or BCG, although effective, is not always sufficient [135]. For this group of patients, the aim would be to avoid cystectomy, prevent local recurrence, and minimalize the risk of progression to muscle-invasive bladder cancer. Regarding experimental studies, electroporation can be potentially used as a drug delivery approach upregulating the local enhancement of cytostatics inside the bladder wall.

4.3. Gene Electrotransfer

EP provides the possibility of non-viral transmission of genes across the cell membrane. Therapeutic use of gene electrotransfer (GET) is focused mainly on two approaches—DNA vaccination and cancer gene therapy [136,137]. The first in vivo GET was carried out in 1991 by Titomirov et al. and since then various experimental attempts were made [138–142]. However, the first clinical application of GET was performed by Daud et al. In 2008 for transfer of interleukin-12 in patients with metastatic melanoma [143]. The mechanism of electroporation-driven gene transfer is a multi-step process. Once the membrane becomes permeable, the cell membrane in the regions opposite to cathode interact with the DNA [144]. The dynamics of that process depend on PEF features such as polarity, repetition, frequency, and duration [145]. It was observed that the application of nanosecond pulses in combination with microsecond or millisecond electric pulses can result in an increase in DNA transfection rate in the targeted cell [146]. DNA diffusion across the membrane takes minutes to hours [144]. The research suggests that the model of endocytosis explains the process of transport of DNA aggregates [147,148]. At first, the electric-field-independent formation of DNA-membrane complex occurs. The aggregation is size-dependent, meaning that the helices containing more than 25 base pairs (bp) aggregate, which cannot be observed for 15 bp helices [149]. The number of small DNA molecules, so-called free DNA, can be directly transported into the cytoplasm [149]. After the aggregation, electropore is formed by the application of PEF, which results in the movement of the genetic material directly to the cytoplasm. The amount of translocated genetic material decreases with the size of the nucleic acid [149]. While crossing the membrane, plasmid interacts with the hydrophilic head groups of membrane phospholipids and cell cytoskeleton [150]. Successful DNA electrotransfer involves the migration of the DNA to the nucleus. DNA may cross the nuclear envelope during the cell division or be actively transported by the nuclear pore complex [151]. The current understanding of the electrotransfer mechanism was reviewed by Rosazza et al. [136] (Figure 3).
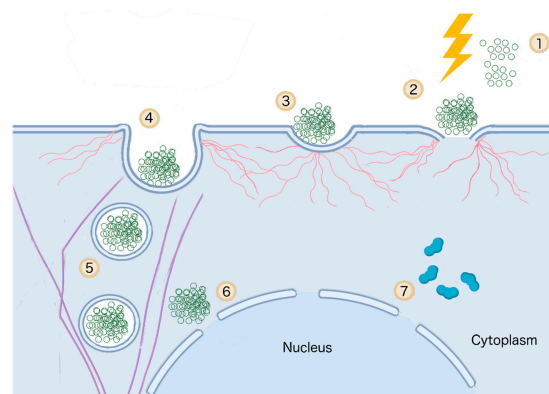

Figure 3. Gene electrotransfer. (1) Plasmid DNA is delivered to the tumor environment; (2) electrical pulses permeabilize the cell membrane; (3) DNA interact with cell membrane on cathode facing site [144]; (4) DNA is inserted into cell membrane with the involvement of actin patches [150]. (5) Plasmids are internalized by endocytosis. Microtubules actively transport DNA molecules through the cytoplasm [136]. (6) DNA leaves endosomes and cross the nuclear envelope [151]. (7) After DNA expression, the proteins are released into the cytoplasm.

GET is commonly performed on muscle or skin tissue. Due to the immunological function and non-restricted access, the skin remains one of the natural candidates for electrotransfer [152]. In general, therapy on the skin is effective. The method found its application in DNA vaccines, skin ischemia treatment, and the stimulation of wound healing [153–157]. GET to muscle provides a high expression of transferred genes for a relatively long period of time and enables the efficient production of transcription factors [158]. The heterogenicity of the cancer tissue makes the transfection directly into the tumor complicated. However, it is possible and effective when the electroporation-based method is properly optimized. [158]. Numerous in vivo and in vitro studies prove the efficiency of GET in gene transfer to tumors [146,159–163].

Cancer gene therapy DNA encoding immunomodulatory factors and cytokines constitute the possible choice for anti-cancer gene transfection [164]. The efficiency of electroporation-based in vitro transfection oscillates around 80%, which is comparable to the standard viral transfection. The electroporated genetic construct does not typically integrate with the genome. Therefore, it is considered safer than other transfection methods [165]. The solution to the lack of integration can be provided by GET of CRISPR/Cas9 nuclease system. CRISP-Cas9 mediated genome editing enables the specific integration of electrotransferred plasmids with the genome in vivo [166].

Apart from the delivery site, the effectiveness of GET depends on length, voltage, number of pulses, kind of used electrodes, and interval time between the injection and pulse delivery [167]. The electric field intensity has to be low enough to ensure the survival of cells. DNA used in GET targeted against tumor generally consists of plasmids encoding cytokines that modulate the tumor and growth factors that induce the antiangiogenic effect in the tumor microenvironment [168–171]. The efficiency of GET was investigated on urological cancers. Since the approach is relatively new, and efficiency strongly depends on pulse parameters, most of the experiments were carried out on animal models. The majority of published trials of GET on urological malignances use plasmids encoding specific tumor antigens. Several strategies of DNA electrotransfer targeted against prostate cancer have been examined in clinical trials.

4.4. GET—Prostate Cancer

DNA-based cancer vaccines have proven their efficiency to induce cytotoxic T lymphocytes specific for prostate antigens. Among antigens of prostate cancer, PSA, PSMA, and PSCA are primary candidates applied in immune therapy [172].

Electroporation has been studied as a possible approach for delivering DNA vaccines to prostate cancer in animal models. *PSA* GET proved to be effective. Nevertheless, the parameters needed to be optimized to achieve both the high efficiency of transfection and immune response against antigens. It appeared that the combination of high short and low long pulses were the most effective [173]. In another two in vivo experiments, plasmids encoding PSA and PSCA antigens were delivered by intramuscular electroporation [174,175]. GET resulted in significant production of IFN-γ, which generated a high level of Th-1 T-cell. The therapy provided the reduction of a tumor mass [175]. In another in vivo experiment, the *p53* mRNA GET achieved the remarkable suppression of prostate tumor growth [176].

In a clinical phase I/II trial on patients with prostate cancer, the plasmid encoding epitope from PSMA was transfected by the electroporation of muscle tissue. The domain of fragment C of tetanus toxin was added to the injected plasmid to upregulate the immune response. Electroporation appeared to be acceptable by patients, although it was painful for a short time. No additional risks or safety concerns connected with electroporation were identified. The response to the therapy was remarkably higher among patients who received DNA injection combined with EP comparing to the control group, where EP did not follow DNA vaccination [79]. The other phase I clinical study evaluated the feasibility of a PSA antigen vaccine combined with intradermal electroporation. Prior to the vaccination, the androgen deprivation therapy (ADT) was performed on patients to induce T-cell infiltration. The electrotransfer successfully increased PSA-specific CD8+ T-cell mediated immune

reaction in patients where ADT primarily triggered the reaction. Moreover, the same effect has been obtained in case of patients where the ADT failed to prime T-cells. The electrotransfer was easy to perform, well-tolerated, and show no severe side effects [80]. A phase I clinical trial evaluating the electrotransfer of DNA Vaccine together with checkpoint inhibitors and PROSTVAC for prostate cancer is currently on-going (NCT03532217).

4.5. GET—Bladder Cancer

The primary trials performed on animal models showed that electroporation is an effective method of gene transfection to submucosal interstitial cells and urothelial cells [177]. Subsequently, two in vivo trials evaluated the effectiveness of GET with the genomic DNA of recombinant bacillus Calmette-Guerin (BCG) with IL-12 [178,179]. Both studies confirm that DNA electrotransfer increased INF-γ and IL-12 secretion inducing infiltration of CD4+/CD8+T-cells and NK cells into the tumor site. Local immune reaction inhibited tumor growth, resulting in significantly prolonged cumulative survival of mice treated with poly-rBCG and mIL-12. The results of both studies suggest that BCG DNA electrotransfer with IL-12 instead of intact live BCG can be effectively applied to stimulate the immune reaction against bladder cancer [180].

4.6. GET—Renal Cancer

The effect of *tumor necrosis factor-related apoptosis-inducing ligand* (*TRAIL*) cDNA plasmid electrotransfer was investigated on the murine model. DNA plasmid injection and electroporation were introduced directly to the tumor. The study shows that *TRAIL* gene therapy induced growth suppression and apoptosis of renal cancer tumor cells. No severe side effects were reported. Moreover, the application of *TRAIL* electrotransfer combined with 5-FU enhanced the outcome of the therapy. The study proved that *TRAIL* GET is a safe and effective treatment method, but further studies are needed to evaluate the feasibility of this approach on humans [181]. Another study on the murine model evaluated the possibility of electrotransfer of plasmids encoding IL-12 for renal cancer treatment. The therapy resulted in significant inhibition of tumor growth after *Il-12* GET compared to GET of empty plasmids [182].

4.7. GET—Adoptive Transfer of Autologous T-Cells

Today, electroporation-based techniques are also used to modulate the immune system to target solid urological tumors or metastatic malignancies. GET can be utilized for the transport of genetic material, encoding the chimeric receptor or specific antigen into immune-competent cells. Modulation of the immune response includes the genetic modification of the immune-competent cells, like the production of chimeric antigen receptor (CAR) T cells, CAR-NK cells, or even the stimulation of NK cells proliferation and killing properties—cytokine-induced killer cells (CIK cells) [183–185]. The advantages of the application of electroporation in CAR-T technology are a simple manufacturing procedure and have a relatively low cost when compared to other methods [165]. Currently, several attempts of CAR-T therapy were successful in treating urological malignances. However, it has to be emphasized that none of the further mentioned trials concerning CAR-T for urological malignancies applies electroporation for gene transfection. Generally, due to the high expression on the prostate gland tissue, PSMA and PSCA are utilized as the targets for the CAR-T cell therapy for prostate cancer [186–188]. High effectivity of the therapy led to the registration of CAR-T against PSMA for phase I clinical trials in patients with metastatic prostate cancer (NCT01140373). Besides, PSCA-CAR-T Cells undergo phase I clinical trials for metastatic PSCA+ castration-resistant prostate cancer (NCT03873805). The therapy seems to be promising for other urological malignancies as well. For instance, EGFR-specific CAR-NK-92 cells were proved in vitro to exhibit a synergistic effect with cabozantinib against renal cell carcinoma [189]. The efficiency of NK cells against the metastatic renal tumor is being evaluated in clinical trials (NCT02843607). Considering bladder cancer, the CAR-T therapy against urothelial tumor undergoes the clinical trial Phase I/II (NCT03185468). Although viral vectors remain the most often used in CAR-T

manufacturing, electroporation seems to be a reasonable and promising alternative, which hopefully can be introduced to urology.

5. Conclusions

The hallmark of EP is the diversity of applications. Depending on the pulse parameters, it can be involved in a wide range of treatments. Considering the focal ablation, IRE has already proven to be the feasible, safe, and effective method of urology cancer treatment. The improved algorithms and the methods of electric field distribution monitoring enable precise ECT and IRE. The need for general anesthesia and muscle relaxation can be overcome by optimal pulse parameters. In the future, electroporation trials should involve the application of immune-stimulating agents and the performance of repetitive therapies. However, no long-term outcome evaluated in a randomized trial restricts the clinical application of electroporation in urology. As previously mentioned, with optimized parameters, GET constitutes a reasonable alternative to the gen vectors in immune therapy. The in vitro efficiency of GET can be compared with viral transfection. The protocols enabling the GET to tumor sites are developing, and studies provide promising results [190]. Prospectively, GET in urology might be applied not only in oncology but also to treat bladder dysfunctions and erectile dysfunction [191]. Thinking globally, the relatively low cost of EP enables less wealthy countries to have access to the therapy [106]. The generator of electric impulses and electrodes can be produced at reasonable prices. Moreover, in the case of IRE, no additional drugs are needed. The cytostatics administrated in ECT can be substituted with already registered and widely available calcium chloride, with similar results [106]. Decisively, the elucidation of the EP potential, in presented approaches in urology, will keep scientists busy for a long time.

References

1. Dy, G.W.; Gore, J.L.; Forouzanfar, M.H.; Naghavi, M.; Fitzmaurice, C.; Catto, J. Global Burden of Urologic Cancers, 1990–2013. *Eur. Urol.* **2016**, *71*, 437–446. [CrossRef] [PubMed]
2. Kurhanewicz, J.; Vigneron, D.; Carroll, P.; Coakley, F. Multiparametric magnetic resonance imaging in prostate cancer: Present and future. *Curr. Opin. Urol.* **2008**, *18*, 71–77. [CrossRef] [PubMed]
3. Nassiri, N.; Chang, E.; Lieu, P.; Priester, A.M.; Margolis, D.J.A.; Huang, J.; Reiter, R.E.; Dorey, F.J.; Marks, L.S. Focal therapy eligibility determined by MRI/US fusion biopsy. *J. Urol.* **2018**, *199*, 453–458. [CrossRef] [PubMed]
4. Lino, C.A.; Harper, J.C.; Carney, J.P.; Timlin, J.A. Delivering CRISPR: A review of the challenges and approaches. *Drug Deliv.* **2018**, *25*, 1234–1257. [CrossRef]
5. Harvey, L.; Arnold, B.; SLawrence, Z.; Matsudaira, P.; Baltimore, D.; Darnell, J. *Molecular Cell Biology*, 4th ed.; Freeman & Co.: New York, NY, USA, 2000; ISBN 0-7167-3136-3.
6. Zimmerman, U. Electric field-medieted fusion and related electrical phenomena. *Biochim. Biophys. Acta* **1982**, *694*, 227–277. [CrossRef]
7. Neumann, E.; Rosenheck, K. Permeability Changes Induced by Electric Impulses in Vesicular Membranes. *J. Membr. Biol.* **1972**, *10*, 279–290. [CrossRef]
8. Kotnik, T.; Pucihar, G.; Miklavcic, D. Induced Transmembrane Voltage and Its Correlation with Electroporation-Mediated Molecular Transport. *J. Membr. Biol.* **2010**, *236*, 3–13. [CrossRef]

9.   Teissie, J.; Marie-Pierre, R. An Experimental Evaluation of the Critical Potential Difference. *Biophys. J. Vol.* **1993**, *65*, 409–413. [CrossRef]

10. Teissie, J.; Tsong, T.Y. Electric Field Induced Transient Pores in Phospholipid Bilayer Vesicles. *Biochemistry* **1981**, *20*, 1548–1554. [CrossRef]

11. Cemazar, M.; Jarm, T.; Miklavcic, D. Effect of Electric-Field Intensity on Electropermeabilization and Electrosensitmty of Various Tumor-Cell Lines In Vitro. *Electro. Magn.* **1998**, *17*, 263–272.

12. Gabriel, B.; Teissie, J. Time Courses of Mammalian Cell Electropermeabilization Observed by Millisecond Imaging of Membrane Property Changes during the Pulse. *Biophys. J.* **1999**, *76*, 2158–2165. [CrossRef]

13. Weavera, J.; Smith, K.; Essera, A.T.; Sona, R.; Gowrishankar, R.T. A brief overview of electroporation pulse strength-duration space: A region where additional intracellular effects are expected. *Bioelectrochemistry* **2012**, *87*, 236–243. [CrossRef] [PubMed]

14. Silve, A.; Guimerà Brunet, A.; Al-Sakere, B.; Ivorra, A.; Mir, L.M. Comparison of the effects of the repetition rate between microsecond and nanosecond pulses: Electropermeabilization-induced electro-desensitization? *Biochim. Biophys. Acta Gen. Subj.* **2014**, *1840*, 2139–2151. [CrossRef]

15. Onik, G.; Mikus, P.; Rubinsky, B. Irreversible Electroporation: Implications for Prostate Ablation. *Technol. Cancer Res. Treat.* **2007**, *6*, 295–300. [CrossRef]

16. Donthula, V.; Camps-Raga, B.; Islam, N.E.; Ślusarz, A.; Lubahn, D.B.; Ganjam, V. Effects of nanosecond pulsed electric fields on the human prostate cancer cell line lncap. *IEEE Trans. Dielectr. Electr. Insul.* **2009**, *16*, 1311–1316. [CrossRef]

17. Gimsa, J.; Wachner, D. Analytical Description of the Transmembrane Voltage Induced on Arbitrarily Oriented Ellipsoidal and Cylindrical Cells. *Biophys. J.* **2001**, *81*, 1888–1896. [CrossRef]

18. Rols, M.; Teissie, J. Electropermeabilization of Mammalian Cells to Macromolecules: Control by Pulse Duration. *Biophys. J.* **1998**, *75*, 1415–1423. [CrossRef]

19. Winterhalter, M.; Helfrich, W. Deformation of Spherical Vesicles by Electric Fields. *J. Colloid Interface Sci.* **1988**, *122*, 583–586. [CrossRef]

20. Chopinet, L.; Roduit, C.; Rols, M.; Dague, E. Destabilization induced by electropermeabilization analyzed by atomic force microscopy. *BBA Biomembr.* **2013**, *1828*, 2223–2229. [CrossRef]

21. Pakhomova, O.N.; Khorokhorina, V.A.; Bowman, A.M.; Rodaite, R. Oxidative effects of nanosecond pulsed electric field exposure in cells and cell-free media. *Arch. Biochem. Biophys.* **2012**, *527*, 55–64. [CrossRef]

22. Olga, M.; Michel, O.; Pakhomov, A.G.; Casciola, M.; Saczko, J.; Kulbacka, J. Electropermeabilization does not correlate with plasma membrane lipid oxidation. *Bioelectrochemistry* **2019**, *132*, 107433.

23. Romeo, S.; Wu, Y.; Levine, Z.A.; Gundersen, M.A.; Vernier, P.T. Water influx and cell swelling after nanosecond electropermeabilization. *Biochim. Biophys. Acta* **2013**, *1828*, 1715–1722. [CrossRef] [PubMed]

24. Teissie, J.; Eynard, N.; Gabriel, B.; Rols, M.P. Electropermeabilization of cell membranes. *Adv. Drug Deliv. Rev.* **1999**, *35*, 3–19. [CrossRef]

25. Rols, M.-P.; Delteil, C.; Golzio, M.; Teissie, J. Control by ATP and ADP of voltage-induced mammalian-cell-membrane permeabilization, gene transfer and resulting expression. *Eur. J. Biochem.* **1998**, *254*, 382–388. [CrossRef] [PubMed]

26. Chakrabarti, R.; Wylie, D.E.; Schuster, S.M. Transfer of Monoclonal Antibodies into Mammalian Cells by Electroporation. *J. Biol. Chem.* **1989**, *264*, 15494–15500.

27. Rols, M. Electropermeabilization, a physical method for the delivery of therapeutic molecules into cells. *Biochim. Biophys. Acta* **2006**, *1758*, 423–428. [CrossRef]

28. Sözer, E.B.; Pocetti, C.F.; Vernier, P.T. Transport of charged small molecules after electropermeabilization—Drift and diffusion. *BMC Biophys.* **2018**, *11*, 1–11. [CrossRef]

29. Rols, M.; Teissie, J. Electropermeabilization of mammalian cells Quantitative analysis of the phenomenon. *Biophys. J.* **1990**, *58*, 1089–1098. [CrossRef]

30. Aycock, K.N.; Davalos, R.V. Irreversible Electroporation: Background, Theory, and Review of Recent Developments in Clinical Oncology. *Bioelectricity.* **2019**, *1*, 214–234. [CrossRef]

31. Saulis, G. Pore disappearance in a cell after electroporation: Theoretical simulation and comparison with experiments. *Biophys. J.* **1997**, *73*, 1299–1309. [CrossRef]

32. Gehl, J.; Skovsgaard, T.; Mir, L.M. Vascular reactions to in vivo electroporation: Characterization and consequences for drug and gene delivery. *Biochim. Biophys. Acta Gen. Subj.* **2002**, *1569*, 51–58. [CrossRef]

33. Blazek, A.D.; Paleo, B.J.; Weisleder, N. Plasma Membrane Repair: A Central Process for Maintaining Cellular Homeostasis. *Physiology* **2015**, *30*, 438–448. [CrossRef] [PubMed]

34. Selma, C.; Zupanic, A.; Kranjc, S.; Al Sakere, B.; Miklavcic, D.; Leroy-Willig, A.; Mir, L.M. The influence of skeletal muscle anisotropy on electroporation: In vivo study and numerical modeling. *Med. Biol. Eng. Comput.* **2010**, *48*, 637–648.

35. Miklavcic, D.; Pavselj, N. Electric Properties of Tissues. In *Wiley Encyclopedia of Biomedical Engineering*; John Wiley & Sons, Inc.: Hoboken, NJ, USA, 2006; pp. 1–12, ISBN 9780471740360.

36. Pavlin, M.; Miklavc, D. Effective Conductivity of a Suspension of Permeabilized Cells: A Theoretical Analysis. *Biophys. J.* **2003**, *85*, 719–729. [CrossRef]

37. Corovic, S.; Lackovic, I.; Sustaric, P.; Sustar, T.; Rodic, T.; Miklavcic, D. Modeling of electric field distribution in tissues during electroporation. *Biomed. Eng. Online* **2013**, *12*, 1–27. [CrossRef]

38. Haemmerich, D.; Staelin, S.T.; Tsai, J.Z.; Tungjitkusolmun, S.; Mahvi, D.M.; Webster, J.G. In vivo electrical conductivity of hepatic tumours. *Physiol. Meas.* **2003**, *24*, 251–260. [CrossRef]

39. Pavselj, N.; Bregar, Z.; Vidmar, E.M.; Miklavcic, D. The Course of Tissue Permeabilization Studied on a Mathematical Model of a Subcutaneous Tumor in Small Animals. *IEEE Trans. Biomed. Eng.* **2005**, *52*, 1373–1380. [CrossRef]

40. Pavlin, M.; Kanduser, M.; Rebers, M.; Pucihar, G.; Hart, F.X.; Magjarevic, R.; Miklavcic, D. Effect of Cell Electroporation on the Conductivity of a Cell Suspension. *Biophys. J.* **2005**, *88*, 4378–4390. [CrossRef]

41. Davalos, R.V.; Otten, D.M.; Mir, L.M.; Rubinsky, B. Electrical Impedance Tomography for Imaging Tissue Electroporation. *IEEE Trans. Biomed. Eng.* **2004**, *51*, 761–767. [CrossRef]

42. Kranjc, M.; Bajd, F.; Sersa, I.; Woo, E.J.; Miklavcic, D. Ex Vivo and In Silico Feasibility Study of Monitoring Electric Field Distribution in Tissue during Electroporation Based Treatments. *PLoS ONE* **2012**, *7*, e45737. [CrossRef]

43. Kranjc, M.; Kranjc, S.; Bajd, F.; Serša, G.; Serša, I.; Miklavčič, D. Predicting irreversible electroporation-induced tissue damage by means of magnetic resonance electrical impedance tomography. *Sci. Rep.* **2017**, *7*, 1–10. [CrossRef] [PubMed]

44. Epstein, B.R.; Foster, K.R. Anisotropy in the dielectric properties of skeletal muscle. *Med. Biol. Eng. Comput.* **1983**, *21*, 51–55. [CrossRef] [PubMed]

45. Pavšelj, N.; Miklavčič, D. Numerical modeling in electroporation-based biomedical applications. *Radiol. Oncol.* **2008**, *42*, 159–168. [CrossRef]

46. Davalos, R.V.; Mir, L.M.; Rubinsky, B. Tissue ablation with irreversible electroporation. *Ann. Biomed. Eng.* **2005**, *33*, 223–231. [CrossRef] [PubMed]

47. Knavel, E.M.; Brace, C.L. Tumor ablation: Common modalities and general practices. *Tech. Vasc. Interv. Radiol.* **2013**, *16*, 192–200. [CrossRef]

48. Jiang, C.; Davalos, R.V.; Bischof, J.C. A Review of Basic to Clinical Studies of Irreversible Electroporation Therapy. *IEEE Trans. Biomed. Eng.* **2015**, *62*, 4–20. [CrossRef]

49. Schoellnast, H.; Monette, S.; Ezell, P.C.; Maybody, M.; Erinjeri, J.P.; Stubblefield, M.D.; Single, G.; Solomon, S.B. The delayed effects of irreversible electroporation ablation on nerves. *Eur. Radiol.* **2013**, *23*, 375–380. [CrossRef]

50. Maor, E.; Rubinsky, B. Endovascular Nonthermal Irreversible Electroporation: A Finite Element Analysis. *J. Biomech. Eng.* **2010**, *132*, 1–7. [CrossRef]

51. Davalos, R.V.; Rubinsky, B.; Mir, L.M. Theoretical analysis of the thermal effects during in vivo tissue electroporation. *Bioelectrochemistry* **2003**, *61*, 99–107. [CrossRef]

52. Wendler, J.; Fischbach, K.; Ricke, J.; Jürgens, J.; Fischbach, F.; Köllermann, J.; Porsch, M.; Baumunk, D.; Schostak, M.; Liehr, U.; et al. Irreversible Electroporation (IRE): Standardization of Terminology and Reporting Criteria for Analysis and Comparison. *Pol. J. Radiol.* **2016**, *81*, 54–64. [CrossRef]

53. Nielsen, K.; Scheffer, H.J.; Vieveen, J.M.; Van Tilborg, A.A.J.M.; Meijer, S.; Van Kuijk, C.; Tol, M.P. Van Den Anaesthetic management during open and percutaneous irreversible electroporation. *Br. J. Anaesth.* **2014**, *113*, 985–992. [CrossRef]

54. Qin, Z.; Zeng, J.; Liu, G.; Long, X.; Fang, G.; Li, Z.; Xu, K.; Niu, L. Irreversible Electroporation Ablation of an Unresectable Fibrous Sarcoma With 2 Electrodes: A Case Report. *Technol. Cancer Res. Treat.* **2017**, *16*, 964–968. [CrossRef] [PubMed]

55. Deodhar, A.; Dickfeld, T.; Single, G.W.; Raymond, H.; Sofocleous, C.T.; Maybody, M.; Solomon, S.B.; Therapies, I.; Sloan, M.; Cancer, K.; et al. Irreversible Electroporation Near the Heart: Ventricular Arrhythmias Can Be Prevented With ECG Synchronization. *AJR Am. J. Roentgenol.* **2011**, *196*, 1–16. [CrossRef] [PubMed]

56. Min, J.; Hyuk, L.; Choi, S.; Jai, H.; Eun, C.; Kim, S.; Keum, B.; Seok, Y.; Yoon, S.; Jeen, T.; et al. EUS-guided irreversible electroporation using endoscopic needle- electrode in porcine pancreas. *Surg. Endosc.* **2019**, *33*, 658–662.

57. Maor, E.; Ivorra, A.; Mitchell, J.J.; Rubinsky, B. Vascular smooth muscle cells ablation with endovascular non thermal irreversible electroporation. *J. Vasc. Interv. Radiol.* **2011**, *21*, 1708–1715. [CrossRef] [PubMed]

58. Chang, T.T.; Zhou, V.X.; Rubinsky, B. Using non-thermal irreversible electroporation to create an in vivo niche for exogenoue cell engrafment. *Biotechniques* **2017**, *62*, 229–231. [CrossRef]

59. Schmidt, C.R.; Shires, P.; Mootoo, M. Real-time ultrasound imaging of irreversible electroporation in a porcine liver model adequately characterizes the zone of cellular necrosis. *Hpb. J.* **2012**, *14*, 98–102. [CrossRef]

60. Vroomen, L.G.P.H.; Scheffer, H.J.; Melenhorst, M.C.A.M. MR and CT imaging characteristics and ablation zone volumetry of locally advanced pancreatic cancer treated with irreversible electroporation. *Eur. Radiol.* **2017**, *27*, 2521–2531. [CrossRef]

61. Neal, R.E., II; Cheung, W.; Kavnoudias, H.; Thomson, K.R. Spectrum of imaging and characteristics for liver tumors treated with irreversible electroporation. *J. Biomed. Sci. Eng.* **2012**, *5*, 813–818. [CrossRef]

62. Deodhar, A.; Monette, S.; Single, G.W.; Hamilton, W.C.; Thornton, R.; Maybody, M.; Coleman, J.A.; Solomon, S.B. Renal Tissue Ablation With Irreversible Electroporation: Preliminary Results in a Porcine Model. *Urology* **2011**, *77*, 754–760. [CrossRef]

63. Johann Jakob, W.; Maciej, P.; Markus, P.; Andreas, J. Urinary Tract Effects After Multifocal Nonthermal Irreversible Electroporation of the Kidney: Acute and Chronic Monitoring by Magnetic Resonance Imaging, Intravenous Urography and Urinary Cytology. *Cardiovasc. Interv. Radiol.* **2012**, *35*, 921–926.

64. Mara, D.X.; Zondervan, J.; De Bruin, M.; van Lienden, K.P. Feasibility and safety of irreversible electroporation (IRE) in patients with small renal masses: Results of a prospective study. *Urol. Oncol. Semin. Orig. Investig.* **2019**, *37*, 183.e1–183.e8.

65. Trimmer, C.K.; Khosla, A.; Morgan, M.; Stephenson, S.L.; Ozayar, A.; Cadeddu, J.A. Minimally Invasive Percutaneous Treatment of Small Renal Tumors with Irreversible Electroporation: A Single-Center Experience. *J. Vasc. Interv. Radiol.* **2015**, *26*, 1–7. [CrossRef] [PubMed]

66. Canvasser, N.E.; Sorokin, I.; Lay, A.H.; Morgan, M.S.C.; Ozayar, A.; Trimmer, C.; Cadeddu, J.A. Irreversible electroporation of small renal masses: Suboptimal oncologic efficacy in an early series. *World J. Urol.* **2017**, *35*, 1–7. [CrossRef] [PubMed]

67. EAU Guidelines. In Proceedings of the EAU Annual Congress Amsterdam 2020, Amsterdam, The Netherlands, 17–26 July 2020; ISBN 978-94-92671-07-3.

68. Zhong, J.; Wah, T.M. Renal ablation: Current management strategies and controversies. *Chin. Clin. Oncol.* **2019**, *8*, 6–13. [CrossRef]

69. Duffey, B.G.; Anderson, J.K. Current and future technology for minimally invasive ablation of renal cell carcinoma. *Indian J. Urol.* **2010**, *26*, 410–417.

70. Donaldson, I.A.; Alonzi, R.; Barratt, D.; Barret, E.; Berge, V.; Bott, S.; Bottomley, D.; Eggener, S.; Ehdaie, B.; Emberton, M.; et al. Focal Therapy: Patients, Interventions, and Outcomes—A Report from a Consensus Meeting. *Eur. Urol.* **2015**, *67*, 771–777. [CrossRef]

71. Blazevski, A.; Scheltema, M.J.; Amin, A.; Thompson, J.; Lawrentschuk, N.; Stricker, P.D. Irreversible electroporation (IRE): A narrative review of the development of IRE from the laboratory to a prostate cancer tratment. *BJU Int.* **2019**, *120*, 1–28. [CrossRef]

72. Van Den Bos, W.; Jurhill, R.R.; De Bruin, D.M.; Postema, A.W.; Wagstaff, P.G.K.; Muller, B.G.; Varkarakis, I.M.; Skolarikos, A.; Zondervan, P.J.; Pes, M.P.L.; et al. Histopathological outcomes after irreversible electroporation in prostate cancer; Results of an ablate-and-resect study. *J. Urol.* **2016**, *196*, 552–559. [CrossRef]

73. Guenther, E.; Klein, N.; Zapf, S.; Weil, S.; Schlosser, C.; Rubinsky, B.; Stehling, M.K. Prostate cancer treatment with Irreversible Electroporation (IRE): Safety, efficacy and clinical experience in 471 treatments. *PLoS ONE* **2019**, *14*, e0215093. [CrossRef]

74. Blazevski, A.; Scheltema, M.J.; Yuen, B.; Masand, N. Oncological and Quality-of-life Outcomes Following Focal Irreversible Electroporation as Primary Treatment for Localised Prostate Cancer: A Biopsy-monitored Prospective Cohort. *Eur. Urol. Oncol.* **2019**, *207*, 1–8. [CrossRef] [PubMed]

75. Dong, S.; Wang, H.; Zhao, Y. First Human Trial of High-Frequency Irreversible Electroporation Therapy for Prostate Cancer. *Technol. Cancer Res. Treat.* **2018**, *17*, 1–9. [CrossRef] [PubMed]

76. Scheltema, M.J.; Van Den Bos, W.; Siriwardana, A.R.; Anton, M.F.; Shnier, R.; Delprado, W.; Stricker, P.D. Feasibility and safety of focal irreversible electroporation as salvage treatment for localized radio-recurrent prostate cancer. *BJU Int.* **2017**, *120*, 51–58. [CrossRef] [PubMed]

77. Van Den Bos, W.; Scheltema, M.J.; Siriwardana, A.R.; Kalsbeek, A.M.F.; Thompson, J.E.; Ting, F.; Maret, B.; Haynes, A.; Shnier, R.; Delprado, W.; et al. Focal irreversible electroporation as primary treatment for localized prostate cancer. *BJU Int.* **2018**, *121*, 716–724. [CrossRef] [PubMed]

78. Klein, N.; Gunther, E.; Zapf, S.; El-idrissi, R.; Atta, J.; Stehling, M. Prostate cancer infiltrating the bladder sphincter successfully treated with Electrochemotherapy: A case report. *Clin. Case Rep.* **2017**, *5*, 2127–2132. [CrossRef] [PubMed]

79. Low, L.; Mander, A.; Mccann, K.; Dearnaley, D.; Tjelle, T. DNA Vaccination with Electroporation Induces Increased Antibody Responses in Patients with Prostate Cancer. *Hum. Gene Ther.* **2009**, *20*, 1269–1278. [CrossRef]

80. Eriksson, F.; Tötterman, T.; Maltais, A.; Pisa, P. DNA vaccine coding for the rhesus prostate specific antigen delivered by intradermal electroporation in patients with relapsed prostate cancer. *Vaccine* **2013**, *31*, 3843–3848. [CrossRef]

81. Van den Bos, W.; De Bruin, D.; Veelo, D.; Postema, A.; Muller, B.G.; Varkarakis, I.M. Quality of Life and Safety Outcomes Following Irreversible Electroporation Treatment for Prostate Cancer: Results from a Phase I-Ii Study. *Cancer Sci. Ther.* **2015**, *7*, 312–321.

82. Hamdy, F.C.; Donovan, J.L.; Lane, J.A.; Mason, M.; Metcalfe, C.; Holding, P.; Davis, M.; Peters, T.J.; Turner, E.L.; Martin, R.M.; et al. 10-Year Outcomes after Monitoring, Surgery, or Radiotherapy for Localized Prostate Cancer. *N. Engl. J. Med.* **2016**, *372*, 1415–1424. [CrossRef]

83. Trial, N.; Haglind, E.; Carlsson, S.; Stranne, J.; Wallerstedt, A.; Wildera, U.; Thorsteinsdottir, T.; Lagerkvist, M.; Damber, J.; Bjartell, A.; et al. Urinary Incontinence and Erectile Dysfunction After Robotic Versus Open Radical Prostatectomy: A Prospective, Controlled, Nonrandomised Trial. *Eur. Urol.* **2015**, *68*, 216–225.

84. Van Der Wielen, G.J.; Mulhall, J.P.; Incrocci, L. Erectile dysfunction after radiotherapy for prostate cancer and radiation dose to the penile structures: A critical review. *Radiother. Oncol.* **2007**, *84*, 107–113. [CrossRef] [PubMed]

85. Liu, M.; Pickles, T.; Berthelet, E.; Agranovich, A.; Kwan, W.; Tyldesley, S.; Mckenzie, M.; Keyes, M.; Morris, J.; Pai, H. Urinary incontinence in prostate cancer patients treated with external beam radiotherapy. *Radiother. Oncol.* **2005**, *74*, 197–201. [CrossRef] [PubMed]

86. Srimathveeravalli, G.; Silk, M.; Wimmer, T.; Monette, S.; Kimm, S.; Maybody, M.; Solomon, S.B.; Coleman, J.; Durack, J.C. Feasibility of Catheter-Directed Intraluminal Irreversible Electroporation of Porcine Ureter and Acute Outcomes in Response to Increasing Energy Delivery. *J. Vasc. Interv. Radiol.* **2015**, *26*, 1059–1066. [CrossRef] [PubMed]

87. Srimathveeravalli, G.; Cornelis, F.; Wimmer, H.; Monette, S.; Kimm, S.Y.; Maybody, M.; Solomon, S.B.; Coleman, J.A.; Durac, J.C. The Normal Porcine Ureter Retains Lumen Wall Integrity but not Patency Following Catheter Directed Irreversible Electroporation: Imaging and Histologic Assessment Over 28 Days. *J. Vasc. Interv. Radiol.* **2018**, *28*, 913–919. [CrossRef] [PubMed]

88. Ivey, J.W.; Latouche, E.L.; Sano, M.B.; Rossmeisl, J.H.; Davalos, R.V.; Verbridge, S.S. Targeted cellular ablation based on the morphology of malignant cells. *Sci. Rep.* **2015**, *5*, 1–17. [CrossRef]

89. Ringel-scaia, V.M.; Beitel-white, N.; Lorenzo, M.F.; Brock, R.M.; Huie, K.E.; Coutermarsh-Ott, S.; Eden, K.; Mcdaniel, D.K.; Verbridge, S.S.; Rossmeisl, J.H.; et al. High-frequency irreversible electroporation is an effective tumor ablation strategy that induces immunologic cell death and promotes systemic anti-tumor immunity. *EBioMedicine* **2019**, *44*, 112–125. [CrossRef]

90. Byron, C.R.; Dewitt, M.R.; Latouche, E.L.; Davalos, R.V.; Robertson, J.L. Treatment of Infiltrative Superficial Tumors in Awake Standing Horses Using Novel High-Frequency Pulsed Electrical Fields. *Front. Vet. Sci.* **2019**, *6*, 1–9. [CrossRef]

91. Arena, C.B.; Sano, M.B.; Rossmeisl, J.H., Jr.; Caldwell, J.L.; Garcia, P.A.; Rylander, M.N.; Davalos, R.V. High-frequency irreversible electroporation (H-FIRE) for non-thermal ablation without muscle contraction. *Biomed. Eng. Online* **2011**, *10*, 1–20. [CrossRef]

92. Reberšek, M.; Connor, R.O.; Miklavc, D.; Dermol–Černe, J.; Polajz, T. Cancellation effect is present in high-frequency reversible and irreversible electroporation. *Bioelectrochemistry* **2020**, *132*, 1–11.

93. Pandit, H.; Hong, Y.K.; Li, Y.; Rostas, J.; Pulliam, Z. Evaluating the Regulatory Immunomodulation Effect of Irreversible Electroporation (IRE) in Pancreatic Adenocarcinoma. *Ann. Surg. Oncol.* **2019**, *26*, 800–8006. [CrossRef]

94. Scheffer, H.J.; Stam, A.G.M.; Geboers, B.; Vroomen, L.G.P.H.; Ruarus, A.; De Bruijn, B.; Van Den Tol, M.P.; Kazemier, G.; Meijerink, M.R.; de Gruijl, T.D. Irreversible electroporation of locally advanced pancreatic cancer transiently alleviates immune suppression and creates a window for antitumor T cell activation. *Oncoimmunology* **2019**, *8*, 1652532. [CrossRef] [PubMed]

95. Perminaite, E.; Zinkevičienė, A. Antitumor Response and Immunomodulatory Effects of Sub-Microsecond Irreversible Electroporation and Its Combination with Calcium Electroporation. *Cancers* **2019**, *11*, 1–18.

96. Beitel-White, N.; Martin, R.C.G.; Li, Y.; Brock, R.M.; Allen, I.C.; Davalos, R. V Real-time prediction of patient immune cell modulation during irreversible electroporation therapy. *Sci. Rep.* **2019**, *9*, 1–8. [CrossRef] [PubMed]

97. Narayanan, J.S.S.; Ray, P.; Hayashi, T.; Whisenant, T.C. Irreversible Electroporation Combined with Checkpoint Blockade and TLR7 Stimulation Induces Anti-Tumor Immunity in a Murine Pancreatic Cancer Model. *Cancer Immunol. Res.* **2019**, *7*, 1714–1726. [CrossRef] [PubMed]

98. He, C.; Lin, X. T-cell activation and immune memory enhancement induced by irreversible electroporation in pancreatic cancer. *Clin. Transl. Med.* **2020**, *10*, 1–14. [CrossRef] [PubMed]

99. Li, X.; Xu, K.; Li, W.; Qiu, X.; Ma, B.; Fan, Q.; Li, Z. Immunologic Response to Tumor Ablation with Irreversible Electroporation. *PLoS ONE* **2012**, *7*, e48749. [CrossRef] [PubMed]

100. Zhao, J.; Wen, X.; Tian, L.; Li, T.; Xu, C.; Wen, X.; Melancon, M.P.; Gupta, S.; Shen, B.; Peng, W.; et al. Irreversible electroporation reverses resistance to immune checkpoint blockade in pancreatic cancer. *Nat. Commun.* **2019**, *10*, 899. [CrossRef]

101. White, S.B.; Zhang, Z.; Chen, J.; Gogineni, V.R.; Larson, A.C. Early Immunologic Response of Irreversible Electroporation versus Cryoablation in a Rodent Model of Pancreatic Cancer. *J. Vasc. Interv. Radiol.* **2018**, *29*, 1–6. [CrossRef]

102. Ii, R.E.N.; Rossmeisl, J.H., Jr.; Robertson, J.L.; Arena, C.B.; Davis, E.M.; Singh, R.N.; Stallings, J.; Davalos, R.V. Improved Local and Systemic Anti-Tumor Efficacy for Irreversible Electroporation in Immunocompetent versus Immunodeficient Mice. *PLoS ONE* **2013**, *8*, e64559.

103. Palucka, A.K.; Coussens, L.M. Review The Basis of Oncoimmunology. *Cell* **2016**, *164*, 1233–1247. [CrossRef]

104. Mir, L.M.; Orlowski, S.; Belehradek, J., Jr.; Paoletti, C. Electrochemotherapy Potentiation of Antitumour Effect of Bleomycin by Local Electric Pulses. *Eur. J. Cancer* **1991**, *27*, 68–72. [CrossRef]

105. Miklavčič, D.; Mali, B.; Kos, B.; Heller, R.; Serša, G. Electrochemotherapy: From the drawing board into medical practice. *Biomed. Eng. Online* **2014**, *13*, 1–20. [CrossRef] [PubMed]

106. Frandsen, S.K.; Vissing, M.; Gehl, J. A Comprehensive Review of Calcium Electroporation—A Novel Cancer Treatment Modality. *Cancers (Basel)* **2020**, *12*, 290. [CrossRef] [PubMed]

107. Mir, L.M. Therapeutic perspectives of in vivo cell electropermeabilization. *Bioelectrochemistry* **2000**, *53*, 1–10. [CrossRef]

108. Calvet, C.Y.; Famin, D.; André, F.M.; Mir, L.M. Electrochemotherapy with bleomycin induces hallmarks of immunogenic cell death in murine colon cancer cells. *Oncoimmunology* **2014**, *3*, e28131. [CrossRef]

109. Sersa, G.; Teissie, J.; Cemazar, M.; Signori, E.; Kamensek, U.; Marshall, G.; Miklavcic, D. Electrochemotherapy of tumors as in situ vaccination boosted by immunogene electrotransfer. *Cancer Immunol. Immunother.* **2015**, *64*, 1315–1327. [CrossRef]

110. Probst, U.; Fuhrmann, I.; Beyer, L.; Wiggermann, P. Electrochemotherapy as a new modality in interventional oncology: A review. *Technol. Cancer Res. Treat.* **2018**, *17*, 153303381878532. [CrossRef]

111. Bellard, E.; Markelc, B.; Pelofy, S.; Le, F.; Sersa, G.; Teissié, J.; Cemazar, M.; Golzio, M. Intravital microscopy at the single vessel level brings new insights of vascular modification mechanisms induced by electropermeabilization. *J. Control. Release* **2012**, *163*, 396–403. [CrossRef]

112. Markelc, B.; Sersa, G.; Cemazar, M. Differential Mechanisms Associated with Vascular Disrupting Action of Electrochemotherapy: Intravital Microscopy on the Level of Single Normal and Tumor Blood Vessels. *PLoS ONE* **2013**, *8*, e59557. [CrossRef]

113. Barve, A.; Jin, W.; Cheng, K. Prostate cancer relevant antigens and enzymes for targeted drug delivery. *J. Control. Release* **2014**, *187*, 118–132. [CrossRef]

114. Vera-donoso, D.; Mar, J.; Rivero-buceta, E.; Vidaurre-agut, C.; Moreno-manzano, V.; Botella, P. PSMA-Targeted Mesoporous Silica Nanoparticles for Selective Intracellular Delivery of Docetaxel in Prostate Cancer Cells. *ACS Omega* **2019**, *4*, 1281–1291.

115. Fang, Y.; Wu, J.; Li, T.; Liu, W.; Gao, L.; Luo, Y. Nanoparticle mediated chemotherapy of hormone refractory prostate cancer with a novel combi-molecule. *Am. J. Transl. Res.* **2015**, *7*, 1440–1449. [PubMed]

116. Ueki, T.; Uemura, H.; Nagashima, Y.; Ohta, S.; Ishiguro, H.; Kubota, Y. Antitumour effect of electrochemotherapy with bleomycin on human prostate cancer xenograft. *BJUI* **2008**, *102*, 1467–1471. [CrossRef] [PubMed]

117. Sylvester, R.J.; Oosterlinck, W.; Holmang, S.; Sydes, M.R.; Birtle, A.; Gudjonsson, S.; De Nunzio, C.; Okamura, K.; Kaasinen, E.; Oddens, J.R.; et al. Systematic Review and Individual Patient Data Meta-analysis of Randomized Trials Comparing a Single Immediate Instillation of Chemotherapy After Transurethral Resection with Transurethral Resection Alone in Patients with Stage pTa–pT1 Urothelial Carcino. *Eur. Urol.* **2016**, *69*, 231–244. [CrossRef]

118. Lerner, S.P.; Tangen, C.M.; Sucharew, H.; Wood, D.; Crawford, E.D. Failure to achieve a complete response to induction BCG therapy is associated with increased risk of disease worsening and death in patients with high risk non-muscle invasive bladder cancer. *Urol. Oncol. Semin. Orig. Investig.* **2009**, *27*, 155–159. [CrossRef]

119. Wirth, M.; Plattner, V.; Gabor, F. Strategies to improve drug delivery in bladder cancer therapy. *Expert Opin. Drug Deliv.* **2015**, *6*, 727–744. [CrossRef]

120. Qiu, H.; Guo, H.; Li, D.; Hou, Y.; Kuang, T.; Ding, J. Intravesical Hydrogels as Drug Reservoirs. *Trends Biotechnol.* **2019**, *38*, 1–4. [CrossRef]

121. Guo, H.; Li, F.; Xu, W.; Chen, J.; Hou, Y.; Wang, C.; Ding, J.; Chen, X. Mucoadhesive Cationic Polypeptide Nanogel with Enhanced Penetration for Efficient Intravesical Chemotherapy of Bladder Cancer. *Adv. Sci.* **2018**, *5*, 1–10. [CrossRef]

122. Tomlinson, B.; Lin, T.; Era, M.D.; Pan, C.; Comprehensive, D. Nanotechnology in bladder cancer: Current state of development and clinical practice. *Nanomedicine* **2015**, *10*, 1189–1201. [CrossRef]

123. Lugnani, F.; Mazza, G.; Cerulli, N.; Rossi, W.; Stephen, R. Iontophoresis of Drugs in the Bladder Wall: Equipment and Preliminary Studies. *Artif. Organs* **1993**, *17*, 8–17. [CrossRef]

124. Colombo, R.; Lev, A.; Da Pozzo, L.F.; Freschi, M.; Gallus, G.; Rigatti, P. A new approach using local combined microwave hepertermia and chemotherapy in superficial transitional bladder carcinoma treatment. *J. Urol.* **1995**, *153*, 959–963. [CrossRef]

125. Arends, T.J.H.; Nativ, O.; Maffezzini, M.; De Cobelli, O.; Canepa, G.; Verweij, F.; Moskovitz, B.; Van Der Heijden, A.G.; Witjes, J.A.; Boorjian, S. Results of a Randomised Controlled Trial Comparing Intravesical Chemohyperthermia with Mitomycin C Versus Bacillus Calmette-Guerin for Adjuvant Treatment of Patients with Intermediate- and High-risk Non—Muscle-invasive Bladder Cancer. *Eur. Urol.* **2016**, *96*, 1046–1052. [CrossRef] [PubMed]

126. Arends, T.J.H.; Van Der Heijden, A.G.; Urology, A.; Witjes, J.A. Combined chemohyperthermia: The 10-years monocentric experience in 160 non-muscle invasive bladder cancer patients. *J. Urol.* **2014**, *192*, 708–713. [CrossRef] [PubMed]

127. Di Stasi, S.M.; Giannantoni, A.; Giurioli, A.; Valenti, M.; Zampa, G.; Storti, L.; Attisani, F.; De Carolis, A.; Capelli, G.; Vespasiani, G.; et al. Sequential BCG and electromotive mitomycin versus BCG alone for high-risk superficial bladder cancer: A randomised controlled trial. *Lancet Oncol.* **2006**, *7*, 43–51. [CrossRef]

128. Kubota, Y.; Mir, L.M.; Nakada, T.; Sasagawa, I.; Suzuki, H.; Aoyama, N. Successful treatment of metastatic skin lesions with electrochemotherapy. *J. Urol.* **1998**, *160*, 1426. [CrossRef]

129. Ogihara, M.; Yamaguchi, O. Potentiation of effects of anticancer agents by local electric pulses in murine bladder cancer. *Urol. Res.* **2000**, *28*, 391–397. [CrossRef]

130. Vásquez, J.L.; Gehl, J.; Hermann, G.G. Electroporation enhances mitomycin C cytotoxicity on T24 bladder cancer cell line: A potential improvement of intravesical chemotherapy in bladder cancer. *Bioelectrochemistry* **2012**, *88*, 127–133. [CrossRef]

131. Kubota, L.E.Y.; Nakada, T.; Yanai, H.; Kakizaki, H.; Sasagawa, I.; Watanabe, M. Electropermeabilization in bladder cancer chemotherapy. *Cancer Chemother. Pharmacol.* **1996**, *39*, 67–70. [CrossRef]

132. Hansen, E.L.; Sozer, E.B.; Romeo, S.; Frandsen, S.K.; Vernier, P.T.; Gehl, J. Dose-Dependent ATP depletion and cancer cell death following calcium electroporation, relative effect of calcium concentration and electric field strength. *PLoS ONE* **2015**, *10*, e0122973.

133. Frandsen, S.K.; Gehl, J. Effect of calcium electroporation in combination with metformin in vivo and correlation between viability and intracellular ATP level after calcium electroporation in vitro. *PLoS ONE* **2017**, *12*, e0181839. [CrossRef]

134. Vasquez, J.L.; Ibsen, P.; Lindberg, H.; Gehl, J. In Vitro and In Vivo Experiments on Electrochemotherapy for Bladder Cancer. *J. Urol.* **2015**, *193*, 1009–1015. [CrossRef] [PubMed]

135. Herr, H.W.; Dalbagni, G. Defining Bacillus Calmette-Guerin refractory superficial bladder tumors. *J. Urol.* **2003**, *169*, 1706–1708. [CrossRef] [PubMed]

136. Rosazza, C.; Meglic, S.H.; Zumbusch, A.; Rols, M.-P.; Miklavcic, D. Gene Electrotransfer: A Mechanistic Perspective. *Curr. Gene Ther.* **2016**, *16*, 98–129. [CrossRef] [PubMed]

137. Bodles-Brakhop, A.M.; Heller, R.; Draghia-Akli, R. Electroporation for the delivery of DNA-based vaccines and immunotherapeutics: Current clinical developments. *Mol. Ther.* **2009**, *17*, 585–592. [CrossRef]

138. Titomirov, A.V.; Sukharev, S.; Kistanova, E. In vivo electroporation and stable transformation of skin cells of newborn mice by plasmid DNA. *BBA Gene Struct. Expr.* **1991**, *1088*, 131–134. [CrossRef]

139. Aihara, H.; Miyazaki, J.I. Gene transfer into muscle by electroporation in vivo. *Nat. Biotechnol.* **1998**, *16*, 867–870. [CrossRef]

140. Suzuki, T.; Shin, B.C.; Fujikura, K.; Matsuzaki, T.; Takata, K. Direct gene transfer into rat liver cells by in vivo electroporation. *FEBS Lett.* **1998**, *425*, 436–440. [CrossRef]

141. Nishi, T.; Yoshizato, K.; Yamashiro, S.; Takeshima, H.; Sato, K.; Hamada, K.; Kitamura, I.; Yoshimura, T.; Saya, H.; Kuratsu, J.; et al. High-Efficiency in Vivo Gene Transfer Using Intraarterial Plasmid DNA Injection following in Vivo Electroporation. *Cancer Res.* **1996**, *56*, 1050–1055.

142. Heller, R.; Jaroszeski, M.; Atkin, A.; Moradpour, D.; Gilbert, R.; Wands, J.; Nicolau, C. In vivo gene electroinjection and expression in rat liver. *FEBS Lett.* **1996**, *389*, 225–228. [CrossRef]

143. Daud, A.I.; DeConti, R.C.; Andrews, S.; Urbas, P.; Riker, A.I.; Sondak, V.K.; Munster, P.N.; Sullivan, D.M.; Ugen, K.E.; Messina, J.L.; et al. Phase I trial of interleukin-12 plasmid electroporation in patients with metastatic melanoma. *J. Clin. Oncol.* **2008**, *26*, 5896–5903. [CrossRef]

144. Faurie, C.; Rebersek, M.; Golzio, M.; Kanduser, M.; Escoffre, J.-M.; Pavlin, M.; Teissie, J.; Miklavcic, D.; Rols, M.-P. 1CNRS Electro-mediated gene transfer and expression are controlled by the life-time of DNA/membrane complex formation. *J. Gene Med.* **2010**, *12*, 117–125. [CrossRef] [PubMed]

145. Henshaw, J.W.; Zaharoff, D.A.; Mossop, B.J.; Yuan, F. Short communication A single molecule detection method for understanding mechanisms of electric field-mediated interstitial transport of genes. *Bioelectrochemistry* **2006**, *69*, 248–253. [CrossRef] [PubMed]

146. Guo, S.; Jackson, D.L.; Burcus, N.I.; Chen, Y.J.; Xiao, S.; Heller, R. Gene electrotransfer enhanced by nanosecond pulsed electric fields. *Mol. Ther. Methods Clin. Dev.* **2014**, *1*, 14043. [CrossRef] [PubMed]

147. Markelc, B.; Skvarca, E.; Dolinsek, T.; Prevodnik, V.; Coer, A.; Sersa, G.; Cemazar, M. Inhibitor of endocytosis impairs gene electrotransfer to mouse muscle in vivo. *Bioelectrochemistry* **2015**, *103*, 111–119. [CrossRef] [PubMed]

148. Rosazza, C.; Deschout, H.; Buntz, A.; Braeckmans, K.; Rols, M.; Zumbusch, A. Endocytosis and Endosomal Trafficking of DNA After Gene Electrotransfer In Vitro. *Mol. Ther. Acids* **2016**, *5*, 1–11. [CrossRef]

149. Sachdev, S.; Moreira, S.F.; Keehnen, Y.; Rems, L.; Kreutzer, M.T.; Boukany, P.E. DNA-membrane complex formation during electroporation is DNA size- dependent. *BBA Biomembr.* **2020**, *1862*, 183089. [CrossRef]

150. Rosazza, C.; Escoffre, J.; Zumbusch, A.; Rols, M. The Actin Cytoskeleton Has an Active Role in the Electrotransfer of Plasmid DNA in Mammalian Cells. *Mol. Ther.* **2011**, *19*, 913–921. [CrossRef]

151. Lechardeur, D.; Lukacs, G.L. Nucleocytoplasmic Transport of Plasmid DNA: A Perilous Journey from the Cytoplasm to the Nucleus. *Hum. Gene Ther.* **2006**, *17*, 882–889. [CrossRef]

152. Roos, A.; Eriksson, F.; Timmons, J.A.; Gerhardt, J.; Nyman, U.; Wahren, B.; Pisa, P.; Bra, A. Skin Electroporation: Effects on Transgene Expression, DNA Persistence and Local Tissue Environment. *PLoS ONE* **2009**, *4*, e7226. [CrossRef]

153. Zampaglione, I.; Simon, A.J.; Capone, S.; Finnefrock, A.C.; Casimiro, D.R.; Kath, G.S.; Tang, A.; Folgori, A.; La Monica, N.; Shiver, J.; et al. Genetic vaccination by gene electro-transfer in non-human primates. *J. Drug Deliv. Sci. Technol.* **2006**, *16*, 85–89. [CrossRef]

154. Pasquet, L.; Chabot, S.; Bellard, E.; Markelc, B.; Rols, M.; Reynes, J.; Tiraby, G.; Couillaud, F.; Teissie, J.; Golzio, M. Safe and efficient novel approach for non-invasive gene electrotransfer to skin. *Sci. Rep.* **2018**, *8*, 1–13. [CrossRef] [PubMed]

155. Gibot, L.; Golberg, A. Electroporation in Scars/Wound Healing and Skin Response. In *Handbook of Electroporation*; Springer International Publishing: Berlin/Heidelberg, Germany, 2016; pp. 1–18.

156. Byrnes, C.K.; Malone, R.W.; Akhter, N.; Nass, P.H.; Wetterwald, A.; Cecchini, M.G.; Duncan, M.D.; Harmon, J.W. Electroporation enhances transfection efficiency in murine cutaneous wounds. *Wound Repair. Regen.* **2004**, *12*, 397–403. [CrossRef] [PubMed]

157. Ferraro, B.; Cruz, Y.L.; Baldwin, M.; Coppola, D.; Heller, R. Increased perfusion and angiogenesis in a hindlimb ischemia model with plasmid FGF-2 delivered by noninvasive electroporation. *Gene Ther.* **2010**, *17*, 763–769. [CrossRef] [PubMed]

158. Mir, L.M.; Moller, P.H.; Franck, A.; Gehl, J. Electric Pulse-Mediated Gene Delivery to Various Animal Tissues. *Adv. Genet.* **2005**, *54*, 84–114.

159. Bettan, M.; Ivanov, M.A.; Mir, L.M.; Boissière, F.; Delaere, P.; Scherman, D. Efficient DNA electrotransfer into tumors. *Bioelectrochem. Bioenerg.* **2000**, *52*, 83–90. [CrossRef]

160. Sieni, E.; Dettin, M.; De Robertis, M.; Bazzolo, B.; Conconi, M.T.; Zamuner, A.; Marino, R.; Keller, F.; Campana, L.G.; Signori, E. The Efficiency of Gene Electrotransfer in Breast-Cancer Cell Lines Cultured on a Novel Collagen-Free 3D Scaffold. *Cancers* **2020**, *12*, 1043. [CrossRef]

161. Znidar, K.; Bosnjak, M.; Semenova, N.; Pakhomova, O.; Heller, L.; Cemazar, M. Tumor cell death after electrotransfer of plasmid DNA is associated with cytosolic DNA sensor upregulation. *Oncotarget* **2018**, *9*, 18665–18681. [CrossRef]

162. Sedlar, A.; Dolinsek, T.; Markelc, B.; Prosen, L.; Kranjc, S.; Bosnjak, M.; Blagus, T.; Cemazar, M.; Sersa, G. Potentiation of electrochemotherapy by intramuscular IL-12 gene electrotransfer in murine sarcoma and carcinoma with different immunogenicity. *Radiol. Oncol.* **2012**, *46*, 302–311. [CrossRef]

163. Heller, R.; Heller, L.C. Gene Electrotransfer Clinical Trials. *Adv. Genet.* **2015**, *89*, 235–262.

164. Lucas, M.L.; Heller, L.; Coppola, D.; Heller, R. IL-12 plasmid delivery by in Vivo electroporation for the successful treatment of established subcutaneous B16.F10 melanoma. *Mol. Ther.* **2002**, *5*, 668–675. [CrossRef]

165. Wang, X.; Rivière, I. Clinical manufacturing of CAR T cells: Foundation of a promising therapy. *Mol. Ther. Oncolytics* **2016**, *3*, 1–7. [CrossRef] [PubMed]

166. Zuckermann, M.; Hovestadt, V.; Knobbe-thomsen, C.B.; Zapatka, M.; Northcott, P.A.; Schramm, K.; Belic, J.; Jones, D.T.W.; Tschida, B.; Moriarity, B.; et al. Somatic CRISPR/Cas9-mediated tumour suppressor disruption enables versatile brain tumour modelling. *Nat. Commun.* **2015**, *6*, 1–9. [CrossRef] [PubMed]

167. Lambricht, L.; Lopes, A.; Kos, S.; Sersa, G.; Vandermeulen, G. Clinical potential of electroporation for gene therapy and DNA vaccine delivery. *Expert Opin. Drug Deliv.* **2015**, *5247*, 1–36. [CrossRef] [PubMed]

168. Choo, A.Y.; Shedlock, D.J.; Muthumani, K. Electroporation of cytokines for cancer gene therapy. *Cancer Biol. Ther.* **2009**, *8*, 2123–2125. [CrossRef]

169. Heller, R.; Lundberg, C.M.; Burcus, N.; Edelblute, C.; Guo, S. Gene electrotransfer of plasmids encoding cytokines as an effective immunotherapy approach for melanoma. *J. Immunol.* **2016**, *196*, 213–216.

170. Shi, G.; Edelblute, C.; Arpag, S.; Lundberg, C.; Heller, R. IL-12 Gene Electrotransfer Triggers a Change in Immune Response within Mouse Tumors. *Cancers* **2018**, *10*, 498. [CrossRef]

171. Verrax, J.; Defresne, F.; Lair, F.; Vandermeulen, G.; Rath, G.; Dessy, C.; Préat, V.; Feron, O. Delivery of soluble VEGF receptor 1 (sFlt1) by gene electrotransfer as a new antiangiogenic cancer therapy. *Mol. Pharm.* **2011**, *8*, 701–708. [CrossRef]

172. Kiessling, R.; Pisa, P.; Miller, A.M.; Volkan, O. Immune Monitoring in a Phase 1 Trial of a PSA DNA Vaccine in Patients with Hormone-Refractory Prostate Cancer. *J. Immunother.* **2005**, *28*, 389–395.

173. Roos, A.; Moreno, S.; Leder, C.; Pavlenko, M.; King, A.; Pisa, P. Enhancement of Cellular Immune Response to a Prostate Cancer DNA Vaccine by Intradermal Electroporation. *Mol. Ther.* **2006**, *13*, 320–327. [CrossRef]

174. Ahmad, S.; Casey, G.; Sweeney, P.; Tangney, M.; Sullivan, G.C.O. Optimised electroporation mediated DNA vaccination for treatment of prostate cancer. *Genet. Vaccines Ther.* **2010**, *8*, 1–13. [CrossRef]

175. Ahmad, S.; Casey, G.; Sweeney, P.; Tangney, M.; Sullivan, G.C.O. Prostate Stem Cell Antigen DNA Vaccination Breaks Tolerance to Self-antigen and Inhibits Prostate Cancer Growth. *Mol. Ther.* **2009**, *17*, 1101–1108. [CrossRef] [PubMed]

176. Mikata, K.; Uemura, H.; Ohuchi, H.; Ohta, S.; Nagashima, Y.; Kubota, Y. Inhibition of Growth of Human Prostate Cancer Xenograft by Transfection of p53 Gene: Gene Transfer by Electroporation. *Mol. Cancer Ther.* **2002**, *1*, 247–252. [PubMed]

177. Harimoto, K.; Sugimura, K.; Lee, C.R.; Kuratsukuri, K.; Kishimoto, T. In vivo gene transfer methods in the bladder without viral vectors. *Br. J. Urol.* **1998**, *81*, 870–874. [CrossRef] [PubMed]

178. Yu, D.-S.Y.; Lee, C.-F.; Hsieh, D.-S.; Chang, S.-Y. Antitumor Effects of Recombinant BCG and Interleukin-12 DNA Vaccines on Xentografted Murine Bladder Cancer. *Urology* **2004**, *63*, 596–601. [CrossRef] [PubMed]

179. Lee, C.; Chang, S.; Hsieh, D.; Yu, D. Immunotherapy for Bladder Cancer using Recombinant Bacillus Calmette-Guerin DNA Vacciner and Interleukin-12 DNA Vaccine. *J. Urol.* **2004**, *171*, 1343–1347. [CrossRef]

180. Lee, C.; Chang, S.; Hsieh, D.; Yu, D. Treatment of bladder carcinomas using recombinant BCG DNA vaccines and electroporative gene immunotherapy. *Cancer Gene Ther.* **2004**, *11*, 194–207. [CrossRef]

181. Matsubara, H.; Mizutani, Y.; Hongo, F.; Nakanishi, H.; Kimura, Y.; Ushijima, S.; Kawauchi, A.; Tamura, T.; Sakata, T.; Miki, T. Gene therapy with TRAIL against renal cell carcinoma. *Mol. Cancer Ther.* **2006**, *5*, 2165–2172. [CrossRef]

182. Tamura, T.; Nishi, T.; Goto, T.; Takeshima, H.; Dev, S.B. Intratumoral Delivery of Interleukin 12 Expression Plasmids with In Vivo Electroporation Is Effective for Colon and Renal Cancer. *Hum. Gene Ther.* **2001**, *12*, 1265–1276. [CrossRef]

183. Wiesinger, M.; März, J.; Kummer, M.; Schuler, G.; Dörrie, J. Clinical-Scale Production of CAR-T Cells for the Treatment of Melanoma Patients by mRNA Transfection of a CSPG4-Specific CAR under Full GMP Compliance. *Cancers (Basel)* **2019**, *11*, 1198. [CrossRef]

184. Ingegnere, T.; Mariotti, F.R.; Pelosi, A.; Quintarelli, C. Human CAR NK Cells: A New Non-viral Method Allowing High Efficient Transfection and Strong Tumor Cell Killing. *Front. Immunol.* **2019**, *10*, 1–10. [CrossRef]

185. Schmidt-wolf, I.G.H.; Finke, S.; Trojaneck, B.; Denkena, A.; Lefterova, P.; Schwella, N.; Heuft, H.; Prange, G.; Korte, M. Phase I clinical study applying autologous immunological effector cells transfected with the interleukin-2 gene in patients with metastatic renal cancer, colorectal cancer and lymphoma. *Br. J. Cancer* **1999**, *81*, 1009–1016. [CrossRef] [PubMed]

186. Feldmann, A.; Arndt, C.; Bergmann, R.; Loff, S.; Cartellieri, M.; Bachmann, D.; Aliperta, R.; Hetzenecker, M.; Ludwig, F.; Albert, S.; et al. Retargeting of T lymphocytes to PSCA- or PSMA positive prostate cancer cells using the novel modular chimeric antigen receptor platform technology "UniCAR". *Oncotarget* **2017**, *8*, 31368–31385. [CrossRef] [PubMed]

187. Schepisi, G.; Cursano, M.C.; Casadei, C.; Menna, C.; Altavilla, A.; Lolli, C.; Cerchione, C.; Paganelli, G.; Santini, D.; Tonini, G.; et al. CAR-T cell therapy: A potential new strategy against prostate cancer. *J. Immunother. Cancer* **2019**, *7*, 258. [CrossRef] [PubMed]

188. Zhong, X.S.; Matsushita, M.; Plotkin, J.; Riviere, I.; Sadelain, M. Chimeric antigen receptors combining 4-1BB and CD28 signaling domains augment PI 3 kinase/AKT/Bcl-X L activation and CD8 T cell-mediated tumor eradication. *Mol. Ther.* **2010**, *18*, 413–420. [CrossRef]

189. Zhang, Q.; Tian, K.; Xu, J.; Zhang, H.; Li, L.; Fu, Q.; Chai, D.; Li, H.; Zheng, J. Synergistic Effects of Cabozantinib and EGFR-Specific CAR-NK-92 Cells in Renal Cell Carcinoma. *J. Immunol. Res.* **2017**, *2017*, 6915912. [CrossRef]

190. Prud'homme, G.J.; Glinka, Y.; Khan, A.S.; Draghia-akli, R. Electroporation-Enhanced Nonviral Gene Transfer for the Prevention or Treatment of Immunological, Endocrine and Neoplastic Diseases. *Curr. Gene Ther.* **2006**, *6*, 243–273. [CrossRef]

191. Mahendran, R.; Mun, S.; Esuvaranath, K. Gene Therapy in Urology. In *Gene Therapy Applications*; InTech: London, UK, 2011.

Praca nr 2

<u>**Tytuł**</u>

In Vitro Study of Calcium Microsecond Electroporation of Prostate Adenocarcinoma

<u>**Autorzy**</u>

Kiełbik, A., Szlasa, W., Michel, O., Szewczyk, A., Tarek, M., Saczko, J., & Kulbacka, J.

In Vitro Study of Calcium Microsecond Electroporation of Prostate Adenocarcinoma Cells

Aleksander Kiełbik [1] [iD]**, Wojciech Szlasa** [1] [iD]**, Olga Michel** [2]**, Anna Szewczyk** [2,3]**, Mounir Tarek** [4]**, Jolanta Saczko** [2] [iD] **and Julita Kulbacka** [2,*] [iD]

1   Faculty of Medicine, Wroclaw Medical University, 50-367 Wroclaw, Poland; aleksander.kielbik@outlook.com (A.K.); wojciech.szlasa@outlook.com (W.S.)
2   Department of Molecular and Cellular Biology, Wroclaw Medical University, 50-556 Wroclaw, Poland; olga.michel@umed.wroc.pl (O.M.); a.szewczyk@umed.wroc.pl (A.S.); jolanta.saczko@umed.wroc.pl (J.S.)
3   Department of Animal Developmental Biology, Institute of Experimental Biology, University of Wroclaw, 50-328 Wroclaw, Poland
4   Université de Lorraine, CNRS, LPCT, F-54000 Nancy, France; mounir.tarek@univ-lorraine.fr
*   Correspondence: Julita.Kulbacka@umed.wroc.pl; Tel.: +48-71-784-06-88

Abstract: Electroporation, applied as a non-thermal ablation method has proven to be effective for focal prostate treatment. In this study, we performed pre-clinical research, which aims at exploring the specific impact of this so-called calcium electroporation on prostate cancer. First, in an in-vitro study of DU 145 cell lines, microsecond electroporation (µsEP) parameters were optimized. We determined hence the voltage that provides both high permeability and viability of these prostate cancer cells. Subsequently, we compared the effect of µsEP on cells' viability with and without calcium administration. For high-voltage pulses, the cell death's mechanism was evaluated using flow-cytometry and confocal laser microscopy. For lower-voltage pulses, the influence of electroporation on prostate cancer cell mobility was studied using scratch assays. Additionally, we applied calcium-binding fluorescence dye (Fluo-8) to observe the calcium uptake dynamic with the fluorescence microscopy. Moreover, the molecular dynamics simulation visualized the process of calcium ions inflow during µsEP. According to our results calcium electroporation significantly decreases the cells viability by promoting apoptosis. Furthermore, our data shows that the application of pulsed electric fields disassembles the actin cytoskeleton and influences the prostate cancer cells' mobility.

Keywords: electroporation; calcium; prostate cancer; focal therapy

1. Introduction

Cell membrane integrity can be largely affected when the latter are exposed to pulsed electric fields (PEFs) of high enough intensity. The application of such electric pulses is believed to trigger formation of highly permeable spots (domains) in their lipid membrane [1,2]. This phenomenon is called electroporation (EP), and the changes induced depend on the intensity of the applied electric fields and can be either reversible, i.e., cells recover their integrity, or irreversible, in which case, the cells turn necrotic [3]. Electroporation has found use in the clinic as a non-thermal focal ablation method and has been applied as a minimal-invasive treatment of patients with internal organs tumors [4–6]. For focal prostate treatments, although several clinical trials showed promising results [7,8], IRE still remains at the investigation stage.

The reversible EP provides a broader spectrum of applications: It allows transfer of genes [9,10], drugs [11,12], small exogenous proteins, and other molecules [13,14]. It has been used, for instance,

in clinic to increase the uptake of cytostatic drugs in a procedure known as electrochemotherapy [15]. Recently, we have described the technique of electroporation-based treatments in urology [16] and its development perspectives.

To avoid the potential harmful systemic effects of electroporation, and other drawbacks such as the difficult preparation and storage of cytostatic drugs, the use of calcium ions has been proposed as an alternative to traditional electrochemotherapy. This novel method termed calcium electroporation (CaEP) had been first presented by Frandsen et al. (2012) [17] and in no time proved its effectiveness in vivo and in vitro for treatments of different cancers [18–20]. Currently, clinical trials involve the application of calcium electroporation for skin malignancies (clinicaltrials.gov #NCT04259658), as a neoadjuvant therapy for early colorectal cancer (clinicaltrials.gov #NCT03694080), as a palliative treatment of head and neck tumors (clinicaltrials.gov #NCT03051269) as well as for advanced, inoperable colorectal cancer (clinicaltrials.gov #NCT03542214).

The present in vitro study aims to evaluate the effect of CaEP on prostate cancer model. Every year over one million patients are diagnosed with prostate cancer (PCa) [21]. The prevalence and mortality rate of PCa increases significantly with age. 55% of all deaths due to PCa concerns patients older than 65 years [22]. Nevertheless, the common risk connected to low and arguably to medium-risk PCa is an overtreatment [23]. The vast prevalence of PCa calls for effective, safe, and minimally-invasive therapy [24]. The fast development of new imaging methods such as multiparametric magnetic resonance imaging inevitably increases the meaning of focal therapies in PCa treatment [25]. Furthermore, recent researches show that access to care and treatment significantly influences the survival rate of patients with prostate cancer [26]. Calcium electroporation requires only readily available calcium chloride and an adequate electric generator with electrodes. Accordingly its simplicity and affordable cost are an undeniable potential for CaEP to become an effective accessible treatment among populations of developing countries [27].

Calcium EP has proved in in vitro and in vivo trials to have a selective effect on cancer cells [28]. To enhance the selectivity, it is required to minimize the occurrence of irreversible electroporation and boost rather the reversible one. Note that during CaEP, the death of reversibly electroporated cells results mainly from calcium influx [29], and cancer cells, with impaired mechanisms of calcium homeostasis, are those predominantly damaged [30,31].

Primary, in this study, the electrical voltage on electrode promoting the reversible electroporation has been determined.

Different cancer types might present different sensitivity to CaEP [32]. To establish whether CaEP has potential as the focal PCa treatment, the impact of CaEP on prostate adenocarcinoma viability was evaluated. The research on other cell lines suggested that the interval time between the drug administration and electroporation may influence the effect of the therapy [33]. As the outcome varies depending on the cell type, consequently, in this study, the optimal time of drug administration has been investigated.

After the unsuccessful treatment of PCa, disease progress often involves the development of metastasis [34]. In around 20% of patients, the recurrence of PCa after the focal treatment with IRE occurs [35]. To prevent the progression of cancer to the metastatic stage, the therapy should decrease the cancer cell motility [36].

Calcium EP may trigger cell death through different mechanisms. The most commonly-evaluated are apoptosis and necrosis. The apoptosis as programmed cell death prevents the development of excessive immune reaction, providing the high selectivity of focal ablation [37]. Conversely, necrosis stimulates immune response resulting in local inflammation. For higher voltage, affecting cell viability, the prostate cancer cell death mechanism after electroporation was evaluated.

Finally, the study of CaEP investigates the dynamics of the process. Firstly, the time dependence between PEFs delivery and calcium influx as well as the dynamic of calcium efflux was observed under the fluorescence microscopy using the calcium-selective Fluo-8 dye. Secondly, microsecond CaEP

was analyzed with the in-silico molecular dynamic study. Both mentioned methods provide excellent insight and a better understanding of CaEP mechanism.

2. Results

2.1. Effects of PEFs on Cancer Cells Viability and Permeability

The impact of standalone microsecond short electric pulses was investigated on cancer cells suspended in the calcium free HEPES buffer. Figure 1 shows that the viability of cells decreases with the increasing intensity of the electric field. The most significant decrease occurs for electric fields intensities laying between 800 and 1200 V/cm. Note that even the highest electric field does not kill 100% of cancer cells. The curves indicate that permeability increases with higher electric fields intensities. The most significant increase in the permeability of the cells is detectable for fields between 400 and 800 V/cm. Above 1200 V/cm PEFs, almost all cells become permeable. Finally, the cells' permeability does not appear to increase remarkably between 1200 and 2000 V/cm.
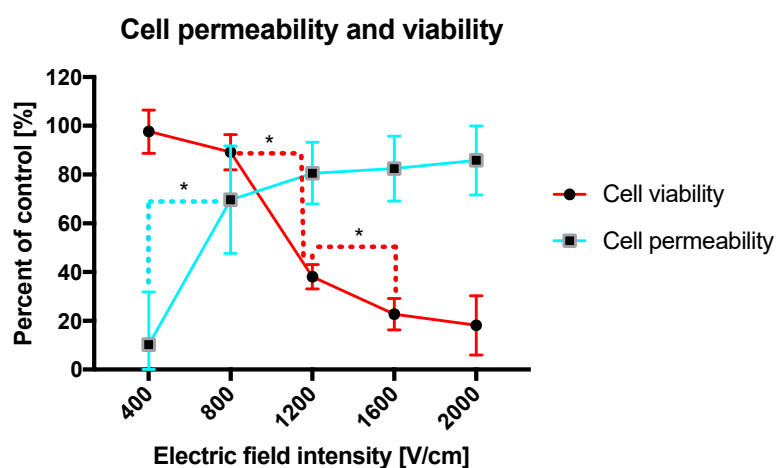
Figure 1. Viability and permeability of DU 145 cells as a function of electric field intensity. Suspended cells were electroporated in 4 mm cuvettes. The viability was assessed with MTT assay and permeability with YO-PRO®-1 uptake on the flow cytometry. Graphs are representative of 3 independent experiments. Data are mean ± SD (*n* = 3 independent experiments). (*) indicates statistically significant differences between the pair of samples electroporated with different electric field intensity (*t*-test, $p < 0.05$).

The results above enable the optimization of pulse parameters. The electric field intensity around 1000 V/cm provides the relatively high cell membrane permeability and does not decrease substantially the cell viability, indicating the highest ratio of reversibly electroporated cells. Once higher voltages on electrodes are applied, the cell permeability increases and viability decreases due probably to an irreversible electroporation of cancer cells.

2.2. The Influence of Time to Extracellular Calcium Application on CaEP Outcome

Figure 2 shows that the largest impact on the cells' viability is achieved when calcium is added 2 min before the PEFs delivery. The administration of calcium after electroporation has a much lower influence on cell viability.
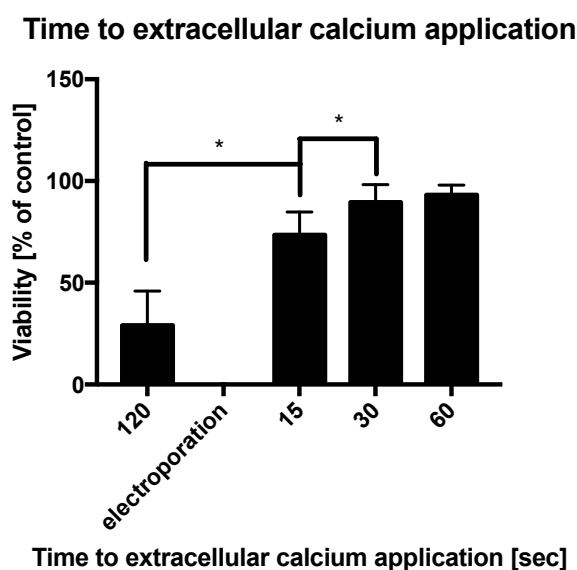
Time to extracellular calcium application

Figure 2. The influence of time to extracellular calcium application on DU 145 cells viability after exposure to pulsed electric fields (PEFs) (1000 V/cm). (*) indicates statistically significant differences between the pair of samples at a different time to calcium chloride administration (*t*-test, $p < 0.05$). Graphs are representative of 3 independent experiments. Data are mean ± SD (*n* = 3 independent experiments).

Overall, these initial data concerning the cells' viability and permeability as well as the time to drug administration enable the optimization of the applied EP protocol for further investigation.

2.3. Effect of CaEP on Cancer Viability

The viability of prostate cancer cells after CaEP was evaluated for different calcium concentrations namely 1 mM, 2 mM, and 5 mM and different pulse parameters (600 V/cm, 800 V/cm, 1000 V/cm, 1200 V/cm). Figure 3 shows viability of DU 145 cells after exposure to PEFs and calcium ions relative to control. Control represents the viability of not treated cells. The cytotoxic effect of the therapy increases with increasing electric field intensity. Higher calcium concentrations significantly lower the viability of the electroporated cells. This effect was not observed at the low electric field intensity of 600 V/cm. The synergistic effect of calcium seems to be most pronounced when 1000 V/cm PEFs follow the drug (Ca) administration. Finally, the standalone incubation with calcium ions without the application of PEFs does not change the viability of cancer cell.

2.4. Calcium Uptake Evaluation

To visualize the calcium uptake, we used the Fluo-8 dye. In cells, the latter is split by esterase to become fluorescent [38]. The intracellular calcium binds to the dye, increasing its fluorescence. The electric pulses of intensity ~800 V/cm were delivered after the onset of the data record. Figure 4 depicts the dynamic of the CaEP. During the delivery of the PEFs, the fluorescence starts to increase. The data indicates that the calcium uptake starts immediately after permeabilization. After reaching the optimum fluorescence, the cells begin to excrete calcium ions. At the beginning of reversion, the fluorescence undergoes an exponential decay and subsequently, the decay constant stabilizes.
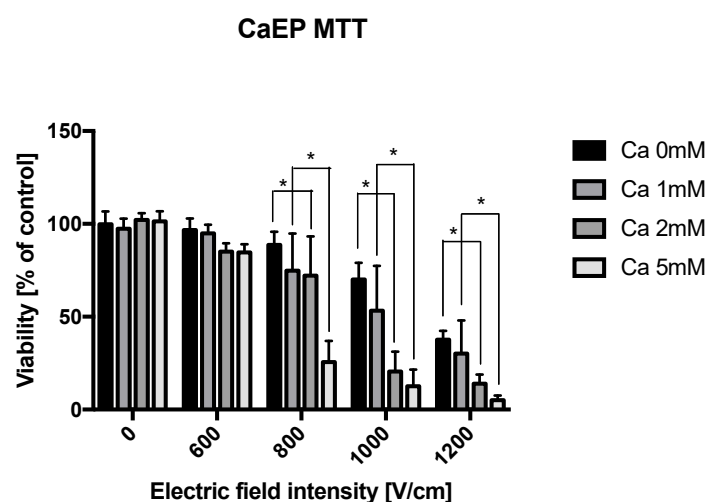
CaEP MTT

Figure 3. Viability of DU 145 cells after exposure to PEFs and calcium ions. The effect of EP was measured at three different calcium concentrations in HEPES buffer and HEPES buffer without calcium. Suspended cells were electroporated in 4 mm cuvettes. Graphs are representative of 3 independent experiments. Data are mean ± SD ($n = 3$ independent experiments). (*) indicates statistically significant differences between the samples at different calcium concentration (two-way analysis of variance (ANOVA) $p < 0.05$).

Calcium uptake by electroporation
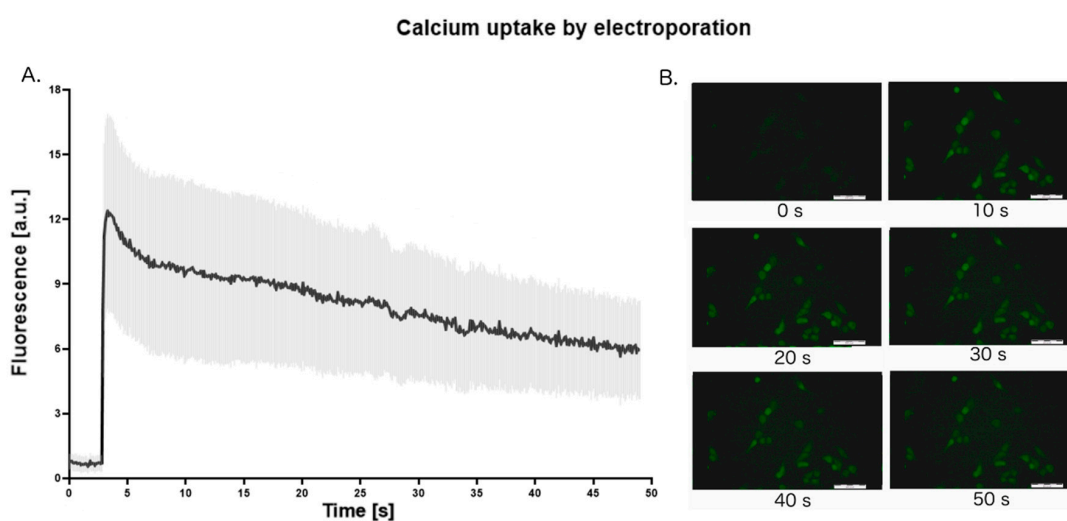
Figure 4. The dynamic of calcium uptake after microsecond electroporation (μsEP). The pulses were delivered after 3 s of initial observation. The whole observation period is 50 s. (**A**): The intensity of fluorescence as a function of time; (**B**): pictures of fluorescent cells taken every 10 s of observation. The graph represents the data form the three replicates of an individual experiment ($n = 3$ replicates).

2.5. Cell Death Quantification Assay after CaEP

To assess the mechanism of cell death following CaEP, we performed flow cytometry studies. 16 h after electroporation the cells were stained with Sytox Green dye and APC-Annexin V. The apoptosis was assessed by measuring the shift of phosphatidylserine to the outer leaflet of the cell membrane. Differently, late apoptotic and necrotic cells were stained with SYTOX™ Green—dye, which inflows only to the permeabilized cells and binds to cellular nucleic acids. Figure 5 shows that the CaEP affects tumor cells by triggering principally apoptosis. Calcium, when combined with PEFs, decreases further the viability of prostate cancer cells promoting hence apoptosis as well. The level of necrotic cells after the therapy does not differ among investigated samples.
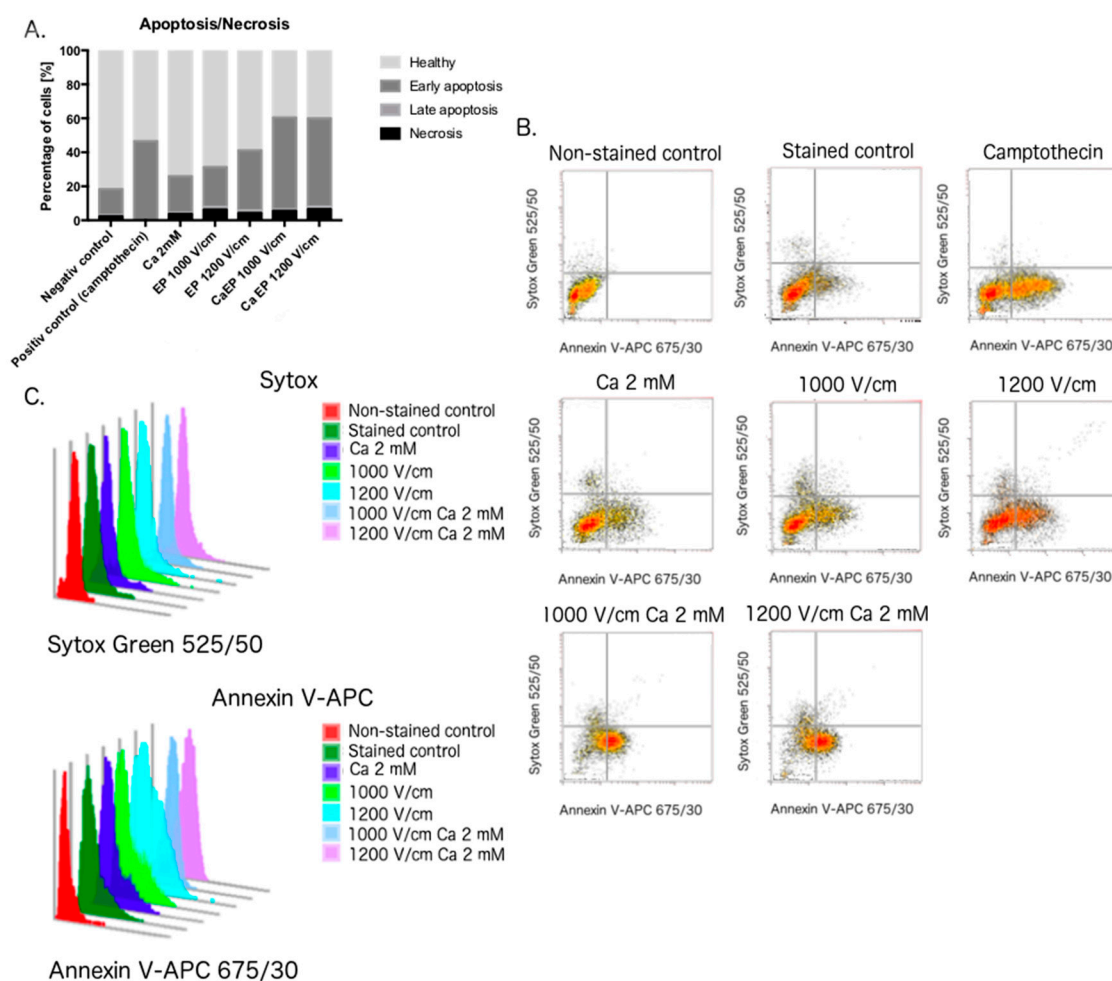
Figure 5. The distribution of apoptosis and necrosis in DU 145 cells after electroporation (EP) and CaEP measured by fluorescence of SYTOX™ Green and APC-Annexin V. The staining was performed 16 h after PEFs delivery. The graph represents the data form one individual experiment. (**A**): The distribution of healthy, early apoptotic, late apoptotic and necrotic cells after the treatment; (**B**): Flow cytometry dot plots. Each event is represented as a single point on a scatter-plot. Cells after 16 h incubation with camptothecin represent positive control for apoptosis. SYTOX™ Green fluorescence—forward scatter height; APC—Annexin V fluorescence—side scatter height; **C**: The overlay of histograms present fluorescence distribution for every sample.

2.6. Immunofluorescence Study of the Expression of Caspase-3

The immunofluorescence experiments were conducted to visualize the caspase-3 expression as key executor of apoptosis [39]. Caspase-3 can be activated via the intrinsic mitochondrial pathway (Bcl-2/Bax, Caspase-9), or via an extrinsic death receptor (Fas/FasL, Caspase-8) route [40]. Figure 6 shows that application of 600 V/cm PEFs with and without calcium does not change the expression of the caspase. In comparison, the fluorescence signal is remarkably stronger after the application of 1000 and 1200 V/cm PEFs (respectively 1.5-fold and 2.5-fold more intense compared to the control). Moreover, there is a difference in the expression between high-voltage PEFs with and without calcium. Namely, the 1000 and 1200 V/cm PEFs with 2 mM of calcium resulted in 2- and 1.25-fold higher fluorescence signal of caspase-3 (1000 V/cm + 2 mM vs. 1000 V/cm; 1200 + 2 mM vs. 1200 V/cm), respectively.
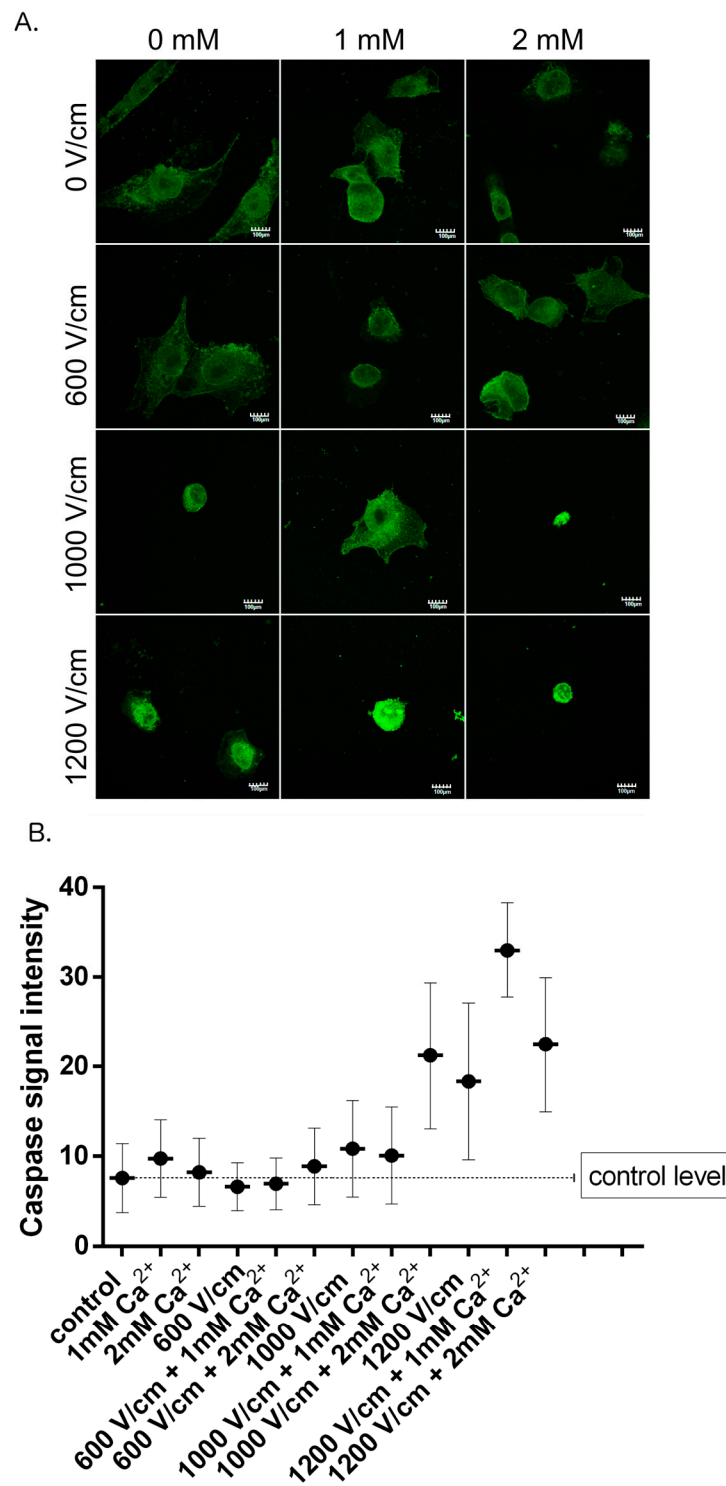
A.

B.

Figure 6. Confocal laser scanning microscopy (CLSM) visualization and intensity measurement of caspase 3 in DU 145 PCa cells after different therapy conditions. (**A**): CLSM pictures show the intensity of caspase-3 expression 16 h after the therapy; scale bar = 100 μm; (**B**): The caspase fluorescence signal intensity was analyzed by ImageJ software; The graph represents the data form the three replicates of an individual experiment. Data are mean ± SD (*n* = 3 replicates).

2.7. Effect of CaEP on Cancer cells Motility

The lower voltage PEFs affect the PCa cell viability significantly less, than the higher intensity electric fields. However, the application of low voltage PEFs has an effect on the mobility of cancer cells. Figure 7 reports the results of the wound healing assays. The cells were seeded inside the silicone inserts for 16 h before the latter were removed. The cells were scrutinized for 10 h until the separated colonies connected. The data shows that the application of PEFs impedes the mobility of cancer cell, while the effect has not been observed for lower-voltage CaEP. Noticeably, the effect of CaEP for higher intensity (1000 V/cm) PEFs could not be assessed as the protocol significantly influenced the cell's viability, precluding the comparison of the created wound. The short time incubation with calcium does not show on the other hand any remarkable effect on the cell mobility.
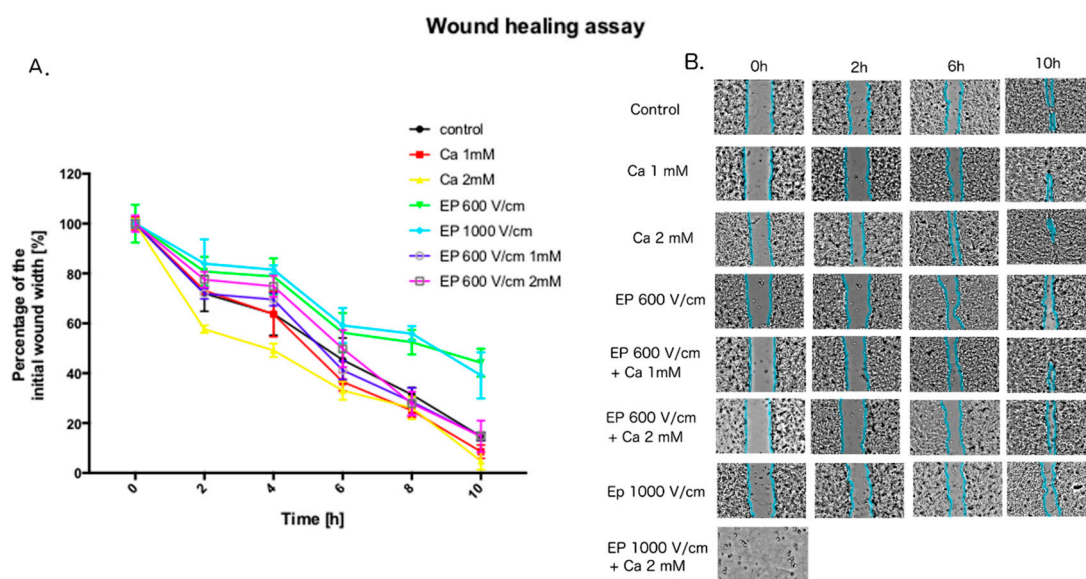
Figure 7. Effect of CaEP on cancer cell motility investigated with wound healing assay. The influence of different therapy protocols was investigated. (**A**): The percentage of a healed wound as a function of time. Images were analyzed by ImageJ software; (**B**): Images of wound gradually invaded by migrating cells. Images were taken in given time intervals. The graph represents the data form the three replicates of an individual experiment. Data are mean ± SD (*n* = 3 replicates).

2.8. Immunofluorescence Study of F-actin

The cells were stained 16 h after the treatment with fluorescein-conjugated phalloidin. Figure 8 shows that non-treated DU 145 cells present a typical organization of F-actin fibers spanning the cytosol. Standalone incubation with calcium in low concentrations, does not influence the cytoskeletal structure of the PCa cells. Higher voltage PEFs increase the number of dying cells that have degranulated and fragmented actin filaments. 16 h after application of a 1000 V/cm PEFs, a loss of stress fibers and rounding of the cells occurs. When submitted to higher-voltage calcium electroporation, the cells create typical honeycomb-like structures due to actin accumulation on the cell periphery.
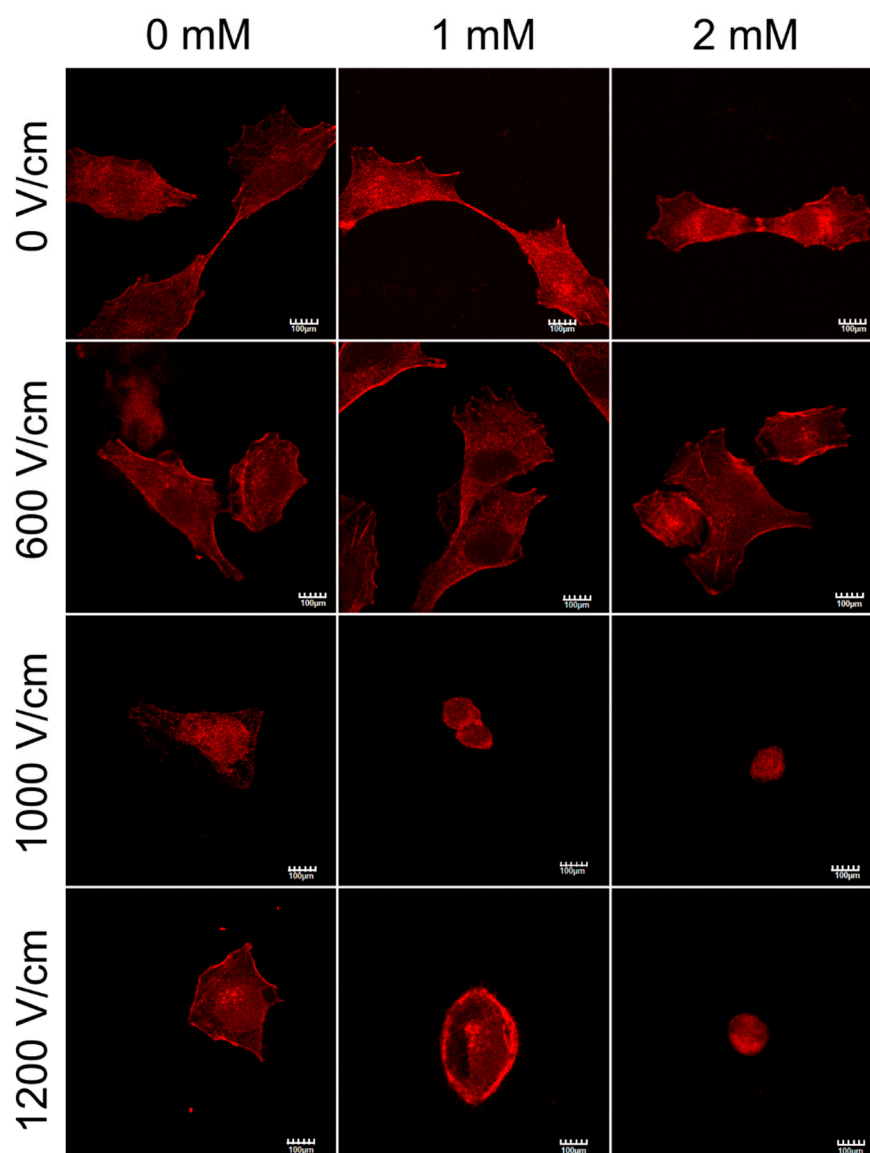
Figure 8. CLSM visualization F-actin structure in DU 145 prostate cancer (PCa) cells after different therapy conditions. Actin filaments were stained with fluorescein-conjugated phalloidin 16 h after the therapy; scale bar = 100 μm.

2.9. Molecular Dynamics Studies of CaEP

Molecular dynamic calculations were carried out to simulate the calcium ions distribution at the vicinity of the model lipid bilayer before and during electroporation. The microsecond electroporation was simulated by introducing the calcium ions imbalance (voltage) between the two compartments above and below the bilayer representing the extra and intra-cellular compartments. The electroporation process is visualized in Figure 9. Initially, calcium ions (green) show extramembrane localization (1). After an application of transmembrane voltage, the water molecules protrude to the membrane. Water fingers emerge on both sides of the lipid bilayer (2). Once, the water appendixes from both sides of the membrane contact, they form the water channel, which eventually spans the membrane. So, conducted electropores provide the possibility of calcium ions transport (3). With the increasing time of pore opening, more Ca^{2+} ions concentrate next to the pore opening, allowing more ions to cross the membrane (4).
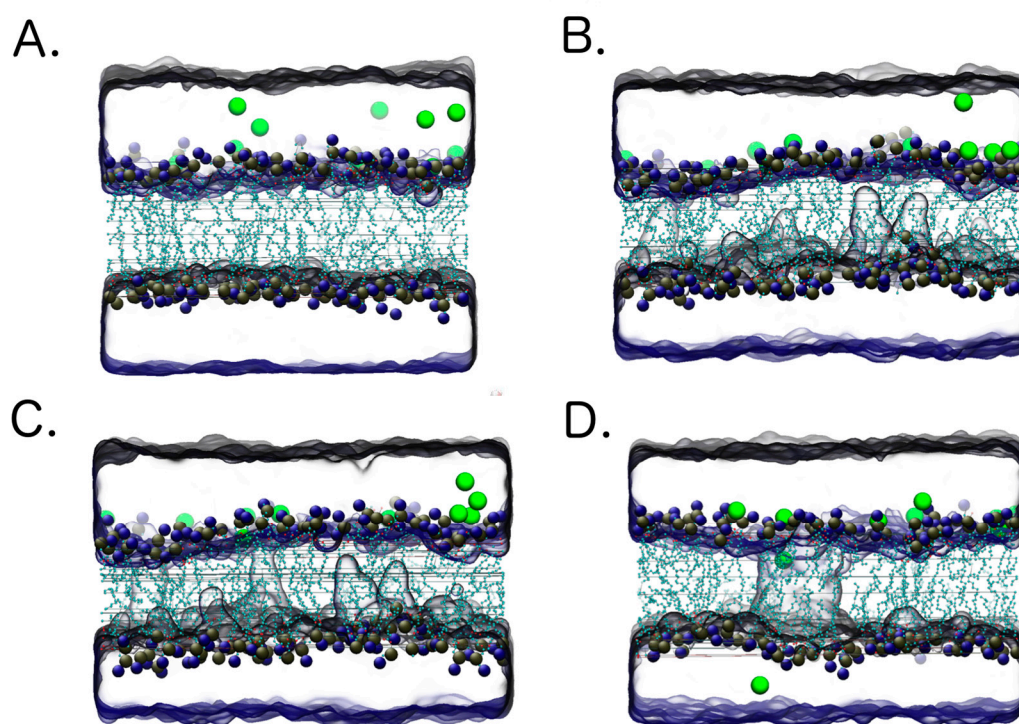
Figure 9. Molecular dynamics simulation of CaEP. Green molecules represent calcium ions. Numbers from (**A–D**) show the evolution of the process.

3. Discussion

The intracellular calcium level is up to a thousand-fold lower than the extracellular one. To maintain this difference, the energy accumulated in ATP is required [41]. Inside the cell, calcium acts as a second messenger in biochemical processes and coordinates the changes in protein confirmations, so its level is required to be strictly controlled [41]. The equilibrium of cytoplasmic Ca^{2+} level is maintained in concentrations about 20 to 40 nM [42].

Electroporation can be used to increase the uptake of calcium and destabilize cancer cells. It was shown that CaEP leads to cancer death, decreasing cellular ATP level [29]. Moreover, it was recently shown that CaEP has an immunomodulatory effect. It converts a tumor microenvironment reducing the number of suppressor cells and increasing cytotoxic T-lymphocytes activity [43]. Besides, calcium electroporation affects tumor vasculature damaging blood vessels and potentiates as well the necrosis of tumor in vivo [44].

In our study, CaEP is shown to decrease the viability of prostate cancer cells triggering apoptosis. High intensity electric fields and calcium concentration enhance the therapy outcome. The apoptosis was assessed by measuring the expression of phosphatidylserine on the cellular surface that binds Annexin V and was confirmed with immunostaining of caspase-3. The mechanism of death induced by CaEP differs between the results published in the literature. Namely, some studies report apoptosis [45,46], others necrosis [17,44]. It is not that surprising, when considering the role of calcium in various paths of cell death's mechanisms [47]. The main cause of death that triggered by standalone intracellular Ca^{2+} overload is generally apoptosis. Increased intracellular Ca^{2+} level activates chains of cell death effectors such as calcineurin, calpain, transglutaminase, endonucleases and phospholipases [48]. Moreover, Ca^{2+} overload results in permeabilization of the outer mitochondrial membrane, the release of mitochondrial proteins, and secondary activation of apoptotic events in other cellular compartments [49].

Necrosis due to calcium overload can also occur, however it would likely be a post-apoptotic necrosis where Ca^{2+} overload triggers caspase cleavage and inactivation of vital Ca^{2+}-extruding

proteins in the plasma membrane [48]. Recently, Gibot et al. (2020) have shown that the cell death after CaEP occurs as a result of mitochondrial dysfunction, without DNA damages, highlighting therefore the safety of such a therapy [50].

Importantly, our research shows that calcium, in order to strengthen the cytotoxic effect of the therapy, should be administrated before PEFs delivery. The effectiveness of CaEP on prostate DU 145 cell line is comparable to the one achieved on other cancer cell lines [17]. Most of the electroporation settings in the experiments followed the standard ESOPE protocol on EP, as it proved efficient and provides the possibility of outcome comparison between different trials [51]. Accordingly, only the applied voltage was adjusted to the initial results of cell permeability and viability after PEFs. In vivo studies showed that CaEP effect is more pronounced on an immunocompetent organism. The stimulation of the immune system results in an even complete tumor regression [52]. The next set of trials should investigate the in vivo effect of CaEP on prostate cancer.

Two classes of Ca^{2+} ATPases provide the stability of Ca^{2+} influx and efflux. In PCa cells the plasma membrane Ca^{2+} ATPase (PMCA) enables the transport of Ca^{2+} across the plasma membrane and SERCA transfer calcium within intracellular pools, as the one located in the endoplasmic reticulum [42]. The other mechanisms described of PCa Ca^{2+} clearance are the mitochondrial uniporter (MCU) and with a more limited scope the sodium-calcium exchanger (NCX) [53]. Moreover, the transient receptor potential superfamily (TRP) of cation channels and store-operated Ca^{2+}-permeable channels (SOC) contribute to Ca^{2+} homeostasis of PCa [54].

A different response to CaEP was observed for healthy cells compared to cancer cells [46,55]. Frandsen et al. (2017) suggested that the rationale behind this is the lower expression of PMCA among cancer cells. Reduced level of PMCA might impede the efflux of calcium ions which results in higher Ca^{2+} concentration in cancer cells after electroporation [30]. Considering prostate cancer, with the progression of PCa to androgen-independent state, the changes of Ca^{2+} homeostasis such us SERCA downregulation and increased Ca^{2+} leak from endoplasmic reticulum occurs [56]. Moreover, the down-regulation of MCU in PCa has been observed [57]. Therefore, prostate cancer cells might have the restricted potential to store intracellular Ca^{2+} in organelles, and consequently exhibit a high susceptibility to CaEP. Undoubtedly, further studies are needed to confirm this hypothesis.

In our study, electroporation with low voltage pulses decreases the mobility of prostate cancer cells in vitro. Surprisingly, the effect was not as prominent once cells are electroporated in presence of calcium at low concentration. However, an extracellular concentration of calcium up to 2 mM is more physiological than no calcium at all. Once low voltage PEFs are delivered, cells electroporated in medium with physiological level of calcium preserve their mobility properties.

The study investigates whether the cell mobility changes observed after EP can be partially due to actin filaments disruption. Actin filaments play an important role in cancer progression and mobility [58]. Calcium is a well-known modulator of the cytoskeleton of the cell plasma membranes. In this study, we have shown that an increased intracellular concentration of calcium enhances the EP-induced actin disruption after higher voltage PEFs. We did not observe any correlation between actin disruption and impeded mobility after an application of PEFs at lower voltage. Several studies investigated the impact of electroporation (with and without calcium) on actin filaments. However, the wide spectrum of possible alterations in cytoskeleton triggered by PEFs application indicates that the effects strongly depend on the cell type [59].

Our study proves that after the application of PEFs prostate cancer cells deal with calcium overload either by extrusion or reuptake into intracellular organelles. After a few seconds, the decay constant stabilizes and cells maintain the high level of intracellular calcium. The possible explanation of this phenomenon might be the beginning of the cells apoptosis, which results in higher concentration of intracellular calcium [60].

Research evaluating the calcium uptake confirmed that Ca^{2+} peaks can be achieved with single pulse delivery [61]. Moreover, even in a calcium-free medium, the peak can be observed. It was demonstrated that a single μs PEF increases the intracellular calcium level acting on the endoplasmic

reticulum [61]. Low-voltage CaEP, which does not affect cell viability, enables the investigation of Ca^{2+} level shifts and their impact on prostate cancer cells' physiology. In this cited study, the fluorescence intensity curve shape is similar to the one obtained in our experiment.

Used in our experimentFluo-8 dye might not be the optimal dye for measuring the calcium uptake after the electroporation. However, this dye indicates the changes in intracellular Ca^{2+}, which can occur either as a result of the inflow of extracellular Ca^{2+} or due to the release of Ca^{2+} from intracellular stores. The latter was not estimated in our study.

The live-cell calcium uptake experiments were performed on adherent cells. The adherent cells have a robust cytoskeleton, with cell-to-cell junctions. The cytoskeleton stabilizes the cell membrane and affects electroporation [62]. Moreover, the difference in shape between adherent cells and cells in suspension indicate that their transmembrane voltage in the same external electric field can differ [63]. Therefore, the calcium uptake curve of suspended cells might have a different shape. Accordingly, the results obtained from the calcium uptake study cannot support and explain the results and conclusion of the experiments performed on suspended cells.

Molecular dynamics simulations help model the phenomena through the numerical integration of multiple particle motion equations. In the case of CaEP it provides a mean of following at the molecular level the calcium uptake and the specifics of the calcium ions interactions with the lipid membrane [64]. Our model proves high affinity of the calcium ions to the bilayer, which results in the accumulation of the calcium beside the cells. We present that the process of calcium ions' transport through the membrane is sequential and not all of the ions penetrate the membrane at once, even though the ionic gradient is present. Moreover, the simulation shows that electroporation does not result in immediately alignment of intracellular and extracellular calcium. MD simulations have already proved that the presence of Ca^{2+} has almost no effect on the pore lifetime [65]. Calcium changes though the conductivity of the electroporation buffer and consequently might have an impact on transmembrane voltage generation [66]. This effect is more pronounced once nanosecond PEFs are applied.

Given the promising in vitro results, a series of clinical studies investigating the outcome of CaEP in vivo have been conducted. In the majority of such studies, a higher calcium concentration of 168 mM calcium was injected into tumor tissues [27]. The volume of injected calcium chloride solution was ~50% of the volume of the tumor [27]. First a CaEP double-blind Phase 2 study on patients with cutaneous metastases proved the effectiveness and safety of the treatment. The Ca^{2+} solution was injected intratumorally, and the EPs were delivered immediately after the calcium administration. No serious adverse events were observed. The outcome of the therapy on cutaneous metastases was similar to that of electrochemotherapy using bleomycin [18]. One case report describes the systematic immune response after the CaEP treatment [67]. In another Phase I study the effect of CaEP was studied on patients with recurrent head and neck cancer [19]. Following CaEP, no serious adverse events were reported. No signs of hypercalcemia, or cardiac arrhythmias were observed after the Ca^{2+} intratumoral injections. Clinical responses were observed in three out of six patients. Moreover, one patient remained without any clinical evidence of cancer during 12 months of observation. Calcium was also applied with IRE for internal organs tumor treatment [68]. Although restricted, the present clinical experience with CaEP did not show any serious side effect of the therapy, thus the CaEP can be further investigated in clinical trials also for broader spectrum of tumors.

The present experience with electroporation-based technologies for PCa treatment concerns predominantly IRE [16]. One case report describes the application of electrochemotherapy with satisfying results [69]. For PCa treatment, the electroporation is applied for focal cancer ablation or in case of spread tumor for the whole gland ablation. Potential candidates for the therapy are patients with intermediate-risk PCa [16]. The electrodes are inserted transperineally under the guidance of ultrasound [35]. During IRE protocols patients require general anesthesia and muscle relaxation [70]. Although effective, IRE not always provides the total oncological control of the tumor [8]. Considering promising results in vitro, EP with calcium has a chance to enhance the oncological outcome of the therapy.

4. Materials and Methods

4.1. Cell Cultures

The human prostate cancer cell line DU 145 was obtained from the American Type Culture Collection. Cells were grown in monolayer cultures in Eagle's Minimum Essential Medium, (EMEM, Sigma-Aldrich, Merck, Poznan, Poland) supplemented with 10% fetal bovine serum (FBS, Sigma-Aldrich) and antibiotics (penicillin/streptomycin; Sigma-Aldrich). Cells were kept under standard culture conditions at 37 °C in a humidified atmosphere containing 5% CO_2. The cells were regularly rinsed with PBS and harvested with 0.025% trypsin solution (EDTA; Sigma-Aldrich).

4.2. Preparation of the Calcium Solutions

The later were prepared from the stock solution of calcium ($CaCl_2$, Sigma-Aldrich dissolved in PBS (Sigma-Aldrich) at a concentration of 100 mM. Subsequently the required concentrations were achieved with dilution of stock in EP buffer to concentrations: 0 mM, 0.5 mM, 1 mM, 2 mM, 5 mM, and 10 mM.

4.3. Electroporation of Cells

The cells in the concentration of 5×10^5 cells/mL were suspended in 300 µL HEPES buffer (10 mM HEPES (Lonza), 250 mM sucrose, and 1 mM $MgCl_2$ in sterile water) with different concentration $CaCl_2$ or in calcium free HEPES for controls. The cells were placed in a 4 mm cuvettes (BTX, Syngen Biotech, Poland). The square wave electroporator was used to deliver the electric pulses (ECM830 Square Wave Electroporation System; BTX, Syngen Biotech, Wroclaw, Poland). The cells were exposed to 8 pulses of 100 µs, 1 Hz, and 400, 800, 1200, 1600, or 2000 V/cm. Subsequently, the cells were incubated for 20 min and then suspended in the culture medium and placed in 96 or 6 well plates. All measurements were performed after a 24 h incubation.

4.4. Cell Viability Assay

To determine the cell viability, the activity of mitochondrial dehydrogenases was measured with MTT assays. First, the electroporation of suspended cells was performed following the protocol described above. Subsequently, after a 24 h incubation, the culture medium from 96 well plate was removed, and 100 µL of 0.5 mg/mL MTT (3-(4,5-dimethylthiazol-2-yl)-2,5-diphenyltetrazolium bromide, Sigma) in PBS buffer was added. After 3 h of incubation at 37 °C, a 100 µL acidified isopropanol (0.04 M HCl in the absolute isopropanol) was added to dissolve formazan crystals. Finally, the multiplate reader (GlowMax, Promega, Walldorf, Germany) was used to measure the absorbance at 570 nm. The results were expressed as the percentage of viable cells relative to untreated (control) cells.

4.5. Evaluation of the Influence of Time to Drug Administration on CaEP Outcome

Calcium chloride was added to the cell suspensions in cuvettes in different time intervals relative to electroporation. Each time, the final concentration of 2 mM calcium in buffer was achieved. To electroporate the cells, 1000 V/cm pulses were delivered according to the protocol described above. The cell viability was measured according to the viability assay.

4.6. Cell Permeability Quantification Assay

The cells were electroporated according to the protocol described above. Prior to electroporation, the green-fluorescent dye YO-PRO®-1 stain (Y3603, Thermo Fisher Scientific Inc., Warsaw, Poland) in the concentration of 100 µL/L was added to buffer. YO-PRO®-1 cellular uptake reflects the degree of the plasma membrane permeabilization [71]. The EP cells were then centrifuged and diluted in 0.5 mL PBS. The green Fluorescent intensities were detected on the Cube 6 flow cytometer. YO-PRO was

excited with a 488 nm laser and measured with the FL-1- detector (525/50). The results are expressed as the percentage of permeabilized cells.

4.7. Cell Death Quantification Assay

The cell death mechanism was detected with flow cytometry. The cells were electroporated according to the description above and left incubating in the culture medium for 24 h. In the next step, the cells were harvested with trypsin and centrifuged. Subsequently, the cells were resuspended in 0.5 mL PBS containing SYTOX™ Green Nucleic Acid Stain (Thermo Fisher Scientific, Warsaw, Poland) and APC bounded Annexin V from the APC Annexin V Apoptosis Detection Kit (BioLegend, San Diego, CA, USA) as described in BioLegend instructions. Flow cytometry was performed with a Cube 6 flow cytometer. The fluorescence of Sytox was excited with a 488 nm laser and measured with the FL-1 detector (525/50) and APC fluorescence was excited with 640 nm laser and measured with the FL-4 detector (675/30).

4.8. Calcium Uptake Evaluation

A volume of 50 μL of cell suspension in the concentration of 10^5 cells/mL was placed on the microscope slide. After 24 h the medium was removed, cells were stained with 4 μM Fluo-8 diluted in PBS and left incubating for 20 min. The slide was placed on the microscope stage with the electrode touching its surface. Cells visible in the objective were directly placed between two needles of the electrode BTX533 (BTX, Syngen Biotech, Poland). The PBS on the microscope slide was replaced with electroporation buffer HEPES with calcium at a 2 mM concentration. Subsequently, the cells were electroporated according to the protocol with field intensity reaching around 1000 V/cm. The increase in cell fluorescence during the electroporation was observed with the fluorescent microscope Olympus BX53F2 (Olympus, Tokyo, Japan). The changes in cell fluorescence were evaluated with ImageJ [72].

4.9. Immunofluorescence Studies of Actin Cytoskeleton and Caspase-3 Expression

The cells were electroporated according to the protocol described above. Subsequently the cells were seeded on glass coverslips places in 6 well plate and incubated for 16 h at 37 °C and 5% CO_2. then the samples were washed with PBS (BioShop, dist. Lab Empire, Rzeszow, Poland), fixed in 4% formaldehyde (Roth, Germany) and washed with PBS again.

For the caspase-3 expression assessment, following fixation, the cells were incubated for 5 min with PBS with 1% Triton 100X, washed with PBS and left for 60 min with 1% HS, and the primary anti-caspase 3 antibody (1:100, sc-7272, Abcam, UK), diluted in PBS and incubated for 60 min at 37 °C and 5% CO_2. Subsequently, the samples were washed 3 times with PBS, and incubated with Alexa Fluor 488 secondary anti-mouse antibody (Ex. 490 nm, Em. 525 nm; 2 μg/mL, A11029, Invitrogen) for 60 min at 37 °C and 5% CO_2. After the washing in PBS, the cells were mounted with DAPI Mounting Medium (Roth, Germany).

For the actin cytoskeleton staining, the cells were incubated for 5 min with PBS with 1% Triton 100X, washed in PBS and left for 60 min with 1% HS, and the Alexa Fluor™ 594 Phalloidin (Ex. 581 nm, Em. 609 nm; 2 μg/mL, A22283, Life Sciences—Thermo Fisher Scientific), diluted in PBS and incubated for 60 min at 37 °C and 5% CO_2. After washing in PBS, the cells were mounted with DAPI Mounting Medium (Roth, Germany).

The samples were analyzed with a confocal laser scanning microscope with using laser wavelengths: 405 nm, 473 nm and 559 nm; 60X oil immersion objective lens with 1.35 NA (Olympus FluoViewer 1000, Tokyo, Japan).

4.10. Wound Healing Assay

To investigate the effect of CaEP on the migratory capacity of cells, the wound healing assay was performed. The cells were electroporated following the protocol described above. After EP, the cells were centrifugated and diluted in the culture medium. The silicone insert was applied in to form a

500-μm ± 50 μm cell-free space between colonies. Cells were incubated at 5% CO_2 and 37 °C for 16 h to stick to the bottom and create the monolayer. Subsequently, the silicone insert was removed. Images of the wounds were captured directly after insert removal and after 2, 4, 6, 8, and 10 h of observation on Leica light microscope (DMi1, Watzlar, Germany).

4.11. Molecular Dynamics Simulations

The MD simulations were performed using the GROMACS 2018.3 software on the computational cluster at the Department of Theoretical Chemistry and Physics of the University of Lorraine. The systems were prepared with the CHARMM-GUI software and visually inspected with VMD. The membrane model was composed of a lipid bilayer composed of 40% POPC, 30% POPEE, 16% POPCE, 4% POPCE, and 10% Cholesterol. 10 calcium ions were added to the system, by replacing two Na^+ cations for one calcium ion in the NaCl solution. The system was initially minimized and equilibrated. Afterwards, 100 ns additional equilibration at constant temperature and constant pressure (NPT simulation) was applied to achieve the lack of surface tension across the simulated membrane. In order to induce transmembrane voltage and mimic the conditions of the EP experiments, we followed the protocols of the charge imbalance developed recently [73,74]: The box size was first extended in the *z*-axis to separate both water baths. Next, a short (10 ns) constant volume and constant temperature (NVT simulation) was performed to evaluate the surface tension on the vacuum-water interphase. This surface tension was applied in the subsequent constant temperature and constant surface tension (NPγT) simulation protocol, which was used to simulate electroporation and still allow as in experiment for a complete relaxation of the membrane surface tension. An ion imbalance of 8 electric charges was applied to induce a transmembrane potential large enough to induce the lipid bilayer electroporation. The simulation described was conducted for over 10 ns and the results were analyzed and visualized using VMD.

4.12. Statistical Analysis

The statistical analysis was performed using the GraphPad Prism 7 (La Jolla, CA, USA). Differences in cell viability were analyzed by two- way ANOVA or student *t*-test depending on the experiment. Results were expressed as mean ± standard deviation of the mean and with $p < 0.05$ being considered statistically significant.

5. Conclusions

This research confirms that calcium electroporation is a potent anti-PCa therapy in vitro. In the future it could potentially be used as an alternative, minimally-invasive focal therapy for prostate cancer. The hallmark of the CaEP is its safety and relatively easy applicability. In the nearest future, we can expect more data from clinical trials, and in case of promising results, extending the therapy to other cancers such prostate adenocarcinoma.

References

1. Neumann, E.; Rosenheck, K. Permeability changes induced by electric impulses in vesicular membranes. *J. Membr. Biol.* **1972**, *10*, 279–290. [CrossRef] [PubMed]
2. Sale, J.H.; Hamilton, W.A. Effects of high electric fields on micro-organisms III. Lysis of erythrocytes and protoplasts. *Biochim. Biophys. Acta* **1968**, *163*, 37–43. [CrossRef]
3. Davalos, R.V.; Mir, L.M.; Rubinsky, B. Tissue Ablation with Irreversible Electroporation. *Ann. Biomed. Eng.* **2005**, *33*, 223–231. [CrossRef]
4. Kalra, N.; Gupta, P.; Gorsi, U.; Bhujade, H.; Chaluvashetty, S.B.; Duseja, A.; Singh, V.; Dhiman, R.K.; Chawla, Y.K.; Khandelwal, N. Irreversible Electroporation for Unresectable Hepatocellular Carcinoma: Initial Experience. *Cardiovasc. Interv. Radiol.* **2019**, *42*, 584–590. [CrossRef] [PubMed]
5. Ruarus, A.H.; Vroomen, L.G.P.H.; Geboers, B.; Van Veldhuisen, E.; Puijk, R.S.; Nieuwenhuizen, S.; Besselink, M.G.; Zonderhuis, B.M.; Kazemier, G.; De Gruijl, T.D.; et al. Percutaneous Irreversible Electroporation in Locally Advanced and Recurrent Pancreatic Cancer (PANFIRE-2): A Multicenter, Prospective, Single-Arm, Phase II Study. *Radiology* **2020**, *294*, 212–220. [CrossRef]
6. Trimmer, C.K.; Khosla, A.; Morgan, M.; Stephenson, S.L.; Ozayar, A.; Cadeddu, J.A. Minimally Invasive Percutaneous Treatment of Small Renal Tumors with Irreversible Electroporation: A Single-Center Experience. *J. Vasc. Interv. Radiol.* **2015**, *26*, 1465–1471. [CrossRef]
7. Van Den Bos, W.; Scheltema, M.J.; Siriwardana, A.R.; Kalsbeek, A.M.F.; Thompson, J.; Ting, F.; Böhm, M.; Haynes, A.-M.; Shnier, R.; Delprado, W.; et al. Focal irreversible electroporation as primary treatment for localized prostate cancer. *BJU Int.* **2017**, *121*, 716–724. [CrossRef]
8. Blazevski, A.; Scheltema, M.J.; Yuen, B.; Masand, N.; Nguyen, T.V.; Delprado, W.; Shnier, R.; Haynes, A.-M.; Cusick, T.; Thompson, J.; et al. Oncological and Quality-of-life Outcomes Following Focal Irreversible Electroporation as Primary Treatment for Localised Prostate Cancer: A Biopsy-monitored Prospective Cohort. *Eur. Urol. Oncol.* **2020**, *3*, 283–290. [CrossRef]
9. Rosazza, C.; Meglic, S.H.; Zumbusch, A.; Rols, M.-P.; Miklavcic, D. Gene Electrotransfer: A Mechanistic Perspective. *Curr. Gene Ther.* **2016**, *16*, 98–129. [CrossRef]
10. Daud, A.I.; DeConti, R.C.; Andrews, S.; Urbas, P.; Riker, A.I.; Sondak, V.K.; Munster, P.N.; Sullivan, D.M.; Ugen, K.E.; Messina, J.L.; et al. Phase I Trial of Interleukin-12 Plasmid Electroporation in Patients With Metastatic Melanoma. *J. Clin. Oncol.* **2008**, *26*, 5896–5903. [CrossRef]
11. Mir, L.M.; Orlowski, S.; Belehradek, J.; Paoletti, C. Electrochemotherapy potentiation of antitumour effect of bleomycin by local electric pulses. *Eur. J. Cancer Clin. Oncol.* **1991**, *27*, 68–72. [CrossRef]
12. Miklavčič, D.; Mali, B.; Kos, B.; Heller, R.; Sersa, G. Electrochemotherapy: From the drawing board into medical practice. *Biomed. Eng. Online* **2014**, *13*, 29. [CrossRef] [PubMed]
13. Chakrabarti, R.; E Wylie, D.; Schuster, S.M. Transfer of monoclonal antibodies into mammalian cells by electroporation. *J. Biol. Chem.* **1989**, *264*, 15494–15500.
14. Kinosita, K.; Tsong, T.Y. Survival of sucrose-loaded erythrocytes in the circulation. *Nat. Cell Biol.* **1978**, *272*, 258–260. [CrossRef] [PubMed]
15. Cemazar, M.; Sersa, G. Recent Advances in Electrochemotherapy. *Bioelectricity* **2019**, *1*, 204–213. [CrossRef]
16. Kiełbik, A.; Szlasa, W.; Saczko, J.; Kulbacka, J. Electroporation-Based Treatments in Urology. *Cancers* **2020**, *12*, 2208. [CrossRef]
17. Frandsen, S.K.; Gissel, H.; Hojman, P.; Tramm, T.; Eriksen, J.; Gehl, J. Direct Therapeutic Applications of Calcium Electroporation to Effectively Induce Tumor Necrosis. *Cancer Res.* **2012**, *72*, 1336–1341. [CrossRef]
18. Falk, H.; Matthiessen, L.; Wooler, G.; Gehl, J. Calcium electroporation for treatment of cutaneous metastases; a randomized double-blinded phase II study, comparing the effect of calcium electroporation with electrochemotherapy. *Acta Oncol.* **2017**, *57*, 311–319. [CrossRef]
19. Plaschke, C.C.; Gehl, J.; Johannesen, H.H.; Fischer, B.M.; Kjaer, A.; Lomholt, A.F.; Wessel, I. Calcium electroporation for recurrent head and neck cancer: A clinical phase I study. *Laryngoscope* **2019**, *4*, 49–56. [CrossRef]
20. Ágoston, D.; Baltás, E.; Ócsai, H.; Rátkai, S.; Lázár, P.G.; Korom, I.; Varga, E.; Nemeth, I.B.; Viharosné, É.D.-R.; Gehl, J.; et al. Evaluation of Calcium Electroporation for the Treatment of Cutaneous Metastases: A Double Blinded Randomised Controlled Phase II Trial. *Cancers* **2020**, *12*, 179. [CrossRef]
21. Rawla, P. Epidemiology of Prostate Cancer. *World J. Oncol.* **2019**, *10*, 63–89. [CrossRef] [PubMed]

22. Zerlay, J.; Colombet, M.; Soerjomataram, I.; Mathers, C.; Parkin, D.M.; Piñeros, M.; Znaor, A.; Bray, F. Estimating the global cancer incidence and mortality in 2018: GLOBOCAN sources and methods. *Int. J. Cancer* **2018**, *144*, 1941–1953. [CrossRef]

23. Hamdy, F.C.; Donovan, J.L.; Lane, J.A.; Mason, M.; Metcalfe, C.; Holding, P.; Davis, M.; Peters, T.J.; Turner, E.L.; Martin, R.M.; et al. 10-Year Outcomes after Monitoring, Surgery, or Radiotherapy for Localized Prostate Cancer. *N. Engl. J. Med.* **2016**, *375*, 1415–1424. [CrossRef] [PubMed]

24. Donaldson, I.A.; Alonzi, R.; Barratt, D.; Barret, E.; Berge, V.; Bott, S.; Bottomley, D.; Eggener, S.; Ehdaie, B.; Emberton, M.; et al. Focal Therapy: Patients, Interventions, and Outcomes—A Report from a Consensus Meeting. *Eur. Urol.* **2015**, *67*, 771–777. [CrossRef] [PubMed]

25. Nassiri, N.; Chang, E.; Lieu, P.; Priester, A.M.; Margolis, D.J.A.; Huang, J.; Reiter, R.E.; Dorey, F.J.; Marks, L.S.; Natarajan, S. Focal Therapy Eligibility Determined by Magnetic Resonance Imaging/Ultrasound Fusion Biopsy. *J. Urol.* **2018**, *199*, 453–458. [CrossRef] [PubMed]

26. Krimphove, M.J.; Cole, A.P.; Fletcher, S.A.; Harmouch, S.S.; Berg, S.; Lipsitz, S.R.; Sun, M.; Nabi, J.; Nguyen, P.L.; Hu, J.C.; et al. Evaluation of the contribution of demographics, access to health care, treatment, and tumor characteristics to racial differences in survival of advanced prostate cancer. *Prostate Cancer Prostatic Dis.* **2018**, *22*, 125–136. [CrossRef] [PubMed]

27. Frandsen, S.K.; Vissing, M.; Gehl, J. A Comprehensive Review of Calcium Electroporation—A Novel Cancer Treatment Modality. *Cancers* **2020**, *12*, 290. [CrossRef]

28. Frandsen, S.K.; Gehl, J. A Review on Differences in Effects on Normal and Malignant Cells and Tissues to Electroporation-Based Therapies: A Focus on Calcium Electroporation. *Technol. Cancer Res. Treat.* **2018**, *17*, 1–6. [CrossRef]

29. Hansen, E.L.; Sözer, E.B.; Romeo, S.; Frandsen, S.K.; Vernier, P.T.; Gehl, J. Correction: Dose-Dependent ATP Depletion and Cancer Cell Death following Calcium Electroporation, Relative Effect of Calcium Concentration and Electric Field Strength. *PLoS ONE* **2015**, *10*, e0128034. [CrossRef]

30. Frandsen, S.K.; Krüger, M.B.; Mangalanathan, U.M.; Tramm, T.; Mahmood, F.; Novak, I.; Gehl, J. Normal and Malignant Cells Exhibit Differential Responses to Calcium Electroporation. *Cancer Res.* **2017**, *77*, 4389–4401. [CrossRef]

31. Szewczyk, A.; Gehl, J.; Daczewska, M.; Saczko, J.; Frandsen, S.K.; Kulbacka, J. Calcium electroporation for treatment of sarcoma in preclinical studies. *Oncotarget* **2018**, *9*, 11604–11618. [CrossRef] [PubMed]

32. Frandsen, S.K.; Gissel, H.; Hojman, P.; Eriksen, J.; Gehl, J. Calcium electroporation in three cell lines: A comparison of bleomycin and calcium, calcium compounds, and pulsing conditions. *Biochim. Biophys. Acta (BBA)-Gen. Subj.* **2014**, *1840*, 1204–1208. [CrossRef] [PubMed]

33. Hoejholt, K.L.; Mužić, T.; Jensen, S.D.; Dalgaard, L.T.; Bilgin, M.; Nylandsted, J.; Heimburg, T.; Frandsen, S.K.; Gehl, J. Calcium electroporation and electrochemotherapy for cancer treatment: Importance of cell membrane composition investigated by lipidomics, calorimetry and in vitro efficacy. *Sci. Rep.* **2019**, *9*, 4758. [CrossRef] [PubMed]

34. Walsh, P.C. Re: The Natural History of Metastatic Progression in Men with Prostate-Specific Antigen Recurrence After Radical Prostatectomy: Long-Term Follow-up. *J. Urol.* **2012**, *188*, 809. [CrossRef]

35. Blazevski, A.; Scheltema, M.J.; Amin, A.; Thompson, J.; Lawrentschuk, N.; Stricker, P.D. Irreversible electroporation (IRE): A narrative review of the development of IRE from the laboratory to a prostate cancer treatment. *BJU Int.* **2019**, *125*, 369–378. [CrossRef]

36. Palmer, T.D.; Ashby, W.J.; Lewis, J.D.; Zijlstra, A. Targeting tumor cell motility to prevent metastasis. *Adv. Drug Deliv. Rev.* **2011**, *63*, 568–581. [CrossRef]

37. Brock, R.M.; Beitel-White, N.; Davalos, R.V.; Allen, I.C. Starting a Fire without Flame: The Induction of Cell Death and Inflammation in Electroporation-Based Tumor Ablation Strategies. *Front. Oncol.* **2020**, *10*, 1235. [CrossRef]

38. Bioquest®, A. Fluo-8®Calcium Reagents and Screen Quest TM Fluo-8 NW Calcium Assay Kits. Available online: https://docs.aatbio.com/products/protocol/A3300d1.pdf (accessed on 24 June 2020).

39. Rudel, T. Caspase inhibitors in prevention of apoptosis. *Herz* **1999**, *24*, 236–241. [CrossRef]

40. Li, J.S.; Yuan, J. Caspases in apoptosis and beyond. *Oncogene* **2008**, *27*, 6194–6206. [CrossRef]

41. Clapham, D.E. Calcium Signaling. *Cell* **2007**, *131*, 1047–1058. [CrossRef]

42. Furuya, Y.; Lundmo, P.; Short, A.D.; Gill, D.L.; Isaacs, J.T. The role of calcium, pH, and cell proliferation in the programmed (apoptotic) death of androgen-independent prostatic cancer cells induced by thapsigargin. *Cancer Res.* **1994**, *54*, 6167–6175. [PubMed]

43. Novickij, V.; Čėsna, R.; Perminaitė, E.; Zinkevičienė, A.; Characiejus, D.; Novickij, J.; Šatkauskas, S.; Ruzgys, P.; Girkontaitė, I. Antitumor Response and Immunomodulatory Effects of Sub-Microsecond Irreversible Electroporation and Its Combination with Calcium Electroporation. *Cancers* **2019**, *11*, 1763. [CrossRef] [PubMed]

44. Staresinic, B.; Jesenko, T.; Kamensek, U.; Frandsen, S.K.; Sersa, G.; Gehl, J.; Cemazar, M. Effect of calcium electroporation on tumour vasculature. *Sci. Rep.* **2018**, *8*, 9412. [CrossRef] [PubMed]

45. Szewczyk, A.; Saczko, J.; Kulbacka, J. Apoptosis as the main type of cell death induced by calcium electroporation in rhabdomyosarcoma cells. *Bioelectrochemistry* **2020**, *136*, 107592. [CrossRef] [PubMed]

46. Zielichowska, A.; Daczewska, M.; Saczko, J.; Michel, O.; Kulbacka, J. Applications of calcium electroporation to effective apoptosis induction in fibrosarcoma cells and stimulation of normal muscle cells. *Bioelectrochemistry* **2016**, *109*, 70–78. [CrossRef] [PubMed]

47. Verkhratsky, A. Calcium Signalling and Disease. *Sub-Cell. Biochem.* **2007**, *45*, 465–480. [CrossRef]

48. Zhivotovsky, B.; Orrenius, S. Calcium and cell death mechanisms: A perspective from the cell death community. *Cell Calcium* **2011**, *50*, 211–221. [CrossRef]

49. Cerella, C.; Diederich, M.; Ghibelli, L. The Dual Role of Calcium as Messenger and Stressor in Cell Damage, Death, and Survival. *Int. J. Cell Biol.* **2010**, *2010*, 1–14. [CrossRef]

50. Gibot, L.; Montigny, A.; Baaziz, H.; Fourquaux, I.; Audebert, M.; Rols, M.-P. Calcium Delivery by Electroporation Induces In Vitro Cell Death through Mitochondrial Dysfunction without DNA Damages. *Cancers* **2020**, *12*, 425. [CrossRef]

51. Romeo, S.; Sannino, A.; Scarfì, M.R.; Vernier, P.T.; Cadossi, R.; Gehl, J.; Zeni, O. ESOPE-Equivalent Pulsing Protocols for Calcium Electroporation: An In Vitro Optimization Study on 2 Cancer Cell Models. *Technol. Cancer Res. Treat.* **2018**, *17*, 1–10. [CrossRef]

52. Falk, H.; Forde, P.F.; Bay, M.L.; Mangalanathan, U.M.; Hojman, P.; Soden, D.M.; Gehl, J. Calcium electroporation induces tumor eradication, long-lasting immunity and cytokine responses in the CT26 colon cancer mouse model. *OncoImmunology* **2017**, *6*, e1301332. [CrossRef] [PubMed]

53. Wolf, A.; Wennemuth, G. Ca^{2+} clearance mechanisms in cancer cell lines and stromal cells of the prostate. *Prostate* **2013**, *74*, 29–40. [CrossRef] [PubMed]

54. Flourakis, M.; Prevarskaya, N. Insights into Ca^{2+} homeostasis of advanced prostate cancer cells. *Biochim. Biophys. Acta (BBA)-Bioenergy* **2009**, *1793*, 1105–1109. [CrossRef] [PubMed]

55. Frandsen, S.K.; Gibot, L.; Madi, M.; Gehl, J.; Rols, M.-P. Calcium Electroporation: Evidence for Differential Effects in Normal and Malignant Cell Lines, Evaluated in a 3D Spheroid Model. *PLoS ONE* **2015**, *10*, e0144028. [CrossRef] [PubMed]

56. Prevarskaya, N.; Skryma, R.; Shuba, Y. Ca^{2+} homeostasis in apoptotic resistance of prostate cancer cells. *Biochem. Biophys. Res. Commun.* **2004**, *322*, 1326–1335. [CrossRef] [PubMed]

57. Cui, C.; Merritt, R.; Fu, L.; Pan, Z. Targeting calcium signaling in cancer therapy. *Acta Pharm. Sin. B* **2017**, *7*, 3–17. [CrossRef]

58. Olson, M.F.; Sahai, E. The actin cytoskeleton in cancer cell motility. *Clin. Exp. Metastasis* **2009**, *26*, 273–287. [CrossRef]

59. Graybill, P.M.; Davalos, R.V. Cytoskeletal Disruption after Electroporation and Its Significance to Pulsed Electric Field Therapies. *Cancers* **2020**, *12*, 1132. [CrossRef]

60. Roy, S.S.; Hajnóczky, G. Calcium, mitochondria and apoptosis studied by fluorescence measurements. *Methods* **2008**, *46*, 213–223. [CrossRef]

61. Hanna, H.; Denzi, A.; Liberti, M.; André, F.M.; Mir, L.M. Electropermeabilization of Inner and Outer Cell Membranes with Microsecond Pulsed Electric Fields: Quantitative Study with Calcium Ions. *Sci. Rep.* **2017**, *7*, 13079. [CrossRef]

62. Kim, H.B.; Lee, S.; Chung, J.H.; Kim, S.N.; Sung, C.K.; Baik, K.Y. Effects of Actin Cytoskeleton Disruption on Electroporation In Vitro. *Appl. Biochem. Biotechnol.* **2020**, *191*, 1545–1561. [CrossRef] [PubMed]

63. Gimsa, J.; Wachner, D. Analytical Description of the Transmembrane Voltage Induced on Arbitrarily Oriented Ellipsoidal and Cylindrical Cells. *Biophys. J.* **2001**, *81*, 1888–1896. [CrossRef]

64. Vernier, P.T.; Ziegler, M.J.; Dimova, R. Calcium Binding and Head Group Dipole Angle in Phosphatidylserine−Phosphatidylcholine Bilayers. *Langmuir* **2009**, *25*, 1020–1027. [CrossRef] [PubMed]

65. Levine, Z.A.; Ziegler, M.J.; Vernier, P.T. Life Cycle of an Electropore: A Molecular Dynamics Investigation of the Electroporation of Heterogeneous Lipid Bilayers (PC:PS) In the Presence of Calcium Ions. *Biophys. J.* **2010**, *98*, 387. [CrossRef]

66. Navickaite, D.; Ruzgys, P.; Novickij, V.; Jakutaviciute, M.; Maciulevičius, M.; Sinceviciute, R.; Šatkauskas, S. Extracellular-Ca^{2+}-Induced Decrease in Small Molecule Electrotransfer Efficiency: Comparison between Microsecond and Nanosecond Electric Pulses. *Pharmaceutics* **2020**, *12*, 422. [CrossRef]

67. Falk, H.; Lambaa, S.; Johannesen, H.H.; Wooler, G.; Venzo, A.; Gehl, J. Electrochemotherapy and calcium electroporation inducing a systemic immune response with local and distant remission of tumors in a patient with malignant melanoma–A case report. *Acta Oncol.* **2017**, *56*, 1126–1131. [CrossRef]

68. Rudno-Rudzińska, J.; Kielan, W.; Guziński, M.; Płochocki, M.; Kulbacka, J. The First Study of Irreversible Electroporation with Calcium Ions and Chemotherapy in Patients with Locally Advanced Pancreatic Adenocarcinoma. *Appl. Sci.* **2020**, *10*, 5163. [CrossRef]

69. Klein, N.; Gunther, E.; Zapf, S.; El-Idrissi, R.; Atta, J.; Stehling, M. Prostate cancer infiltrating the bladder sphincter successfully treated with Electrochemotherapy: A case report. *Clin. Case Rep.* **2017**, *5*, 2127–2132. [CrossRef]

70. Nielsen, K.; Scheffer, H.J.; Vieveen, J.M.; Van Tilborg, A.A.J.M.; Meijer, S.; Van Kuijk, C.; Van Den Tol, M.P.; Meijerink, M.R.; Bouwman, R.A. Anaesthetic management during open and percutaneous irreversible electroporation. *Br. J. Anaesth.* **2014**, *113*, 985–992. [CrossRef]

71. Napotnik, T.B.; Miklavčič, D. In vitro electroporation detection methods—An overview. *Bioelectrochemistry* **2018**, *120*, 166–182. [CrossRef]

72. Schindelin, J.; Arganda–Carrera, I.; Frise, E.; Verena, K.; Mark, L.; Tobias, P.; Stephan, P.; Curtis, R.; Stephan, S.; Benjamin, S.; et al. Fiji-an open platform for biological image analysis. *Nat. Methods* **2009**, *9*, 10–38. [CrossRef] [PubMed]

73. Casciola, M.; Tarek, M. A molecular insight into the electro-transfer of small molecules through electropores driven by electric fields. *Biochim. Biophys. Acta (BBA)-Biomembr.* **2016**, *1858*, 2278–2289. [CrossRef] [PubMed]

74. Casciola, M.; Kasimova, M.A.; Rems, L.; Zullino, S.; Apollonio, F.; Tarek, M. Properties of lipid electropores I: Molecular dynamics simulations of stabilized pores by constant charge imbalance. *Bioelectrochemistry* **2016**, *109*, 108–116. [CrossRef] [PubMed]

Sample Availability: Samples of the compounds are not available.

Publisher's Note: MDPI stays neutral with regard to jurisdictional claims in published maps and institutional affiliations.

Praca nr 3

scientific reports

OPEN

Effects of high-frequency nanosecond pulses on prostate cancer cells

Aleksander Kiełbik[1,2✉], Wojciech Szlasa[3], Vitalij Novickij[4], Anna Szewczyk[2,5], Magdalena Maciejewska[6], Jolanta Saczko[2] & Julita Kulbacka[2✉]

Electroporation with pulsed electric fields show a potential to be applied as an experimental focal therapy of tumors. Sub-microsecond regime of electric pulses displays unique electrophysical features operative in cells and membranes. Recently, MHz compression of nanosecond pulses electric fields (nsPEFs) bursts proved to enhance the effectiveness of the therapy. High morbidity of prostate cancer (PCa) and risk of overtreatment associated with this malignancy call for new minimal-invasive treatment alternative. Herein we present the in vitro study for developing applications based on this new technology. In this study, we used flow cytometric analysis, cell viability assay, caspase activity analysis, wound healing assay, confocal microscopy study, and immunofluorescence to investigate the biological effect of high-frequency nsPEFs on PCa cells. Our results show that high-frequency nsPEFs induces the permeabilization and cell death of PCa cells. The cytotoxicity is significantly enhanced in MHz compression of pulses and with the presence of extracellular Ca^{2+}. High-frequency nsPEFs trigger changes in PCa cells' cytoskeleton and their mobility. The presented data show a therapeutic potential of high-frequency nsPEFs in a PCa setting. The sub-microsecond regime of pulses can potentially be applied in nanosecond electroporation protocols for PCa treatment.

Intense pulsed electric fields (PEFs) can be applied to permeabilize biomembranes[1]. This phenomenon is known as electroporation and found its use among others in the minimal-invasive treatment of different types of cancer. Clinically, commonly series of microsecond pulses are applied in various approaches such as electrochemotherapy or irreversible electroporation. Schoenbach and Beebe (2001) presented that biomembranes can also be permeabilized with 60 ns pulses and initiated a series of studies investigating the effect of sub-microsecond PEFs[2].

Initially, it was observed that nanosecond pulsed electric fields (nsPEFs) preferably affect cells interior acting on intracellular biomembranes[3]. Indeed, ns electroporation induces the dissipation of mitochondria membrane potential what eventually leads to cell death[4,5]. The permeabilization of other intracellular compartments such as the endoplasmic reticulum triggers the release of calcium and apoptosis of the cells[6]. Apart from intracellular compartments, multiple studies confirm that high-voltage submicrosecond PEFs can permeabilize plasma membrane[7,8]. The nsPEFs, similar to longer microsecond PEFs, trigger permeabilization increasing the transmembrane voltage[9]. However, comparing to standard microsecond PEFs, the size of permeable spots is smaller, so they can not always be detected by conventional dyes[10]. The permeabilization induced by ns pulses is a long-lived process that enables small molecules uptake for a longer time[11]. Consequently, the permeabilization is followed by ions inflow[12], cell swelling[13], cytoskeleton destabilization[11] and eventually necrotic or apoptotic cell death[14].

In vivo studies presented that nsPEFs trigger apoptotic cell death and result in the restriction of tumor vascularization[15,16]. Moreover, research on the animal models show signs of the systemic anti-cancer immune response[17,18].

Prostate cancer (PCa) remains the second most often diagnosed malignancy among men worldwide[19]. A systematic review of autopsy studies reported a prevalence ranging from 48 to 71% by patients over 79 years[20]. However, in most cases, PCa is associated with long life expectancy, and the radical therapy of low and intermediate-risk PCa is often unnecessary. Therefore, few focal therapies were developed to prevent overtreatment and provide patients with the alternative to radical prostatectomy. Among others, electroporation constitutes a new

[1]Medical University Hospital, Borowska 213, 50-556 Wrocław, Poland. [2]Department of Molecular and Cellular Biology, Faculty of Pharmacy, Wroclaw Medical University, Wrocław, Poland. [3]Faculty of Medicine, Wroclaw Medical University, Wrocław, Poland. [4]Institute of High Magnetic Fields, Vilnius Gediminas Technical University, Vilnius, Lithuania. [5]Department of Animal Developmental Biology, Institute of Experimental Biology, University of Wroclaw, 50-328 Wrocław, Poland. [6]Hirszfeld Institute of Immunology and Experimental Therapy, Polish Academy of Sciences, 53-114 Wrocław, Poland. ✉email: aleksander.kielbik@outlook.com; julita.kulbacka@umed.wroc.pl

promising treatment modality for PCa[21]. Differently from commonly used microsecond pulses, we propose the application of pulses in the nanosecond range.

The major limitation for sub-microsecond pulses is the need for high-voltage bursts to induce the cellular response. Therefore, usually pulses up over 10 kV/cm are applied. Novickij et al. (2018) presented that to overcome this limitation short pulses can be delivered in higher frequencies[22]. Namely, pulses should be applied in intervals shorter than the relaxation time of induced transmembrane potential. MHz monopolar nsPEFs remained poorly investigated due to the technological challenges of generating high voltage monopolar pulses in the MHz range[22]. Recent research proved that MHz ns pulses could be applied for gene delivery[23] and nerve excitation[24].

Primary, we determined the correlation between the frequency of pulses and permeabilization of cells. Secondly, we evaluated the cytotoxic effect of conventional and high-frequency nsPEFs in the buffer with and without a high concentration of extracellular Ca^{2+}. The Ca^{2+} uptake dynamic after bursts with different frequency PEFs was determined by a fluorescence microscopy study. The biological effects of MHz nsPEFs remain poorly investigated. Therefore, our experiments aimed at defining the effect of high-frequency bursts on the cytoskeleton and mobility of the cells.

Results

The permeabilization rate of PCa cells depends on the electric field intensity and frequency of PEFs.
Initially, PEFs parameters were optimized to achieve a high rate of responding cells. Figure 1 presents the effect of the standalone series of 200 ns pulses in different frequencies on the DU 145 cells permeabilization. The permeabilization depends on the electric field intensity and frequency of PEFs. Pulses delivered at MHz are significantly more efficient in electroporating cells. 25, 7 kV/cm PEFs in MHz frequency result in comparable permeabilization to 25, 10 kV/cm PEFs in lower frequencies (Fig. 1b).

The antitumor effect of PEFs is potentiated by the increasing number of pulses in MHz frequency and administration of Ca^{2+}.
We evaluated the impact of PEFs on the PCa cells' viability. The series of 25, 200 ns pulses has little impact on the DU 145 cells survival (Fig. 2a). A significant decrease is observed only when pulses in MHz frequency are applied. The effect of PEFs is more evident on the LNCaP cells (Fig. 2b). However, the LNCaP cells lethality is independent of PEFs frequency. A profound increase in cell death is achieved after exposure to PEFs in a buffer containing Ca^{2+}. High Ca^{2+} concentration facilitates the cytotoxicity of 25, 200 ns PEFs on both cell lines in all investigated frequencies (Fig. 2c, d).

Bursts with a higher number of 200 ns PEFs increase the cytotoxicity of the therapy. Figure 3e presents the correlation between the number of applied pulses and cancer cell viability. Results suggest that if pulses are delivered in MHz frequency, their increasing number significantly affects cell viability. Moreover, the effect is more pronounced when MHz PEFs are delivered in one burst, not intervals. Differently, kHz compression of 200 ns PEFs shows no significant difference in cytotoxicity between PEFs in one or two bursts. The cytotoxic effect of a higher numer of 200 ns pulses was potentiated by the addition of Ca^{2+} to the electroporation medium (Fig. 3e). In those probes, MHz compression of PEFs showed significant superiority to kHz PEFs and very high efficiency in decreasing PCa cells viability.

Figures 3a–d show apoptotic death markers activity after delivery of different 200 ns high-frequency ns bursts. Caspase 3 and 7 activity was studied to validate whether high-frequency nsPEFs trigger apoptosis. The time courses of caspases activity indicate the highest expression of caspase 3 and 7 4 h after the exposure to PEFs. The cells subjected to PEFs with Ca^{2+}, show low expression of apoptotic death markers after the therapy. After permeabilization without Ca^{2+} in EP buffer cells enter the apoptotic pathways, partially contributing to the observed decrease of cell viability after 24 h. Interestingly, the expression of apoptotic markers is significantly higher after bursts in kHz frequency comparing to MHz.

Ca^{2+} transients dynamic evoked by ns bursts depends on the frequency of PEFs.
Figure 4 shows visible differences in Ca^{2+} uptake and efflux dynamic after bursts with 25, 200 ns PEFs in different frequencies. Cells exposed to PEFs without extracellular Ca^{2+} do not respond with a detectable Ca^{2+} rise. The shapes of the response of cells subjected to PEFs with Ca^{2+} vary depending on the frequency. The fluorescence rise and fall time are notably different. Bursts of MHz pulses resulted in the sharp rise of intracellular Ca^{2+} with subsequent smooth and fast (60 s) return to the resting level (Fig. 4a). After the exposure to pulses in kHz and Hz frequency, Ca^{2+} transients do not occur immediately after bursts. Moreover, the increase of intracellular Ca^{2+} level is lower than MHz pulses (Fig. 4b, c).

High-frequency nsPEFs trigger changes in PCa cells' cytoskeleton and their mobility.
Fluorescence staining after exposure to 25, 200 ns PEFs revealed changes in the cell morphology (Fig. 5a). High-frequency PEFs trigger the disruption of lamellipodia and stress fibers. F-actin after high-frequency ns bursts accumulates in peripheral parts of cells. This effect is less evident after exposure to PEFs in 1 Hz frequency. High-frequency PEFs in buffer containing Ca^{2+} ions trigger prominent changes in cell morphology. The latter results in cell rounding and the creation of honeycomb-like structures. In untouched cells, zyxin localizes with actin fibers on the membrane protrusions. Figure 5a shows that standalone bursts of 25, 200 ns high-frequency PEFs have a mild effect on zyxin localization. However, the changes after permeabilization with Ca^{2+} are remarkable and indicate zyxin translocalization from focal adhesions. Cells after PEFs application present impaired mobility. Figure 5b–e reports the results of the wound healing assays. The cells were scrutinized for 15 h until the colonies of the control group connected. This assay shows a slight difference between probes permeabilized with and without Ca^{2+} ions.
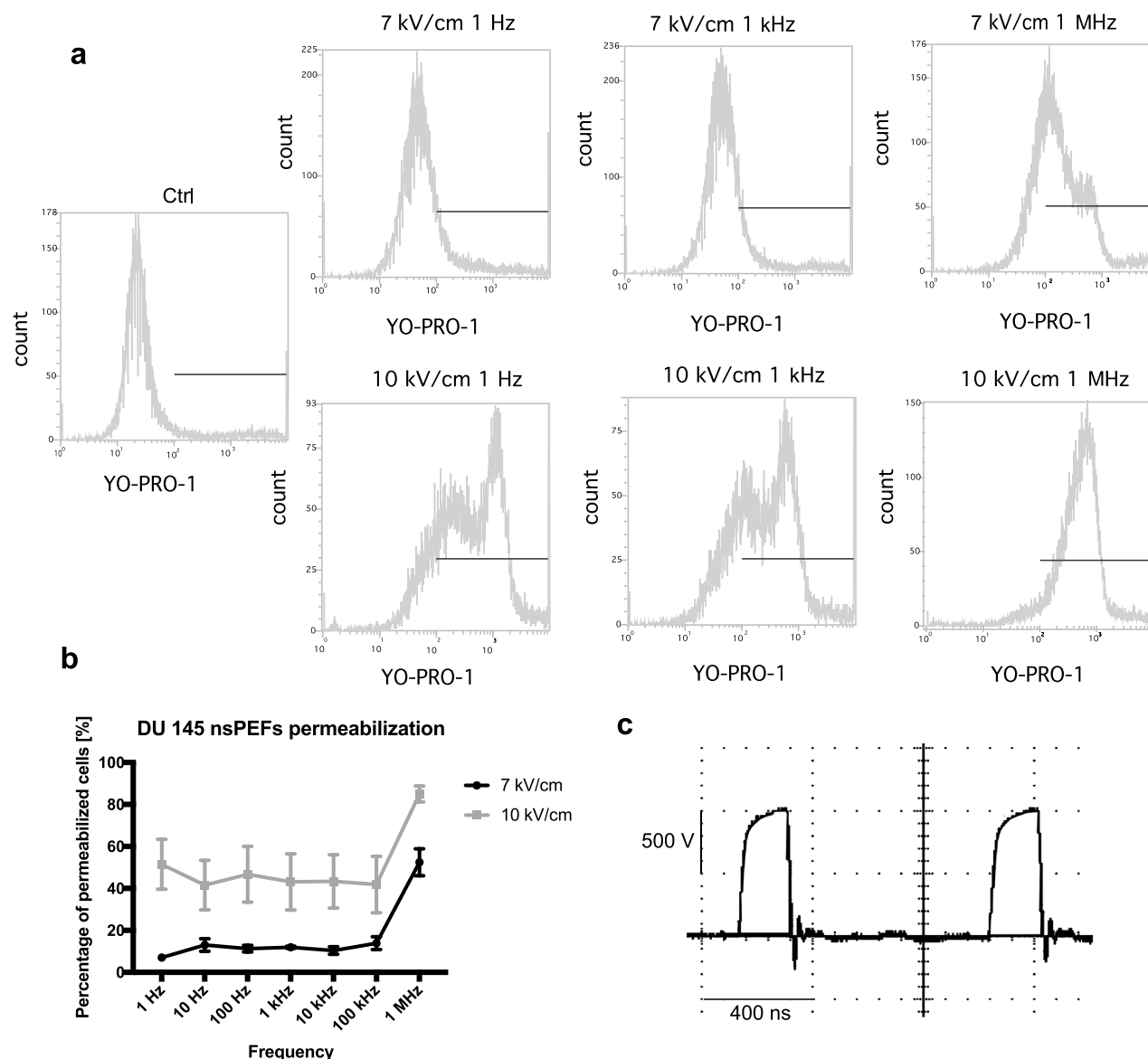
Figure 1. Permeabilization of DU 145 cells by 25, 200 ns PEFs bursts evidenced by YO-PRO-1 dye uptake. Cells were permeabilized in suspension in a 1-mm gap electroporation cuvette. (**a**) Flow cytometry analysis data presented on one-dimensional histograms. The graphs represent the data form one representative experiment. (**b**) The permeability of cells as a function of electric field frequency. The graph is representative of three independent experiments. Data are mean ± SD (n = 3 independent experiments). The effect of nsPEF was measured at two different electric field intensities. 25-pulse, 200-ns bursts become significantly more efficient at MHz. (**c**) The shape of high-frequency nsPEF delivered to 1 mm electroporation cuvettes.

Discussion

Our in vitro study shows the potential of high-frequency nsPEFs for prostate cancer treatment. Bursts of 25, 200 ns pulses result in a high permeability rate of the cells. Nevertheless, the latter is not reflected by their high mortality. However, note that cells after treatment were kept in the optimal condition in a growth medium containing serum what might significantly increase their viability after PEFs application[30,31]. For consistency, we also provide the data for LNCaP cells, but most experiments were performed on DU 145 cells. LNCaP cells do not produce a uniform monolayer but grow in clusters. Moreover, they attach only lightly to the substrate. Consequently, we choose DU 145 cell line as more appropriate for the study. In our experiments, two PCa cell lines show different sensitivity to ns bursts. The cytotoxic effect of nsPEFs varies across different cell lines with no visible dependence on cell size and other morphology features[32].

Herein we studied two approaches to enhance the effectiveness of high-frequency nsPEF. Namely, we increased the number of pulses and applied calcium ions. The increase of high-frequency PEFs number significantly upregulates the cytotoxic effect of the therapy. In our study, the latter is more pronounced when pulses in MHz frequencies are delivered. We also detected the favorable effect of unfractionated MHz PEFs. The pause between the series of pulses can result in the sensitization of cells, which increases the cytotoxicity of fractionated
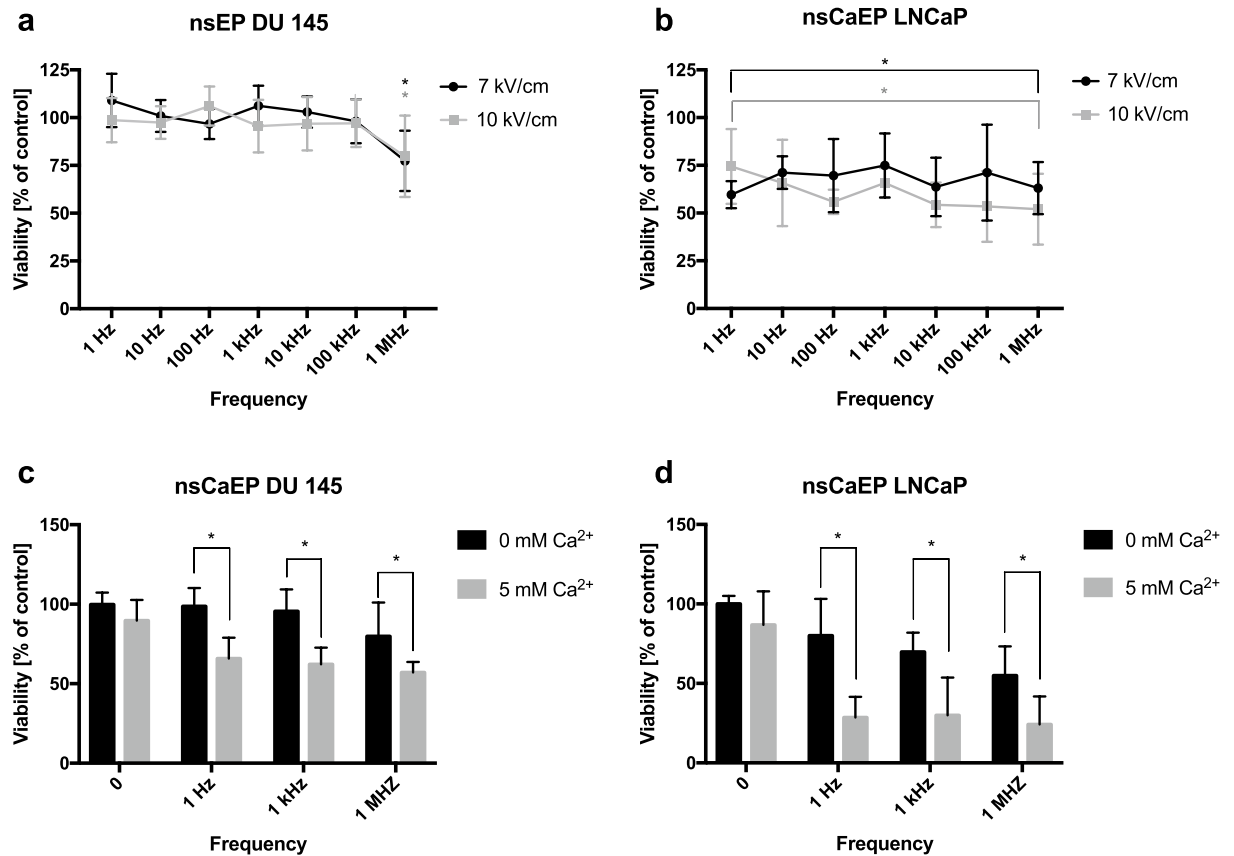
Figure 2. Viability of DU 145 and LNCaP cells after exposure to 25, 200 ns PEFs (**a–d**). Cells were permeabilized in suspension in a 1-mm gap electroporation cuvette. Viability of the cells as a function of electric field frequency. (**a, b**) The effect of PEFs was measured at two different electric field intensities. (**c, d**) Viability of cells after exposure to PEFs in medium with different Ca^{2+} concentration. Viability was assessed with MTT assay. Graphs are representative of at least 3 independent experiments. Data are mean ± SD (n = 3–5 independent experiments). (*) indicates statistically significant differences between the sample and control (**a, b**), or pair of samples (**c, d**) (ANOVA, $p < 0.05$).

therapy[33]. The effect of cell sensitization was not observed in our experiment. The result can be explained by the fact that the cells were electroporated in cuvettes. The applied method does not prevent the cells' sedimentation and their random rotation, affecting the sensitization[33]. Recently we proved that calcium ions could enhance the cytotoxicity of microsecond electroporation of prostate adenocarcinoma cells[34]. This study confirms that a burst of high-frequency nsPEFs with the presence of the extracellular Ca^{2+} also triggers extensive cell death. After 24 h the population of cells permeabilized with Ca^{2+} was significantly reduced. We observed higher activity of casp-3/7 8 h after standalone PEFs delivery. Moreover, an increase in apoptotic markers after kHz PEFs over MHz PEFs was detected. We hypothesize that MHz and permeabilization with extracellular Ca^{2+} pulses could result in extensive non-apoptotic early cell death. Consequently, in those probes, after PEFs exposure, even if the apoptosis pathway was activated, there were fewer cells left to enter the apoptosis[27].

Some other studies indeed suggest that the main cell death mechanism induced by standalone nanosecond PEFs is apoptosis. Several phenomena associated with apoptosis were observed after the application of nsPEFs i.e. cytochrome c release[35], caspase activation[35] and DNA fragmentation[36]. In our study, the intensity of apoptosis was assessed by measuring the activation of caspase 3 and 7.

Ca^{2+} disturbances after nsPEFs were pointed to be one of the critical events leading to cell death[37]. NsPEFs trigger the increase of intracellular Ca^{2+} by its influx from the extracellular medium and efflux from the intracellular compartments[38]. Our study shows various Ca^{2+} transients evoked by ns bursts in different frequencies. Considering MHz pulses, the Ca^{2+} transients are similar to those obtained by a single longer pulse[24]. Bursts of kHz and Hz PEFs triggered variable responses. Ca^{2+} inflow has not occurred immediately after the delivery of pulses what suggests the involvement of different mechanisms. Dissynhronized response is likely caused by a delayed Ca^{2+} release from the intracellular compartments[38].

Herein, we tried to find a correlation between cytoskeleton disruption and impaired cancer cell motility. Ns bursts affect the cytoskeleton as a result of permeabilization and subsequent cell swelling[39]. Presented confocal microscopy study showed more extensive cytoskeleton disruption after permeabilization with Ca^{2+}. The observation has not been represented in the motility test. Exposure to PEFs, independent of extracellular Ca^{2+} concentration, affected the motility of cells. A small and insignificant difference between various therapy protocols could
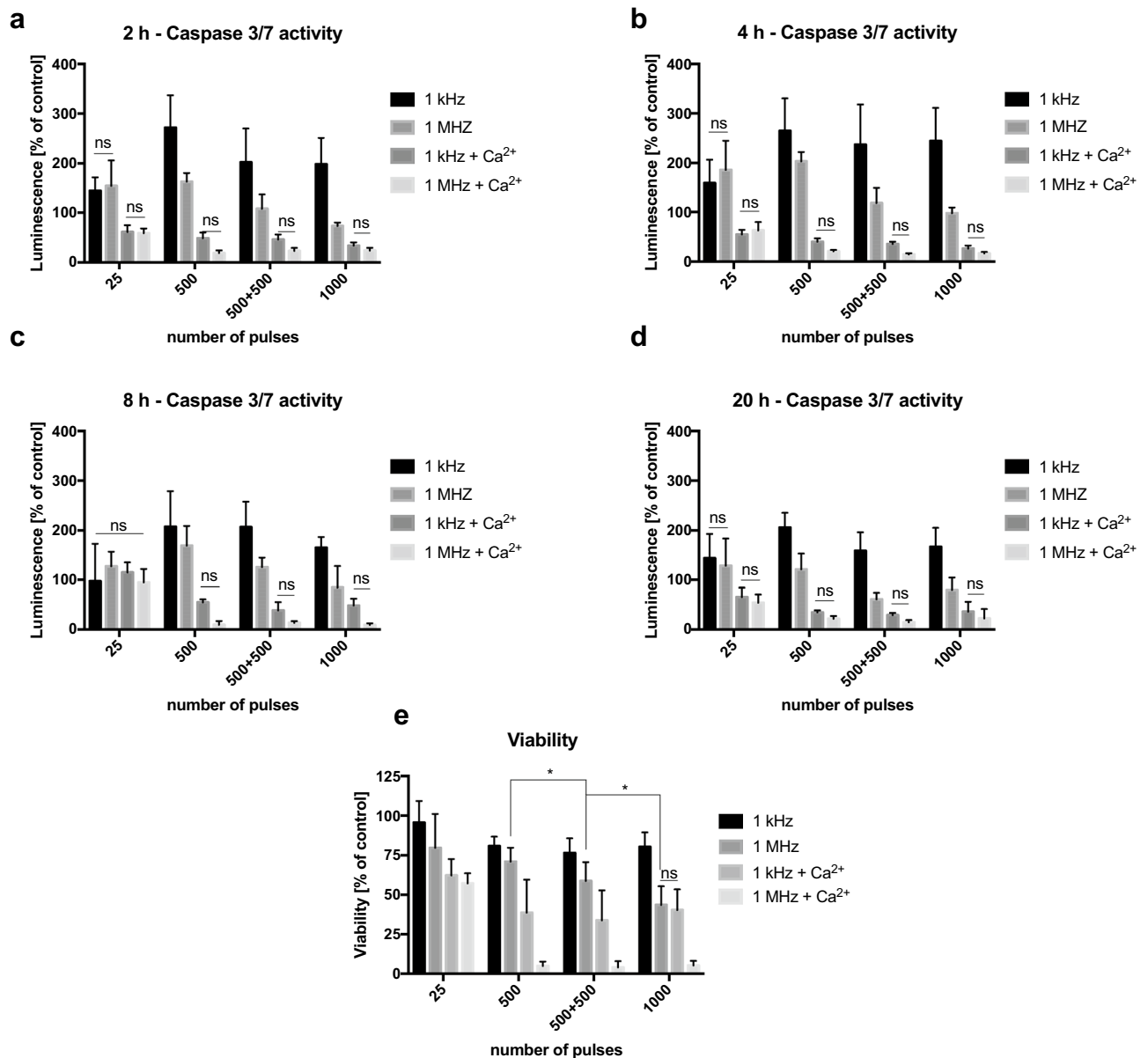
Figure 3. Viability and Caspase 3/7 activity of the DU 145 cells after high-frequency PEFs application. Cells were exposed in suspension in a 1-mm gap electroporation cuvette (200 ns duration, 10 kV). (**e**) The effect of pulse number in two different frequencies and different extracellular calcium concentration. The viability was assessed with MTT assay 24 h after PEFs exposure. (**a–d**) The Caspase 3/7 activity in the cells after exposure to a different number of PEFs in two frequencies and different extracellular Ca^{2+} concentration. The caspase 3/7 activity was determined with Caspase-Glo 3/7 Assay from Promega 2, 4, 8 and 20 h after electroporation. Graphs are representative of at least 3 independent experiments. Data are mean ± SD (n = 3–4 independent experiments). (ns) indicates no statistically significant difference between the pair of samples (*) indicates statistically significant differences between the pair of samples (ANOVA, $p < 0.05$).

emerge from minor inequalities of viable cells seeded inside silicon inserts. Motility is a complex process, and apparently, changes in cytomechanics can not be entirely explained by actin and zyxin disruption.

Our study presented differences between high and low-frequency PEFs. High-frequency bursts introduce parametric flexibility. The extent of electroporation can be controlled solely by the frequency without altering the pulse energy, i.e., 1 kHz same parameters nsPEF will deliver lower electroporation than MHz. Moreover, some features of MHz compression of nsPEFs seem to be distinct from PEFs in other frequencies. Viability assays showed a more potent cytotoxic effect of MHz PEFs when applied in higher numbers and with extracellular Ca^{2+}, over lower frequency pulses. Another interesting distinction was presented by Ca^{2+} uptake analysis. Previously it was speculated that the observed effects in MHz range are due to the accumulation of transmembrane potential and slow relaxation[22]. There are no data contradicting this hypothesis; thus, plasma membrane charge and discharge dynamics are considered primary mechanisms.
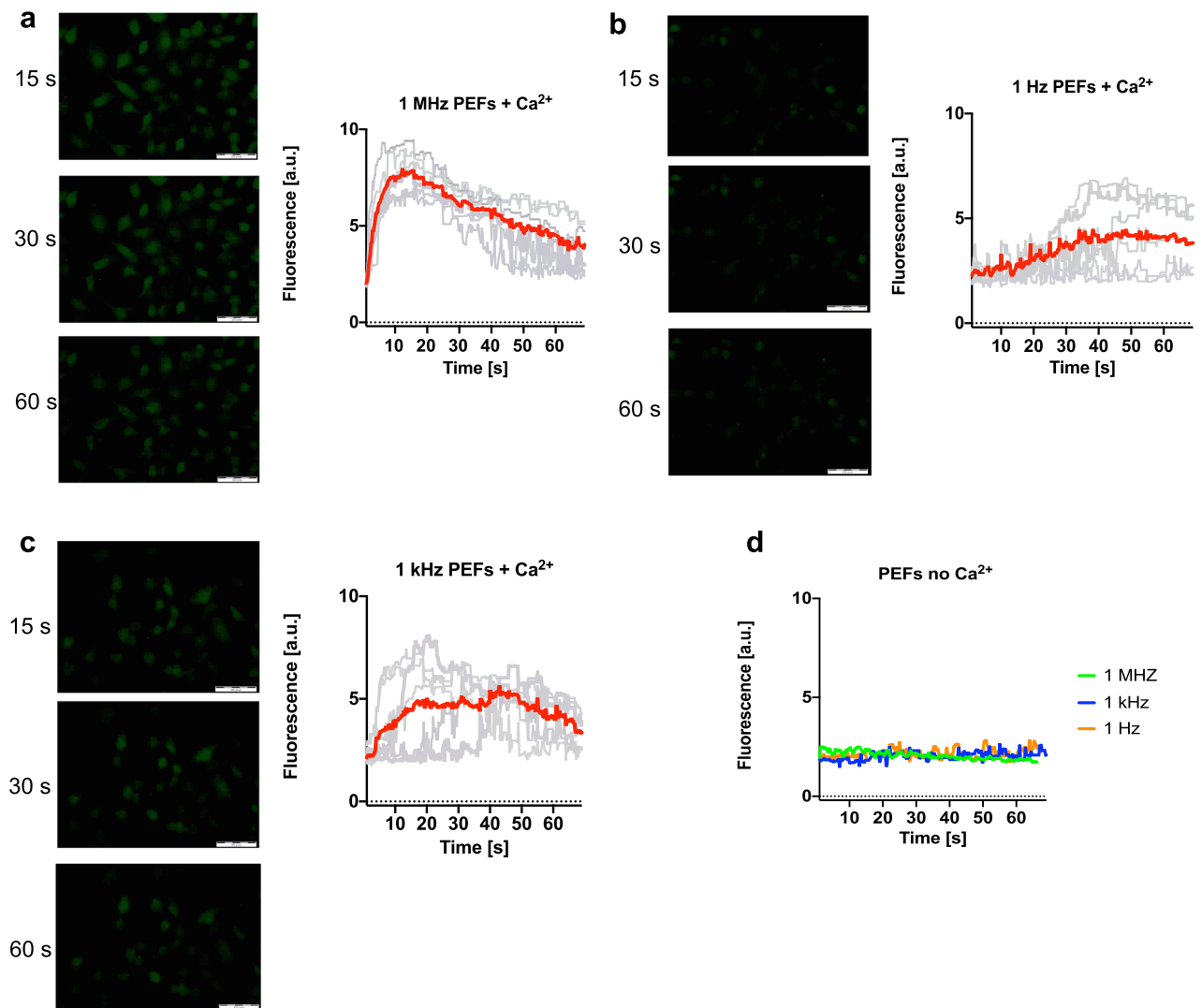
Figure 4. Ca²⁺ transients dynamic evoked by 200 ns bursts. The adherent cells were permeabilized with two needle electrode with bursts of 25, 5 kV/cm, 200 ns PEFs in different frequencies. The dynamic of Ca²⁺ uptake after nanosecond permeabilization was presented as traces of response in selected individual cells (grey lines, 7 cells per plot) and their average (colour lines). The cells were stained with Fluo-8 dye. Pulses were delivered at the beginning of the observation and the cells were observed for 60 s. Images were analyzed by ImageJ software (Version: 2.1.0/1.53C; https://imagej.net/Fiji)[28].

The possible effect of MHz nsPEFs on intracellular biomembranes is not yet understood. In theoretical analysis of MHz pulses, Sözer et al. (2021) denied charge accumulation and pointed at possible oscillations of the potential of intracellular membranes after MHz PEFs exposure[40]. It requires further experimental analysis to settle the question if MHz pulses have the potential of inducing the intracellular effects similar to nsPEFs in lower frequencies.

One of the rationales of applying short PEFs for the focal therapy of PCa is the possibility of ablations without thermal damage. However, the current flow results in the temperature rise due to Joule heating. In vivo nsPEFs showed rather a low capability of inducing the heating of tissue[41]. In our study, we applied ns pulses in a high-frequency range in a low conductivity medium. Considering the short duration (200 ns) and relatively low amplitude of pulses, the total energy of the highest intensity burst (1000 pulses) was low (< 0.25 J). Nevertheless, if the number of pulses and the amplitude is increased in the future, the induction of Joule heating should be considered. Other studies indicated an increase of the frequency from 1 Hz to 1 kHz showed the temperature rise of 3 °C of the electroporated tissue[42]. Another multi-parameter analysis of temperature rise after high-frequency electroporation shows that MHz compression of nanosecond pulses indeed has the potential of causing thermal damage due to Joule heating. The simulation performed on the electrical properties of liver tissue presented that burst of 100, 1 MHz pulses when the higher voltage is applied are likely to increase the tissue temperature by 8 °C[43]. In the in vitro study of Pakhomov et al., the calculated temperature rise after MHz PEFs did not exceed 6 °C[24]. It implies that Joule heating is specific to the case, but it is easy to control if the input energy is well defined.
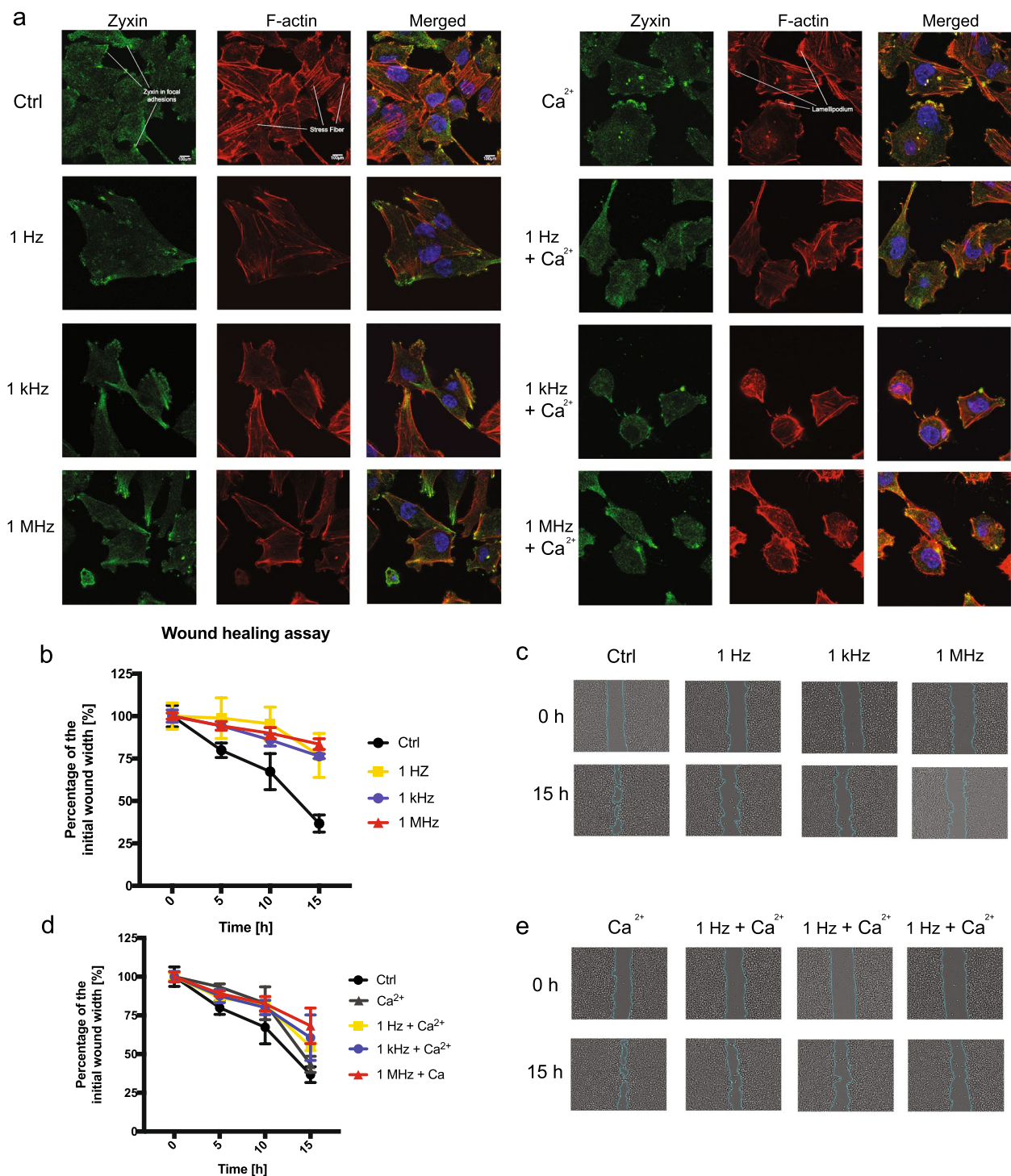
Figure 5. PCa cells morphology and mobility after exposure to 25, 10 kV/cm, 200 ns pulses in different frequencies with and without extracellular Ca^{2+}. (**a**) The representative photographs of cells exposed to bursts of nsPEFs. Confocal laser scanning microscopy visualize the rearrangement of zyxin (green fluorescent dye), F-actin (red fluorescent dye) nucleus (blue florescent dye) structure in DU 145 cells. (**b**, **c**) The percentage of a healed wound as a function of time. Images were analyzed by ImageJ software (Version: 2.1.0/1.53C; https://imagej.net/Fiji)[28]. (**d**, **e**) Images of wound gradually invaded by migrating cells. Images were taken in a given time interval. The graph represents the data from the three replicates of an individual experiment. Data are mean ± SD (n = 3 replicates).

In our study, we can entirely exclude the thermal effect contributed to the observed cell death. However, if high conductivity (> 1 S/m) buffer is used in the future, the thermal effect should be reconsidered.

In this study, we proved the in vitro effectiveness of high-frequency nsPEFs for PCa treatment. Prospectively, ns pulses might provide additional advantages over μsPEFs, which are already applied for irreversible electroporation of PCa. High-frequency nsPEF allows mitigation of impedance changes. Therefore, a more uniform exposure of the tumor can be ensured. The inhomogeneity of various layers and structures is less a concern[44,45]. Bursts of ns pulses allow better control of the total treatment energy than protocols involving single pulses or low amplitude pulses. The ablation can be controlled in a more flexible and precise way if the number of pulses is high. Moreover, high-frequency nsPEFs are characterized by their low excitatory efficacy compared to longer pulses. With ns bursts, the permeabilization threshold for cancer cells can be exceeded, and simultaneously, the excitation threshold for surrounding neurons and muscle cells will not be reached[46]. Accordingly, the electroporation of cancer cells is possible without unwanted neuronal or muscular excitation and damage. That gives ns bursts an advantage namely, it excludes the need for complete muscle relaxation and general anesthesia during focal ablation of PCa.

Materials and methods

Cell culture. The androgen-independent prostate cancer cell line DU 145 and androgen-dependent prostate cancer cell line LNCaP were obtained from American Type Culture Collection and propagated as recommended by the supplier. Both media (RPMI 1640 and EMEM Sigma-Aldrich, St. Louis, MO, USA) were supplemented with 10% fetal bovine serum (FBS, Sigma-Aldrich) and 1% antibiotics (penicillin/streptomycin; Sigma-Aldrich). Cells were kept under standard culture conditions at 37 °C in a humidified atmosphere containing 5% CO_2.

Preparation of drug. Calcium solutions were prepared from the stock solution of calcium chloride (67 mg/ml, calcium chloratum WZF, Polfa Warszawa S.A., Poland). The required concentrations were achieved with a dilution of stock in EP buffer to 5 mM concentration.

Permeabilization of cells. 50 μl of cells in the concentration of 2×10^6/ml, suspended in HEPES buffer (10 mM HEPES (Sigma-Aldrich), 250 mM sucrose (Chempur), and 1 mM $MgCl_2$ (Sigma-Aldrich) in milliQ water) with or without $CaCl_2$, were placed in 1 mm cuvettes with aluminium electrodes (BTX, Syngen Biotech, Poland). The square wave electroporator (100 ns–1 ms) developed in the Institute of High Magnetic Fields (VGTU, Vilnius, Lithuania) was used to deliver electric pulses[25]. Cells were exposed to 25 pulses of 200 ns, 7000 or 1000 V/cm and different frequencies ranging from 1 Hz to 1 MHz. Pulse shapes and amplitudes were controlled with an MDO3052 oscilloscope (Tektronix, Beaverton, OR). Subsequently, the cells were left incubating for 20 min and then suspended in a culture medium and placed in 96 or 6 well plates.

Cell viability and caspase 3/7 activity assays. After permeabilization, the viability of cells was measured in 24 h with MTT assay[26]. We utilized a Caspase-Glo 3/7 Assay from Promega (Madison, WI,) to assess the caspase 3/7 activity in 8 h[27]. The luminescence and absorbance were measured with the multiplate reader GloMax (Promega, Madison, WI). The experiment was performed in triplicate.

Cell permeability quantification assay. The cells were permeabilized according to the description of permeabilization of cell suspension. However, before PEFs delivery, the green-fluorescent YO-PRO-1 stain (Y3603, Thermo Fisher Scientific, Waltham, MA) in the concentration of 1 μl/ml was added to EP buffer. YO-PRO-1 cellular uptake reflects the degree of plasma membrane's permeabilization[38]. After permeabilization cells were incubated for 3 min. Green Fluorescent intensities were detected on Cube 6 flow cytometer (Sysmex, Germany). The fluorescence of YO-PRO-1 was excited with 488 nm wavelength and measured with the FL-1- detector (525/50). The results were expressed as the percentage of permeabilized cells. The experiment was performed in triplicate.

Calcium uptake evaluation. Cells were placed in a well of 6 wells plate. After 24 h the medium was removed, cells were stained with 4 μM Fluo-8 (ab142773, Abcam, UK) diluted in PBS and left incubating for 20 min. Subsequently, the buffer was replaced with HEPES or with HEPES with calcium chloride at a 5 mM concentration. The plate was placed on the microscope stage with the electrode touching the surface of the well. Cells visible in the objective were directly placed between two needles of the electrode BTX533 (BTX, Syngen Biotech, Poland). Subsequently, the cells were subjected to 200 ns PEFs with field intensity reaching around 5 kV/cm. The increase in cell fluorescence during the permeabilization was observed with the fluorescent microscope Olympus IX53 (Olympus, Japan). The changes in cell fluorescence were evaluated with ImageJ software (Version:2.1.0/1.53C; https://imagej.net/Fiji)[28]. The experiment was performed in triplicate.

Qualitative evaluation of the cytoskeletal organization. The cells were permeabilized according to the protocol described above. Subsequently, the cells were seeded on glass coverslips placed and stained with primary zyxin antibody (MAB6977, RD systems, Minneapolis, MN) at 3 μg/ml and a mixture of Alexa Fluor 488 dye (Ex. 490 nm, Em. 525 nm; 2 μg/ml, A11029, Thermo Fisher Scientific Waltham, MA) and Alexa Fluor 546 Phalloidin (Ex. 556 nm, Em. 570 nm; 2 μg/ml, A22283, Thermo Fisher Scientific, Waltham, MA) according to the protocol[29]. Eventually, cells were mounted with DAPI Mounting Medium (ab104139, Abcam, UK). The samples were analyzed with a confocal laser scanning microscope using laser wavelengths: 405 nm, 490 nm, and 556 nm; 60 × oil immersion objective lens with 1.35 NA (Olympus FluoViewer 1000, Japan).

Wound healing assay. After permeabilization, cells were seeded inside the silicone inserts (Ibidi, Germany) for 24 h to form a monolayer. Subsequently, the inserts were removed. The cells were scrutinized until the colonies of the control group connected. Note that PEFs with calcium as well as standalone MHz nsPEFs resulted in decreased viability of cell compared to control. Consequently, the proportionally higher number of cells that underwent the therapy was placed in the silicone insert for those samples. The changes in wound width were evaluated with ImageJ software (Version:2.1.0/1.53C; https://imagej.net/Fiji)[28].

References

1. Neumann, E. & Rosenheck, K. Permeability changes induced by electric impulses in vesicular membranes. *J. Membr. Biol.* **10**, 279–290 (1972).
2. Schoenbach, K. H., Beebe, S. J. & Buescher, E. S. Intracellular effect of ultrashort electrical pulses. *Bioelectromagnetics* **22**, 440–448 (2001).
3. Tekle, E. *et al.* Selective field effects on intracellular vacuoles and vesicle membranes with nanosecond electric pulses. *Biophys. J.* **89**, 274–284 (2005).
4. Beebe, S. J., Chen, Y., Sain, N. M., Schoenbach, K. H. & Xiao, S. Transient features in nanosecond pulsed electric fields differentially modulate mitochondria and viability. *PLoS One* **7**, e51349 (2012).
5. Napotnik, T. B., Wu, Y.-H., Gundersen, M. A., Miklavcic, D. & Vernier, P. T. Nanosecond electric pulses cause mitochondrial membrane permeabilization in Jurkat cells. *Bioelectromagnetics* **33**, 257–264 (2012).
6. Beebe, S. J. *et al.* Diverse effects of nanosecond pulsed electric fields on cells and tissues. *DNA Cell Biol.* **22**, 785–796 (2003).
7. Pakhomov, A. G. *et al.* Membrane permeabilization and cell damage by ultrashort electric field shocks. *Arch. Biochem. Biophys.* **465**, 109–118 (2007).
8. Vernier, P. T., Sun, Y. & Gundersen, M. A. Nanoelectropulse-driven membrane perturbation and small molecule permeabilization. *BMC Cell Biol.* **7**, 1–16 (2006).
9. Frey, W. *et al.* Plasma membrane voltage changes during nanosecond pulsed electric field exposure. *Biophys. J.* **90**, 3608–3615 (2006).
10. Bowman, A. M., Nesin, O. M., Pakhomova, O. N. & Pakhomov, A. G. Analysis of plasma membrane integrity by fluorescent detection of Tl⁺ uptake. *J. Membr. Biol.* **236**, 15–26 (2010).
11. Pakhomov, A. G. *et al.* Multiple nanosecond electric pulses increase the number but not the size of long-lived nanopores in the cell membrane. *BBA Biomembr.* **1848**, 958–966 (2015).
12. Pakhomov, A. G. *et al.* Cancellation of cellular responses to nanoelectroporation by reversing the stimulus polarity. *Cell. Mol. Life Sci* **71**, 4431–4441 (2014).
13. Romeo, S., Wu, Y., Levine, Z. A., Gundersen, M. A. & Vernier, P. T. Water influx and cell swelling after nanosecond electropermeabilization. *Biochim. Biophys. Acta* **1828**, 1715–1722 (2013).
14. Pakhomova, O. N., Gregory, B. W., Semenov, I. & Pakhomov, A. G. Two modes of cell death caused by exposure to nanosecond pulsed electric field. *PLoS One* **8**, e70278 (2013).
15. Chen, X., Zhuang, J., Kolb, J. F., Schoenbach, K. H. & Beebe, S. J. Long term survival of mice with hepatocellular carcinoma after pulse power ablation with nanosecond pulsed electric fields. *Technol. Cancer Res. Treat.* **11**, 83–93 (2012).
16. Nuccitelli, R. *et al.* A new pulsed electric field therapy for melanoma disrupts the tumor's blood supply and causes complete remission without recurrence. *Int. J. Cancer* **125**, 438–445 (2009).
17. Nuccitelli, R. *et al.* Non-thermal nanoelectroablation of UV-induced murine melanomas stimulates an immune response. *Pigment Cell Melanoma Res.* **25**, 618–629 (2012).
18. Novickij, V. *et al.* Antitumor response and immunomodulatory effects of sub-microsecond irreversible electroporation and its combination with calcium electroporation. *Cancers (Basel)* **11**, 1–18 (2019).
19. Bray, F. *et al.* Global Cancer Statistics 2018: GLOBOCAN estimates of incidence and mortality worldwide for 36 cancers in 185 countries. *CA Cancer J. Clin.* **68**, 394–424 (2018).
20. Bell, K. J. L., Mar, C. D., Wright, G., Dickinson, J. & Glasziou, P. Prevalence of incidental prostate cancer: A systematic review of autopsy studies. *Int. J. Cancer* **137**, 1749–1757 (2015).
21. Kiełbik, A., Szlasa, W., Saczko, J. & Kulbacka J. Electroporation-based treatments in urology. *Cancers (Basel)* **12**, 1–26 (2020).
22. Novickij, V., Ruzgys, P., Grainys, A. & Saulius, Š. High frequency electroporation efficiency is under control of membrane capacitive charging and voltage potential relaxation. *Bioelectrochemistry* **119**, 92–97 (2018).
23. Ruzgys, P., Novickij, V., Novickij, J. & Šatkauskas, S. Nanosecond range electric pulse application as a non-viral gene delivery method: Proof of concept. *Sci. Rep.* **8**, 1–8 (2018).
24. Pakhomov, A. G. *et al.* Excitation and electroporation by MHz bursts of nanosecond stimuli. *Biochem. Biophys. Res. Commun.* **518**, 759–764 (2019).
25. Novickij, V. *et al.* High-frequency submicrosecond electroporator. *Biotechnol. Biotechnol. Equip.* **30**, 607–613 (2016).
26. Szlasa, W. *et al.* Oxidative effects during irreversible electroporation of melanoma cells—In vitro study. *Molecules* **26**, 1–17 (2021).
27. Pakhomova, O. N., Gregory, B., Semenov, I. & Pakhomov, A. G. Calcium-mediated pore expansion and cell death following nanoelectroporation. *BBA Biomembr.* **1838**, 2547–2554 (2014).
28. Schindelin, J. *et al.* Fiji—An open source platform for biological image analysis. *Nat. Methods* **9**, 676–682 (2012).
29. Szewczyk, A. *et al.* Calcium electroporation for treatment of sarcoma in preclinical studies. *Oncotarget* **9**, 11604–11618 (2018).
30. Delteil, C., Teissie, J. & Rols, M. Effect of serum on in vitro electrically mediated gene delivery and expression in mammalian cells. *Biochim. Biophys. Acta* **1467**, 362–368 (2000).
31. Sukhorukov, V. L. *et al.* Surviving high-intensity field pulses: Strategies for improving robustness and performance of electrotransfection and electrofusion. *J. Membr. Biol.* **201**, 187–201 (2005).
32. Gianulis, E. C. *et al.* Selective susceptibility to nanosecond pulsed electric field (nsPEF) across different human cell types. *Cell. Mol. Life Sci.* **74**, 1741–1754 (2017).
33. Muratori, C., Pakhomov, A. G., Xiao, S. & Pakhomova, O. N. Electrosensitization assists cell ablation by nanosecond pulsed electric field in 3D cultures. *Sci. Rep.* **6**, 1–9 (2016).
34. Kiełbik, A. *et al.* In vitro study of calcium microsecond electroporation of prostate adenocarcinoma cells. *Molecules* **25**, 1–19 (2020).
35. Beebe, S. J., Fox, P. M., Rec, L. J., Willis, L. K. & Schoenbach, K. H. Nanosecond, high-intensity pulsed electric fields induce apoptosis in human cells. *FASEB J.* **17**, 1493–1495 (2003).
36. Beebe, S. J. *et al.* Nanosecond pulsed electric field (nsPEF) effects on cells and tissues: Apoptosis induction and tumor growth inhibition. *IEEE Trans. Plasma Sci.* **30**, 286–292 (2002).
37. Beebe, S. J., Sain, N. M. & Ren, W. Induction of cell death mechanisms and apoptosis by nanosecond pulsed electric fields (nsPEFs). *Cells* **2**, 136–162 (2013).

38. Semenov, I., Xiao, S. & Pakhomov, A. G. Primary pathways of intracellular Ca^{2+} mobilization by nanosecond pulsed electric field. *BBA Biomembr.* **1828**, 981–989 (2013).
39. Pakhomov, A. G. *et al.* Disassembly of actin structures by nanosecond pulsed electric field is a downstream effect of cell swelling. *Bioelectrochemistry* **100**, 88–95 (2014).
40. Sözer, E. B. *et al.* Bioelectrochemistry analysis of electrostimulation and electroporation by high repetition rate bursts of nanosecond stimuli. *Bioelectrochemistry* **140**, 107811 (2021).
41. Nuccitelli, R. *et al.* Nanosecond pulsed electric fields cause melanomas to self-destruct. *Biochem. Biophys. Res. Commun.* **343**, 351–360 (2006).
42. Lacković, I., Magjarević, R. & Miklavčič, D. A multiphysics model for studying the influence of pulse repetition frequency on tissue heating during electrochemotherapy. In *4th European Conference of the International Federation for Medical and Biological Engineering* (eds Vander Sloten, J., Verdonck, P., Nyssen, M. & Haueisen, J.) 2609–2613 (Springer, 2009).
43. Mi, Y., Rui, S., Li, C., Yao, C. & Xu, J. Multi-parametric study of temperature and thermal damage of tumor exposed to high-frequency nanosecond-pulsed electric fields based on finite element simulation. *Med. Biol. Eng. Comput.* **55**, 1109–1122 (2017).
44. Gowrishankar, T. R. & Weaver, J. C. Electrical behavior and pore accumulation in a multicellular model for conventional and supra-electroporation. *Biochem. Biophys. Res. Commun.* **349**, 643–653 (2007).
45. Xie, F. *et al.* Ablation of myocardial tissue with nanosecond pulsed electric fields. *PLoS One* **10**, 1–15 (2015).
46. Pakhomov, A. G. & Pakhomova, O. N. The interplay of excitation and electroporation in nanosecond pulse stimulation. *Bioelectrochemistry* **136**, 107598 (2020).

Acknowledgements

Author contributions

A.K. research conception, design of experiments, data acquisition, interpretation and visualization of data, manuscript preparation; W.S. data acquisition, interpretation of data; V.N. the creation of new electroporator used in the work, supervision, funding acquisition; A.S. data acquisition, manuscript revision; M.M. data acquisition; J.S. supervision, project administration, funding acquisition; J.K. supervision, project administration, funding acquisition; All authors have read and agreed to the published version of the manuscript.

Competing interests

The authors declare no competing interests.

Additional information

Correspondence and requests for materials should be addressed to A.K. or J.K.

Reprints and permissions information is available at www.nature.com/reprints.

Publisher's note Springer Nature remains neutral with regard to jurisdictional claims in published maps and institutional affiliations.

11. Oświadczenia współautorów

dr hab. inż. Julita Kulbacka, Prof. UMW   Wrocław 30.08.2021

Afiliacja: Katedra i Zakład Biologii Molekularnej i Komórkowej Uniwersytetu Medycznego im. Piastów Śląskich we Wrocławiu

OŚWIADCZENIE WSPÓŁAUTORA

Oświadczam, że w pracy **"Electroporation-Based Treatments in Urology"** Cancers (Basel). 2020 Aug 7;12(8):2208, mój udział polegał na kierowaniu projektem naukowym, którego częścią jest powyżej opisana praca przeglądowa, korekcie manuskryptu oraz pozyskaniu funduszy na pokrycie kosztów publikacji.

Podpis

dr hab. inż. Julita Kulbacka, Prof. UMW   Wrocław 30.08.2021

Afiliacja: Katedra i Zakład Biologii Molekularnej i Komórkowej Uniwersytetu Medycznego im. Piastów Śląskich we Wrocławiu

OŚWIADCZENIE WSPÓŁAUTORA

Oświadczam, że w pracy **„Effects of high-frequency nanosecond pulses on prostate cancer cells",** Scientific Reports vol.11, 15835 (2021), mój udział polegał na kierowaniu projektem naukowym obejmującym badania opisane w tej pracy, krytycznej ocenie wyników, doradzaniu przy planowaniu eksperymentów, korekcie manuskryptu oraz pozyskaniu funduszy na pokrycie kosztów eksperymentów oraz publikacji.

Podpis

dr hab. inż. Julita Kulbacka, Prof. UMW   Wrocław 30.08.2021

Afiliacja: Katedra i Zakład Biologii Molekularnej i Komórkowej Uniwersytetu Medycznego im. Piastów Śląskich we Wrocławiu

OŚWIADCZENIE WSPÓŁAUTORA

Oświadczam, że w pracy "**In Vitro Study of Calcium Microsecond Electroporation of Prostate Adenocarcinoma Cells**" Molecules. 2020 Nov; 25(22): 5406. mój udział polegał na kierowaniu projektem naukowym obejmującym badania opisane w tej pracy, krytycznej ocenie wyników, doradzaniu przy planowaniu eksperymentów, korekcie manuskryptu oraz pozyskaniu funduszy na pokrycie kosztów eksperymentów.

Julita Kulbacka

Podpis

Wojciech Szlasa   Wrocław 30.08.21

Afiliacja: Uniwersytet Medyczny im. Piastów Śląskich we Wrocławiu

OŚWIADCZENIE WSPÓŁAUTORA

Oświadczam, że w pracy **Electroporation-Based Treatments in Urology** mój udział polegał na edycji wizualnej, końcowej korekcie manuskryptu oraz pozyskaniu funduszy na pokrycie kosztów publikacji.

.

Podpis

Wojciech Szlasa   Wrocław 30.08.21

Afiliacja: Uniwersytet Medyczny im. Piastów Śląskich we Wrocławiu

OŚWIADCZENIE WSPÓŁAUTORA

Oświadczam, że w pracy **Effects of high−frequency nanosecond pulses on prostate cancer cells** mój udział polegał na pomocy przy wykonywaniu doświadczeń techniką mikroskopii fluorescencyjnej oraz cytometrii przepływowej. Ponadto pomagałem w pozyskaniu funduszy na pokrycie kosztów publikacji.

.

Podpis

Wojciech Szlasa   Wrocław 30.08.21

Afiliacja: Uniwersytet Medyczny im. Piastów Śląskich we Wrocławiu

OŚWIADCZENIE WSPÓŁAUTORA

Oświadczam, że w pracy **In Vitro Study of Calcium Microsecond Electroporation of Prostate Adenocarcinoma Cells** mój udział polegał na wykonaniu symulacji dynamiki molekularnej, opisaniu jej rezultatów oraz przygotowaniu ryciny 9. Ponadto pomagałem przy wykonywaniu doświadczeń techniką mikroskopii fluorescencyjnej.

.

Podpis

prof. dr hab. Jolanta Saczko   Wrocław 07.09.21

Afiliacja: Katedra i Zakład Biologii Molekularnej i Komórkowej Uniwersytetu Medycznego im. Piastów Śląskich we Wrocławiu

OŚWIADCZENIE WSPÓŁAUTORA

Oświadczam, że w pracy przeglądowej **Electroporation-Based Treatments in Urology** mój udział polegał na korekcie manuskryptu oraz pozyskaniu funduszy na pokrycie kosztów publikacji.

Podpis

prof. dr hab. Jolanta Saczko   Wrocław 07.09.21

Afiliacja: Katedra i Zakład Biologii Molekularnej i Komórkowej Uniwersytetu Medycznego im. Piastów Śląskich we Wrocławiu

OŚWIADCZENIE WSPÓŁAUTORA

Oświadczam, że w pracy **Effects of high−frequency nanosecond pulses on prostate cancer cells** mój udział polegał na kierowaniu Katedrą i Zakładem Biologii Molekularnej i Komórkowej w których przeprowadzono badania opisane w tej pracy, krytycznej ocenie wyników, doradzaniu przy planowaniu eksperymentów, korekcie manuskryptu oraz pozyskaniu funduszy na pokrycie kosztów eksperymentów.

Podpis

prof. dr hab. Jolanta Saczko   Wrocław 07.09.21

Afiliacja: Katedra i Zakład Biologii Molekularnej i Komórkowej Uniwersytetu Medycznego im. Piastów Śląskich we Wrocławiu

OŚWIADCZENIE WSPÓŁAUTORA

Oświadczam, że w pracy **In Vitro Study of Calcium Microsecond Electroporation of Prostate Adenocarcinoma Cells** mój udział polegał na kierowaniu Katedrą i Zakładem Biologii Molekularnej i Komórkowej w których przeprowadzono badania opisane w tej pracy, krytycznej ocenie wyników, doradzaniu przy planowaniu eksperymentów, korekcie manuskryptu oraz pozyskaniu funduszy na pokrycie kosztów eksperymentów oraz publikacji.

Podpis

Prof. Mounir Tarek - Senior Research Director   Nancy 30.08.21

Affiliation: CNRS- Université de Lorraine, Nancy, France

Author's contribution

This letter confirms that my contribution in work entitled **In Vitro Study of Calcium Microsecond Electroporation of Prostate Adenocarcinoma Cells** included correction of manuscript, coordination and performance of molecular dynamics simulation and presentation of its results (figure 9).

Signature:

Mounir Tarek

dr Anna Szewczyk   Wrocław 30.08.21

Afiliacja: Katedra i Zakład Biologii Molekularnej i Komórkowej Uniwersytetu Medycznego im. Piastów Śląskich we Wrocławiu

OŚWIADCZENIE WSPÓŁAUTORA

Oświadczam, że w pracy **Effects of high−frequency nanosecond pulses on prostate cancer cells** mój udział polegał na poradzie przy wyborze przeciwciał oraz wykonaniu zdjęć preparatów za pomocą mikroskopii konfokalnej. Wykonane zdjęcia zaprezentowano na rycinie 5a.

.

Podpis

dr Anna Szewczyk   Wrocław 30.08.21

Afiliacja: Katedra i Zakład Biologii Molekularnej i Komórkowej Uniwersytetu Medycznego im. Piastów Śląskich we Wrocławiu

OŚWIADCZENIE WSPÓŁAUTORA

Oświadczam, że w pracy **In Vitro Study of Calcium Microsecond Electroporation of Prostate Adenocarcinoma Cells** mój udział polegał na wykonaniu zdjęć preparatów za pomocą mikroskopii konfokalnej (rycina 6. i 8.), pomocy przy opisie rezultatów oraz analizie fluorescencji kaspazy 3. (rycina 6.).

Podpis

Dr Olga Michel   Wrocław 30.08.21

Afiliacja: Katedra i Zakład Biologii Molekularnej i Komórkowej Uniwersytetu Medycznego im. Piastów Śląskich we Wrocławiu

OŚWIADCZENIE WSPÓŁAUTORA

Oświadczam, że w pracy **In Vitro Study of Calcium Microsecond Electroporation of Prostate Adenocarcinoma Cells** mój udział polegał na obsłudze cytometru i na koordynowaniu wykonywania doświadczeń techniką cytometrii przepływowej (rycina 5). Ponadto, w projekcie dokonałam krytycznej oceny rezultatów doświadczeń oraz korekcji manuskryptu.

.

Podpis

Prof. Vitalij Novickij   Vilnius 30.08.21

Affiliation: Institute of High Magnetic Fields, Vilnius Gediminas Technical University, Vilnius, Lithuania

Author's contribution

This letter confirms that my contribution in work entitled Effects of high - frequency nanosecond pulses on prostate cancer cells included the development of square wave electroporator, project supervision and funding acquisition. Moreover, I helped to respond to reviewers' comments.

Signature:

mgr inż. Magdalena Maciejewska   Wrocław 30.08.21

Afiliacja: Instytut Immunologii i Terapii Doświadczalnej im. Ludwika Hirszfelda Polskiej Akademii Nauk

OŚWIADCZENIE WSPÓŁAUTORA

Oświadczam, że w pracy **Effects of high-frequency nanosecond pulses on prostate cancer cells** mój udział polegał na doradzaniu przy wyborze linii komórkowych oraz udzieleniu wskazówek dotyczących hodowli modeli nowotworu prostaty.

Podpis

M. Maciejewska

12. Życiorys

Dane osobowe

- Imię i nazwisko: Aleksander Kiełbik
- Data i miejsce urodzenia: 24.06.1995 Wałbrzych
- Adres korespondencyjny: ul. Ełcka 15a 51-427 Wrocław
- Adres mailowy: aleksander.kielbik@outlook.com

Aktualne miejsce i stanowisko pracy

- Uniwersytecki Szpital Kliniczny we Wrocławiu. ul. Borowska 213. 50-556 Wrocław - lekarz stażysta

Edukacja

- 2014-2020 Uniwersytet Medyczny we Wrocławiu, Wrocław
- 2018-2019 Technische Universität Dresden, Drezno, Niemcy (program Erasmus)
- 2016-2017 Philipps-Universität Marburg, Marburg, Niemcy (program Erasmus)

Nagrody

- Stypendium Fundacji Kościuszkowskiej - Exchange to the U.S. na rok akademicki 2021-2022
- Stypendium Ministra Zdrowia za wybitne osiągnięcia na rok akademicki 2019-2020
- Pierwsza nagroda w sesji Oncology, Hematology and Radiotherapy oraz druga nagroda w Golden Session podczas 18th International Congress of Young Medical Scientists (czerwiec 2018, Poznań) za pracę pod tytułem "*The influence of photodynamic therapy with curcumin as a photosensitizer on human Glioblastoma multiforme SNB19 cells*".

Doświadczenie kliniczne oraz praktyki zawodowe

- 2019 sierpień – wrzesień: praktyki zawodowe na Oddziale Ginekologii, Pediatrii oraz Neurologi, Facoltà di Medicina e Chirurgia dell'Università degli Studi di Perugia, Włochy
- 2019 luty -marzec: praktyki zawodowe na Oddziale Urologii, Technische Universität Dresden, Niemcy
- 2018 sierpień: praktyki zawodowe na oddziale Anestezjologii i intensywnej terapii, Charité – Universitätsmedizin Berlin, Berlin, Niemcy

- 2018 lipiec: praktyki zawodowe na oddziale Chirurgii ogólnej, Charité – Universitätsmedizin Berlin, Niemcy

Udział w warsztatach i kursach

- Electroporation Based Technologies and Treatments 2019, Lublana, Słowenia

Prezentacje na zjazdach i kongresach

Zagraniczne

- "*The effect of Irradiation with Curcumin as a Possible Form of Amelanotic Melanoma Treatment*"; Prezentacja plakatu podczas AACR Special Conference on Melanoma: From Biology to Target, Houston 2019, USA

Krajowe

- "*The influence of photodynamic therapy with curcumin as a photosensitizer on human Glioblastoma multiforme SNB19 cells*" Prezentacja ustna podczas sesji Oncology, Hematology and Radiotherapy na 18th International Congress of Young Medical Scientists, Poznań 2018, Polska

Doświadczenie Naukowe

- „*Efekty terapii fotodynamicznej z kurkuminą jako fotouczulaczem na komórkach glejaka wielopostaciowego*".
  Opiekun naukowy: dr hab. inż. Julita Kulbacka, Prof. UMW

- „*Wpływ elektroporacji mikrosekundowej z wapniem na przeżywalność i mobilność komórek nowotworu prostaty (DU145)*" – kierownik grantu – program FAST I edycja, WCA (Wrocławskie Centrum Akademickie)
  Opiekun naukowy: dr hab. inż. Julita Kulbacka, Prof. UMW

- „*Wpływ mikrosekundowej elektroporacji na ekspresję markerów powierzchniowych MAGE czerniaka barwnikowego (A375) i bezbarwnikowego (C32) – badania in vitro*" – wykonawca grantu –program FAST II edycja, WCA (Wrocławskie Centrum Akademickie);
  Opiekun naukowy: dr hab. inż. Julita Kulbacka, Prof. UMW

Języki obce: Angielski (C1); **Niemiecki** (C1)

Publikacje:

Publikacje pełnotekstowe: 12; łączna punktacja IF: 31,789; Pkt. MNiSW/KBN: 845

1. **Aleksander Kiełbik,** Wojciech Szlasa, Anna Szewczyk, Vitalij Novickij, Jolanta Saczko, Julita Kulbacka: *Effects of high‑frequency nanosecond pulses on prostate cancer cells*, Scientific Reports 2021 Vol. 11 no. 5=15835; IF: 4,379

2. **Aleksander Kiełbik,** Wojciech Szlasa, Olga Michel, Anna Szewczyk, Mounir Tarek, Jolanta Saczko, Julita Kulbacka: *In vitro study of calcium microsecond electroporation of prostate adenocarcinoma cells*, Molecules 2020 Vol. 25 no. 5406; IF: 4.411

3. **Aleksander Kiełbik,** Wojciech Szlasa, Jolanta Saczko, Julita Kulbacka.: *Electroporation-Based Treatments in Urology,* Cancers 2020 Vol.*12* no. 2208; IF: 6.639

4. **Aleksander Kiełbik**, Piotr Wawryka, Dawid Przystupski, Joanna Rossowska, Anna Szewczyk, Jolanta Saczko, Julita Kulbacka, Agnieszka Chwiłkowska.: *Effects of photosensitization of curcumin in human glioblastoma multiforme cells,* In Vivo 2019 Vol.33 no.6; page:1857-1864; IF: 1.541

5. **Aleksander Kiełbik**, Piotr Wawryka, Agnieszka Chwiłkowska.: *Immunotherapy for melanoma - the newest therapeutic possibilities targeting cancer immunity cycle and tumor microenvironment*, Post.Biol.Kom. 2019 T.46 no 2; page:129-146; IF: 0.163

6. Wojciech Szlasa**, Aleksander Kiełbik,** Anna Szewczyk, Nina Rembiałkowska, Vitalij Novickij, Mounir Tarek, Jolanta Saczko, Julita Kulbacka: *Oxidative Effects during Irreversible Electroporation of Melanoma Cells—In Vitro Study***,** Molecules 2021 Vol. 26 no. 154; IF: 4.411

7. Wojciech Szlasa, Anna Szewczyk, Małgorzata Drąg-Zalesińska, Hanna Czapor-Irzabek, Olga Michel, **Aleksander Kiełbik**, Karolina Cierluk, Aleksandra Zalesińska, Vitalij Novickij, Mounir Tarek, Jolanta Saczko, Julita Kulbacka: *Mechanisms of curcumin-based photodynamic therapy and its effects in combination with electroporation: an in vitro and molecular dynamics study*, Bioelectrochemistry Vol. 140; IF 5.373

8. Dawid Przystupski, Magdalena J. Niemczura, Agata Górska, Stanisław Supplitt, Krzysztof Kotowski, Piotr Wawryka, Paulina Rozborska, Kinga Woźniak, Olga Michel,

Aleksander Kiełbik, Weronika Bartosik, Jolanta Saczko, Julita Kulbacka.: *In search of panacea - review of recent studies concerning nature-derived anticancer agents*, Nutrients 2019 Vol.11 no.6; art.1426 IF: 4.546

9. Piotr Wawryka, **Aleksander Kiełbik**, Małgorzata Moszyńska, Gracjan Iwanek, Nina Rembiałkowska.: *Cellular and molecular mechanisms of electrochemotherapy, sonoporation, photodynamic therapy and sonodynamic therapy in terms of oncological treatment*, Post.Biol.Kom. 2019 T.46 no 2; page: 205-220; IF: 0.163

10. **Aleksander Kiełbik**, Piotr Wawryka, Agnieszka Chwiłkowska, Jolanta Saczko, Julita Kulbacka.: *Signaling pathways in melanoma biology and new targeted therapeutic approaches*. Med.Res.J. 2019 Vol.4 no.3; page: 184-188

11. Staniław Supplitt, Weronika Bartosik, Krzysztof Kotowski, **Aleksander Kiełbik**, Dagmara Baczyńska, Julia Rudno-Rudzińska, Julita Kulbacka.: *Car T-Cell Therapy as an Innovative Approach in Cancer Immunotherapy*, Post.Biol.Kom. 2019 T.46 no 2; page: 159-172; IF: 0.163

12. Wojciech Szlasa, Kamila Wala, **Aleksander Kiełbik**, Aleksandra Zalesińska, Jolanta Saczko, Julita Kulbacka.: *Connection between Warburg effect and oncometabolites biosynthesis with its clinical implications*. Org.Med.Chem.Int.J. 2020 Vol.9 no.5 Publikacja w czasopiśmie spoza listy MNiSW.